Modeling and Performance Enhancement of Hybrid Fiber Network-PON/DPPM-DWDM-FSO Communications under Atmospheric Turbulence Conditions

Ebrahim E. Elsayed (engebrahem16@gmail.com)

Electronics and Communications Engineering Department, Faculty of Engineering, Mansoura University, Mansoura 35516, El-Dakahilia Governorate, Egypt. https://orcid.org/0000-0002-7208-2194

Research Article

Keywords: Hybrid fiber/free-space optical communications, DWDM systems, DPPM modulation, Optical cross-connect, Inter-channel crosstalk, Amplified spontaneous emission (ASE) noise

Posted Date: April 26th, 2021

DOI: https://doi.org/10.21203/rs.3.rs-460066/v1

Modeling and Performance Enhancement of Hybrid Fiber Network-PON/DPPM-DWDM-FSO Communications under Atmospheric Turbulence Conditions

Ebrahim E. Elsayed

Electronics and Communications Engineering Department, Faculty of Engineering, Mansoura University, Mansoura 35516, El-Dakahilia Governorate, Egypt.
Author's email address: engebrahem16@gmail.com

Abstract

A Wavelength Division Multiplexing (WDM) access network using high-speed free-space optical (FSO) communication based on the passive optical networks (PONs) for the distribution link is proposed. In such network architecture, the FSO link can extend the system to areas where an optical fiber link is not feasible, and or provide limited mobility for indoor coverage. The performance of Hybrid Fiber/FSO (HFFSO) network based on digital pulse position modulation (DPPM), for both the indoor and outdoor environments of the optical access network, are compared with the performance of such a network that is based on conventional On-Off Keying Non-Return-to-Zero (OOK-NRZ) modulation using results obtained through computational and analytical modeling. The WDM channels suffer from inter-channel crosstalk, while the HFFSO communication performance in a clear atmosphere is limited by atmospherically induced scintillation. The impairments, plus the amplified spontaneous emission noise from optical amplification, combining in a potentially problematic way, particularly in the upstream direction, which is investigated here. The results obtained indicate that in a clear atmosphere with a sufficiently high signal to crosstalk ratio the proposed system can achieve a human-safe and high-capacity access network. Dense Wavelength Division Multiplexing (DWDM) has dramatically increased the capacity of optical transmission systems. Its inherent advantages have made it the current favorite multiplexing technology for an optical network, also used on fiber optic backbones and long-distance transmission. The crosstalk due to inter-band crosstalk for Ultra-Dense WDM systems causes higher noise and degrades the network performance and analyzed the performance of DWDM-PON link that is corrupted crosstalk for Optical Cross-Connect (OXC). Then the analysis of BER with crosstalk was done. Using the equation for crosstalk number of channels was plotted using Matlab. An analysis is carried out to find the amount of crosstalk considering a WDM-FSO over OOK-NRZ and DPPM based OXC. The bit error rate performance

degradation due to crosstalk is evaluated for the OXC parameter and number of wavelength per fiber.

Keywords: Hybrid fiber/free-space optical communications; DWDM systems; DPPM modulation; Optical cross-connect; Inter-channel crosstalk; Amplified spontaneous emission (ASE) noise.

1. Introduction

Over the years, there has been an exponential rise in the demand for broadband applications and Services [1, 2]. Optical carrier technologies can be a good solution for the access networks since they potentially offer huge bandwidth [2-6]. Passive Optical Networks (PONs) (i.e. the last mile connection between individual homes and businesses and the public network) and have gradually replaced the copper-based access network technologies. Optical fiber has many advantages (low cost, no electromagnetic interference problems, and less power loss) over the incumbent copper system [7, 8]. At the moment, Time Division Multiplexing (TDM/TDMA) systems are the most popular architecture for PONs although they are only suitable for a limited number of optical network units (ONUs) (unless augmented by optical amplification [9] and they typically use power splitter. Wavelength Division Multiplexing (WDM) systems, on other hand, allow more ONUs to be connected at high data rates and assign a distinct pair of dedicated wavelengths to each ONU such that a point-to-point connection is established between the ONU and the Optical Line Terminator (OLT) [1]. The WDM-PON increases the bandwidth and the greater data security that can be offered to the ONUs compared to the (TDM / TDMA) system [1, 2, 10-12]. One of the popular modulation schemes widely applied in the free-space optical (FSO) communications in Digital Pulse Position Modulation (DPPM). This scheme is well known to be attractive in different (FSO) environments including inter-satellite atmospheric and indoor wireless channels [12]. DPPM has been proposed and intensively investigated for optical fiber systems [2] with the availability of bandwidth-intensive services such as Video On Demand (VOD), Internet Protocol Television (IPTV), IP Telephony and interactive gaming/video conferencing, there has been a rapid rise in bandwidth demand from users [10, 12]. In response to this increase in bandwidth demand, Wavelength Division Multiplexing (WDM) systems have been investigated and/or deployed for optical fiber, Optical

Wireless Communications (OWC), and atmospheric indoor wireless optical network [2]. WDM could also be applied in multiple user access networks, for example, the WDM Passive Optical Network (PON) is generally considered as a good solution to the bandwidth requirements for future access networks, with potential for higher data rate, improved data security and longer reach [1, 2]. Dense Wavelength Division Multiplexing (DWDM) operates in the 1528 nm to 1568 nm wavelength range and can combine up to 32 signals on one fiber, 4 channels – 8 channels – 16 channels or 32 channels DWDM with 200 GHz. Free Space Optical (FSO) communications simply entail transmission of the optical signal through the earth's atmosphere and its subsequent reception. FSO communications have been successfully applied for short-distance link (up to 4 km) [5]. Relative to fiber systems, FSO communications has the advantages of ease of set-up and technology provision of access in difficult locations, and relatively lower cost (i.e. no purchasing and installing of fiber, especially if it otherwise had to go underground) [13-16]. FSO communication-based access networks have competitive advantages over RF (or millimeter-wave) systems such as improved security, no spectrum licensing, and faster speed over the short-haul-access [4, 5]. Despite the advantages of FSO communications, is faced with considerable challenges such as the effects of atmospheric attenuation and turbulence-induced scintillation, which have severe effects on the propagation field [4, 5, 7, 14, 17, 18]. A DWDM access network using FSO communications in the distribution link is a realistic proposition since both optical fiber and FSO systems operate using similar optical transmission wavelength and system components [7, 10, 17, 19]. Therefore, the integration of both technologies may yield a cost-effective and reliable hybrid optical access network solution. For long propagation distances, the use of an optical amplifier becomes necessary. However, the optically amplified signal is accompanied by ASE noise which somewhat offsets the performance benefits of the amplifier and complicates performance calculations [20-22]. The presence of inter-channel crosstalk in WDM systems is well reported [8, 23, 24]. However, it will be seen that the turbulent nature of the atmospheric channel in the distribution link of the hybrid optical access network causes fluctuation inter-channel crosstalk effects that significantly exacerbates its negative impact on performance. The probability of crosstalk power exceeding the signal power (either by the turbulent increase of crosstalk or turbulent decrease of signal or both) provides an ultimate performance limit. Experimental work has demonstrated the feasibility of WDM-FSO networks

[10, 25, 26]. Optical Wavelength Division Multiplexing (WDM) networks are very promising due to their large bandwidth, their large flexibility, and the possibility to upgrade the existing optical fiber networks to WDM networks [27]. WDM has already been introduced in commercial systems. All-Optical Cross-Connect, however, has not yet been used for the routing of the signal in any of these commercial systems [1]. One key advantage of DWDM is that the gain region of Erbium-Doped Fiber Amplifiers (EDFA) is also in C-band, which enables all the wavelengths to be amplified to overcome loss over long spans of fiber and high passive losses (e.g. From splitting, multiplexing, etc.). The OXC is an essential network element in a WDM optical network [27]. A number of OXC architectures have been proposed in each of which have its own unique features, strengths, and limitations.

2. Network (Down / Up) Stream Transmission

The network components as shown in Figs. 1, 2 include a transmitter module which comprises of a laser driver (LD) and laser for optical signal generation, the input message signal (data), PPM modulator (PPM Mod), and a receiver module made up of a photodetector (PD), electrical amplifier and filter (EA) and the integrate and compare circuitry (ICC) for system decision [27]. Thus the system is intensity-modulated and the signal is received by direct detection.

2.1. Downstream Transmission:

In the downstream, N separates OLT laser transmit signals belonging to each ONU on a particular wavelength in a point-to-point fashion. In the downstream performance calculations, the same assumption as in the upstream is made for the optical wavelengths, channel spacing, and use of optimal threshold in the OOK scheme. However, maximum OLT transmits powers are lower (typically 10 dBm) [2, 27] to fiber nonlinearity. The downstream architecture is similar to the upstream but the system operation is different. Each wavelength at the OLT has a separate laser source which transmits the signal for the group of ONUs on its wavelength. As shown in fig 1, the signal on each wavelength is split into the number of ONUs on the wavelength and separately encoded with the Optical Orthogonal Code (OOC) for each ONU before being recombined for wavelength multiplexing [27]. The multiplexed signals propagate through the feeder fiber to the remote node for optical amplification and demultiplexed before each wavelength's signal is split into each ONUs signal and

further transmitted the FSO link for decoding and reception [27]. The downstream crosstalk arises for the imperfect performance of the demux at the remote node. Compared to the upstream transmission, there is additional splitter loss in the downstream; this is an optional operational cost that reduces the number of optical sources required at the OLT to the number of wavelengths (N), instead of one per user (i.e. NK) as is obtained in the upstream [27].

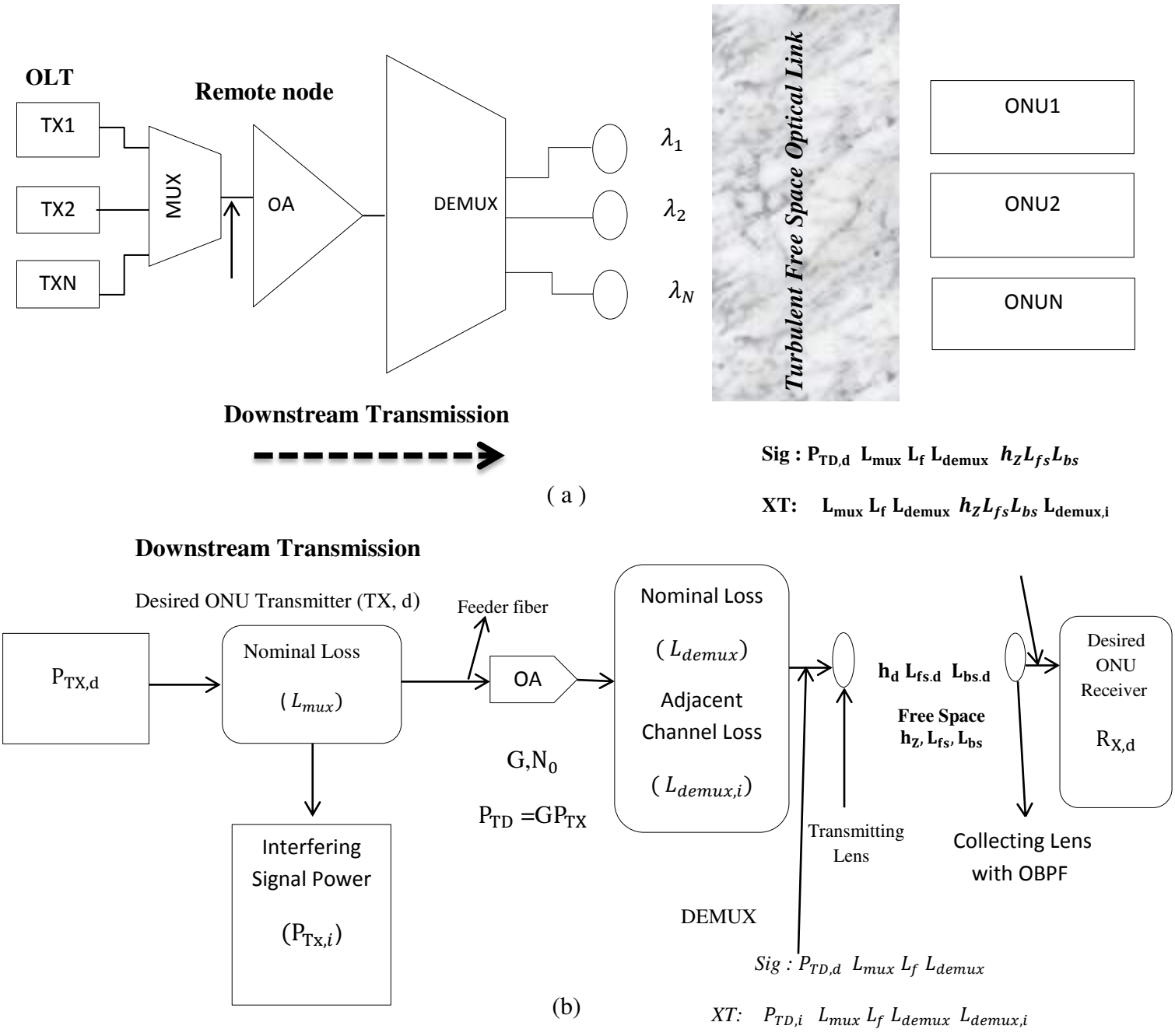

Fig. 1 Optically Pre-amplified WDM DPPM Network: a) Downstream system diagram and b) (Downstream) functional diagram.

2.2. Upstream Transmission:

In the upstream, each ONU has a dedicated independent point-to-point optical link to the OLT with a laser of its own specific fixed wavelength. The distribution network (atmospheric channel) conveys the signal from the ONUs to a mux, which combines and transmits them through a single optical feeder fiber to the OLT as shown in Fig 2. At the OLT the demux separates the multiplexed optical signals into constituent wavelengths. Several (WDM/mux-demux) technologies exist [27]. The arrayed waveguide grating (AWG) based devices are very popular, mainly because of their low chromatic dispersion loss, however, production complexity, cost, and temperature-dependent loss variation are drawbacks [1, 8, 27]. The optical wavelengths are assumed to be in the C band (i.e. around 1550 nm) with channel spacing of 100 GHz [2] on the (ITU-T grid) thus benefiting from the low signal attenuation and developed optical device technology in those range of wavelengths. Each group of ONUs transmitting on a fixed wavelength uses the same laser transmitters operating at a set central wavelength. Optically encoded signals from the ONUs located at homes, buildings, or kerb are transmitting upstream through a turbulent FSO link to the remote node. The Average optical received power at the OLT photodiode from an ONU on the desired signal wavelength and an ONU on the crosstalk wavelength are respectively written as [18, 27]. Each RCL, located at the remote, collects the corresponding incident optical signal and then couples it through a short length of fiber using a fiber collimator as per [20] to the mux. An optical preamplifier of gain G and noise figure NF can be placed either at the remote node output to effectively increase the transmit power of the feeder fiber or at the demux input to help the effective OLT receiver sensitivity. A PIN photodiode with quantum efficiency η is placed after the demux to convert the information-bearing light into an electric signal. An integrate-and-dump receiver is assumed at the decision circuit with electrical bandwidth $B_e = {}^{1}/_{2\mathrm{T_b}}$, where $T_b = {}^{1}/_{R_b}$ and Rb is the data rate. For the OOK-NRZ assumed here, the Kalman filtering method [27] represents a realistic adaptive approach of achieving a near-optimal threshold for each instantaneous level [27].

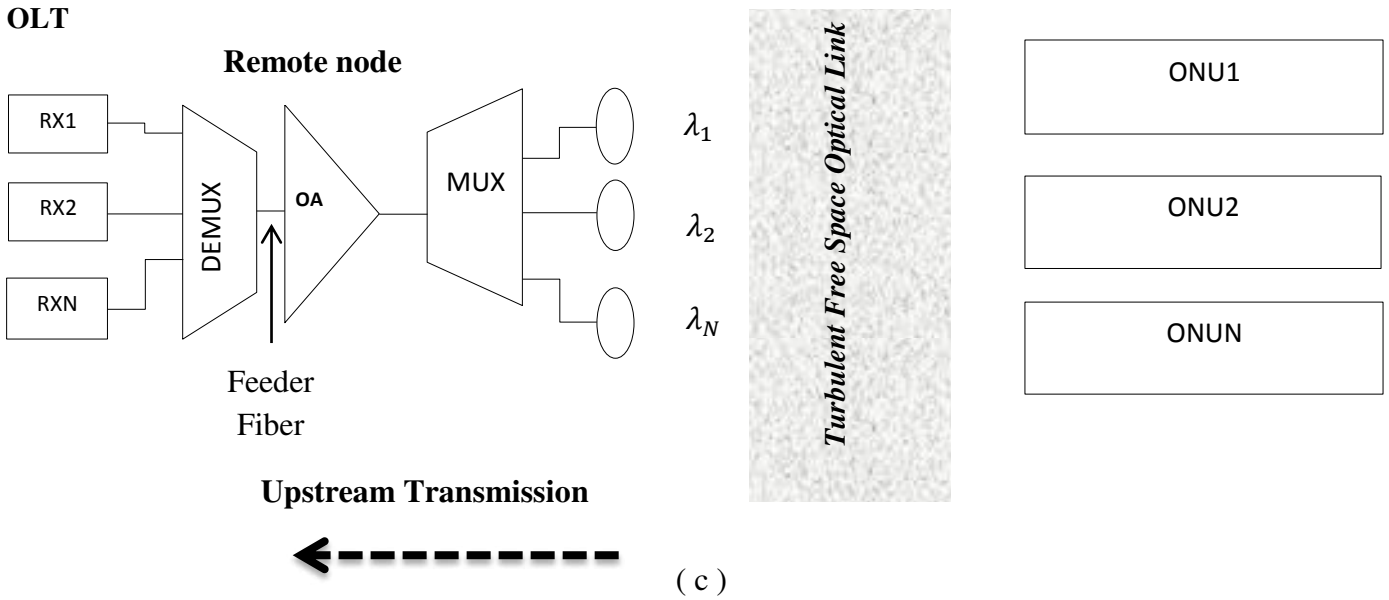

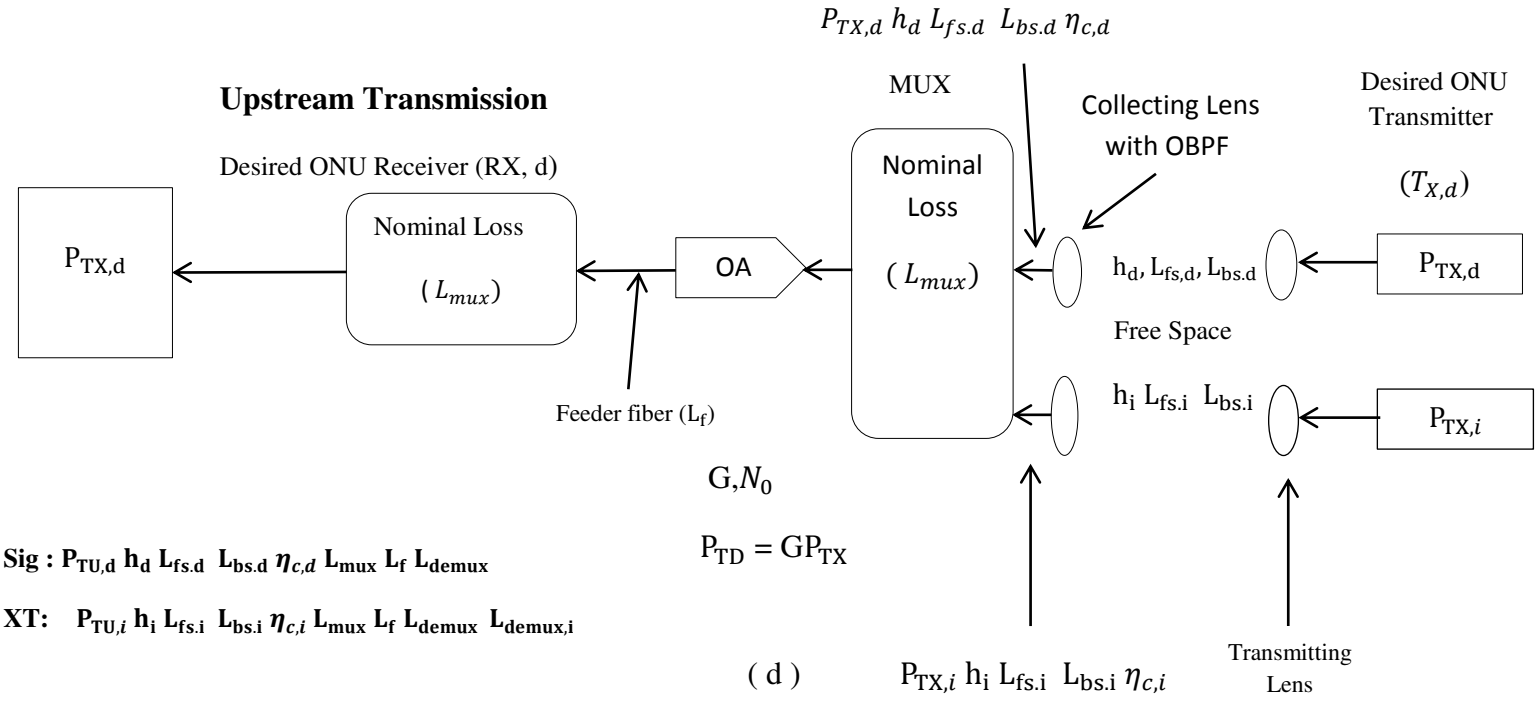

Fig. 2 Optically Pre-amplified WDM DPPM Network: (c) Upstream system diagram (d) Upstream functional diagram.

2.3. Optical amplifier placement:

There are two Cases. Case A is when the optical amplifier is placed at the remote node [27]. Case B is when the optical amplifier is placed at the OLT. In upstream Case A, the ASE noise loss due to feeder fiber attenuation and OLT demux loss, while in upstream Case B, the ASE noise suffers from OLT demux loss only [27]. In the downstream Case A, the ASE noise suffers remote node demux loss, atmospheric attenuation, and beam spreading. Case A and Case B for ≈20 Km fiber, which is not particularly significant when OSNR is good [27].

3. Turbulence Channel Modeling

Atmospheric scintillation occurs due to thermally induced refractive index changes of the air along with the optical link, causing rapid fluctuation of signal irradiance at the receiver, reduction in the degree of coherence of the optical signal [27, 28], and potentially poor Bit-Error Rate (BER) [2, 27].The Gamma-Gamma (GG) distribution is widely used for characterizing the whole range of turbulence effects, i.e., weak, moderate, and strong, not only because closed-form expressions exist but also because of their direct dependence on turbulence parameters and the closeness to experimental results [14, 16, 18, 27, 28].

$$P_{GG}(h_X) = \frac{2(\alpha\beta)^{(\alpha+\beta)/2}}{\Gamma(\alpha)\Gamma(\beta)} h_X^{(\alpha+\beta)/2-1} K_{\alpha-\beta}(2\sqrt{\alpha\beta h_X}); \qquad h_X > 0, \tag{1}$$

Where h_X is the attenuation due to atmospheric turbulence for the signal (h_{sig}) or interferer (h_{int}), α is the effective number of large-scale eddies of the scattering process, β is the effective number of small-scale eddies of the scattering process, $K_n(\cdot)$ is the gamma function. The signal and interferer travel over physically distinct paths in the upstream as written in [27, 28-32].

$$\alpha = \left\{ \exp\left[\frac{0.49\sigma_R^2}{(1+0.65d^2+1.11\sigma_R^{12/5})^{7/6}} \right] - 1 \right\}^{-1}, \tag{2}$$

$$\beta = \left\{ \exp\left[\frac{0.51\sigma_R^2 \left(1+0.69\sigma_R^{12/5}\right)^{-5/6}}{1+0.9d^2+0.62d^2\sigma_R^{12/5}} \right] - 1 \right\}^{-1}, \tag{3}$$

Where $d = \sqrt{KD_{RX}^2/4l_{fso}}$ is the normalized RCL radius, $\sigma_R^2 = 1.23C_n^2 k^{7/6} l_{fso}^{11/6}$ is the Rytov variance [18, 27, 28-32], C_n^2 is the refractive index structure constant (ranging from ~ $10^{-17}m^{-2/3}$ to $\sim 10^{-13}m^{-2/3}$), l_{fso} is the FSO link length, $k = 2\pi/\lambda$ is the wave-number [27].

4. BER Analysis

In its most general form, under the assumption of independent signal and crosstalk channels (e.g., as in the upstream), the average (turbulence-accentuated) BER [for given fixed transmitter powers for the signal, crosstalk, and attenuation written in [18, 2, 27-31].

$$\overline{\mathrm{BER}} = \iint_0^{\infty} \mathrm{BER}(\mathrm{h_{sig}},\mathrm{h_{int}})\mathrm{P_{GG,sig}}(\mathrm{h_{sig}}) \times \mathrm{P_{GG,int}}\,\mathrm{h_{int}})\mathrm{dh_{sig}d}, \quad 4$$

Where $P_{GG,sig}(h_{sig})$ and $P_{GG,sig}(h_{int})$ are respectively, the signal and interferer GG pdfs (each with different α, β and σ_R^2) as written in [2, 27, 31]

$$\mathrm{BER}\left(\mathrm{h_{sig}}, \mathrm{h_{int}}\right) = \frac{1}{4}\ \mathrm{erfc}\left(\frac{\mathrm{Q}(\mathrm{h_{sig}},\mathrm{h_{int}}}{\sqrt{2}}\right) \quad 5$$

5. Results

BER versus average received power results, for FSO communication system under various atmospheric turbulence conditions, with the main focus on the turbulence – accentuated of inter-channel crosstalk.

The parameters

Laser wavelength (λ) =1.55 μm, data rate (R_b) = 2.5 Gb/ps, Extinction ration (r) = 10 dB (for signal and interferer), Optical band pass-filter (B_0)= 60 GHz, Quantum efficiency (η) = 0.8, amplifier noise figure (NF) = 4.77 dB and Optical gain (G) =30 dB, the thermal noise current is assumed to be 7×10^{-7} with back-to-back sensitivity of -20 dBm at BER of 10^{-12}.

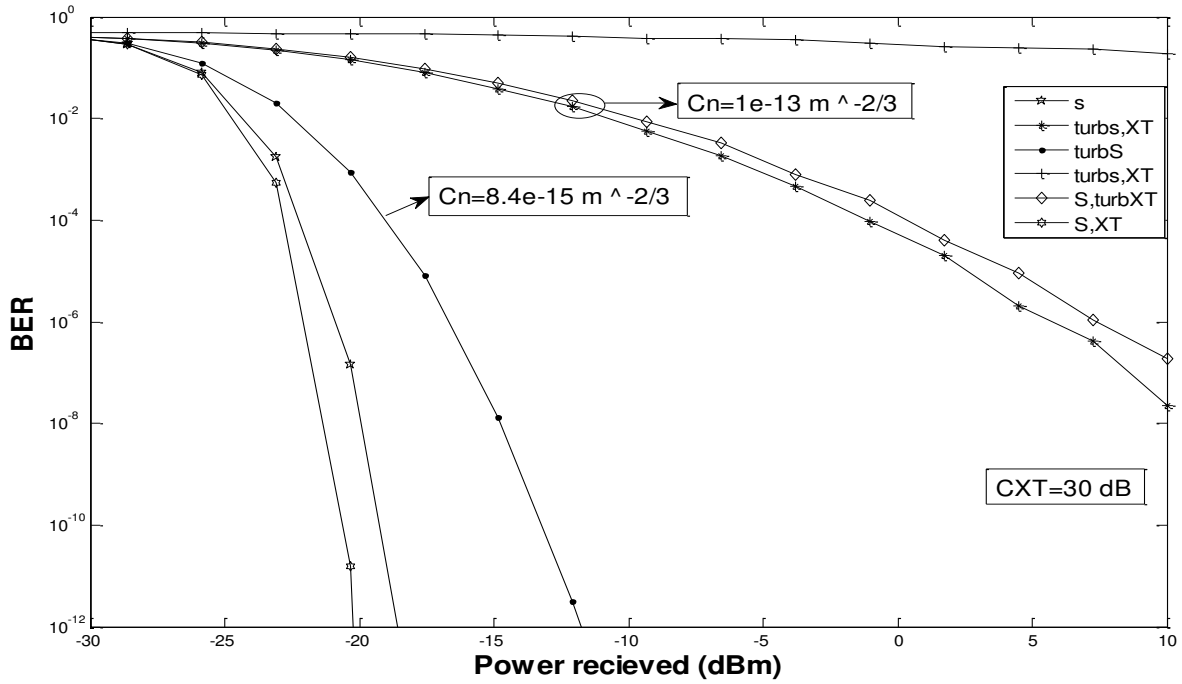

Fig. 3 BER versus average received signal optical power (dBm) for WT and ST (no amplifier) with crosstalk CXT= 30 dB.

In the weak turbulence cases; error floors occur at much lower BER, then range shown, using a signal-to-crosstalk ration of 30 dB. To understand turbulence accentuation of crosstalk considers firstly the (S, turb XT) CASE (interferer with turbulence) and note that turbulent crosstalk sometimes increases its 1 value so that {data 0, crosstalk 1} is greater than {data 1, crosstalk 0} (neglecting receiver noises) [27]. In the non-amplified case in Fig. 3, the (S, turb XT interferer with turbulence case) and the (turb S, XT interferer with no turbulence) can superficially seem at the same, as the instantaneous crosstalk ratio (not the same as CXT) which used the average or turbulence-free values in its definition will have the same statistics in both cases. The difference that is one (S, turbXT) the ratio between the signal power and the noise does not change, while in the other (turb, XT), the ratio between the signal power and noise varies – greatly [27].

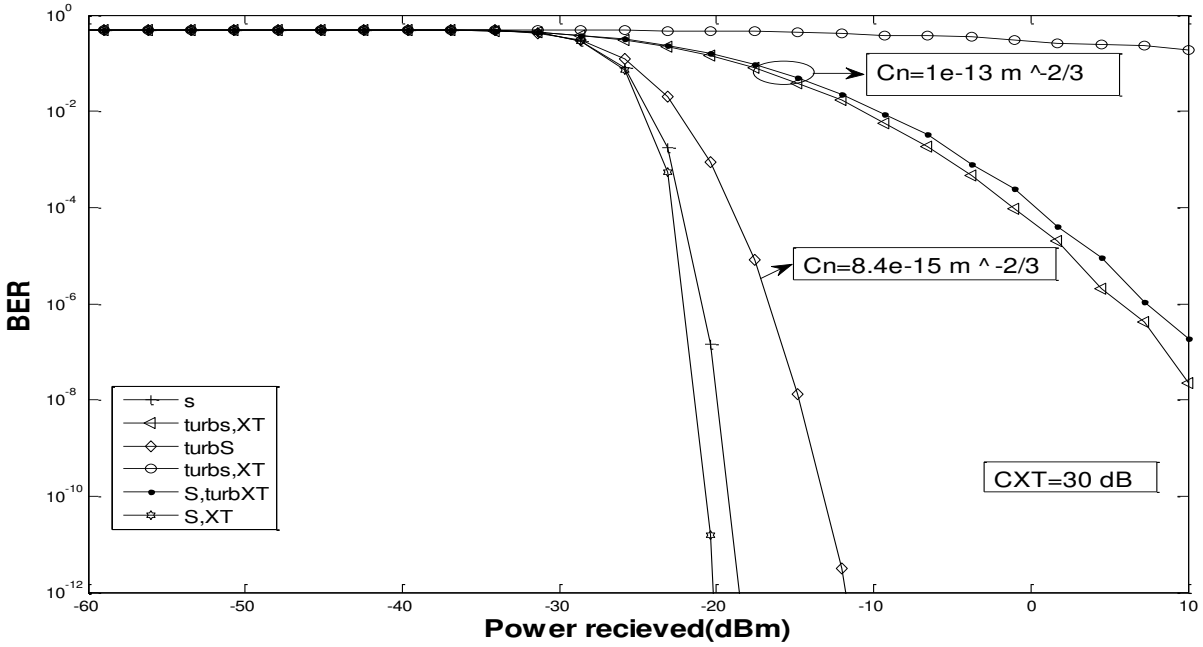

Fig. 4 BER versus average received signal optical power (dBm) for WT and ST (with amplifier) with crosstalk CXT= 30 dB.

In Fig. 4, the same effect is observed when an optical amplifier is placed in the signal path (on the assumption that the optical filtering) provided by WDM or an optical band pass-filter does not reduce the crosstalk power while still being inter-channel of the optical amplifier case is presented in Fig. 4 for a signal to crosstalk ratio of 30 dB. It takes into account a specific crosstalk rejection by the optical filtering instead [27].

6. BER Evaluation for Hybrid WDM-PON-FSO System

6.1. Upstream transmission:

The single crosstalk can be used in situations where a dominant interferer exists (e.g. in some sparsely populated DWDM grids or where particular interferer transmitters are higher powered). Now the average received optical power at the OLT photodiode for the desired signal and an interferer is given, respectively, as equation written in [2. 21, 27-31].

$$P_{R,sig}(h_{turb,sig}) = GP_{UT,sig}\, L_{fso.sig}\, L_{bs,sig}\, L_{c,si} L_{mux} L_{fiber} L_{demux} \quad 6$$

$$P_{R,int} = GP_{UT,int}\, h_{turb,int}\, L_{fso.int}\, L_{bs,int}\, L_{c,int} L_{mux} L_{fiber} L_{demux}\, L_{demux,XT} \quad 7$$

Where $L_{demux,XT}$ is the crosstalk i.e. additional loss (above L_{demux}) the interferer has when coupled onto the signal photodiode by the demux. Also $P_{UT,sig}$ and $P_{UT,int}$ are the ONU transmit power of the signal and interfere, in principle, these could be allowed to differ in a power control algorithm [27-31]. $L_{fiber} = 10^{-\propto_{(fiber/fiber)}/10}$ is the loss due to fiber attenuation and $-\propto_{(fiber)}$ is the fiber attenuation factor in dB/Km. The loss due to beam spreading L_{bs} in the FSO link for signal and interferer can be calculated from [3, 14, 27].

$$L_{bs} = \left[\frac{D_{RX}}{\theta_{lfso}}\right]^2 \quad 8$$

And can of course be stated separately for the signal and the interferer [27].

L_C — is the coupling loss for the signal and interferer can be calculated from [2, 27, 29].

$$L_C = 1 - \left\{8a^2 \iint_0^1 \exp\left[-\left[a^2 + \frac{A_{RX}}{Ac}\right]\right] (X1^2 + X2^2) \times I_0\left[\frac{2A_{RX}}{Ac} X1X2\ dx1dx2\right]\right\} \quad 9$$

a— is the ratio of the RCL radius to the radius of the back-propagated fiber mode,

$A_{RX} = \frac{\pi D_{RX}^2}{4}$, $Ac = \pi\rho_c^2$ is the spatial coherence area of the incident plane wave

.$\rho_c = \left(1.46\, Cn^2 K^2\, l_{fso}\right)^{-3/5}$ ρ_c is the spatial coherence radius, and $I_{\circ =}(\cdot)$ is the modified Bessel function of the first kind and zero-order. At the amplifier output, the ASE Power Spectral Density (PSD) is $N_{0\ OA=}$ 0.5(NFG-1) E.

6.2. Downstream Transmission:

The inter-channel crosstalk present here is treated as non-turbulence-accentuated as (setting aside wavelength difference impact on σ_R^2) it travel on the same path of atmospheric of the signal.

The downstream BER is given by [21, 27, 31]

$$\mathrm{BER_d}\,(\mathrm{h_{turb}}) = \frac{1}{4}\mathrm{erfc}\left[\frac{\mathrm{Q_d(h_{turb})}}{\sqrt{2}}\right] \quad 10$$

$$\mathrm{Q_d(h_{turb})} = \frac{\mathrm{id_{1,0}(h_{turb}) - id_{0,1}(h_{turb})}}{\sigma\mathrm{d_{1,0}(h_{turb}) + \sigma d_{0,1}(h_{turb})}} \quad 11$$

The average received optical power at the ONU photodiodes for desired signal and interferer are given, respectively, as [21, 27, 31]:

$$\mathrm{P_{dR,sig}(h_{turb}) = GP_{dT,sig}h_{turb}\ L_{mux}L_{fiber}L_{demux}\ L_{fso}\,L_{bs}} \quad 12$$

$$\mathrm{P_{dR,int}(h_{turb}) = GP_{dT,int}h_{turb}\ L_{mux}L_{fiber}L_{demux,XT}\ L_{fso}\,L_{bs}} \quad 13$$

Where $P_{dR,sig}$ and $P_{dR,int}$ are the OLT transmitter power can used for the electric domain noises [27].

7. The Calculations Results

Results in terms of required optical power are presented to predict the performance for various scenarios of the hybrid WDM network.

Table 1 List of key parameters used in the calculation for both transmissions.

Parameter	Description	Value
$\boldsymbol{\lambda_{sig}}$	Desired signal wavelength	1550 nm
$\boldsymbol{R_b}$	Data rate	2.5 Gb/ps
$\boldsymbol{D_{RX}}$	RCL diameter	13 mm
G	Optical amplifier gain	30 dB
NF	Noise figure	4.77 dB
$\boldsymbol{B_0}$	Demux channel bandwidth	60 GHz
r	Extinction ratio	10 dB (signal and interferer)
$\boldsymbol{l_{fiber}}$	Feeder fiber length	20 km [1]
$\boldsymbol{l_{fso}}$	Maximum FSO length	2≈5 km
$\boldsymbol{\alpha_{fiber}}$	Feeder fiber attenuation	0.2 dB/km [1, 2]
$\boldsymbol{\alpha_{fso}}$	Atmospheric channel attenuation	0.2 dB/km (very λ clear air) [1, 12, 13]
$\boldsymbol{\theta}$	Transmission divergence angle	0.2 m/rad
$\boldsymbol{l_{demux}}$	Signal mux/ demux loss	3.5 dB [1, 2, 24]
η	Quantum efficiency	0.8

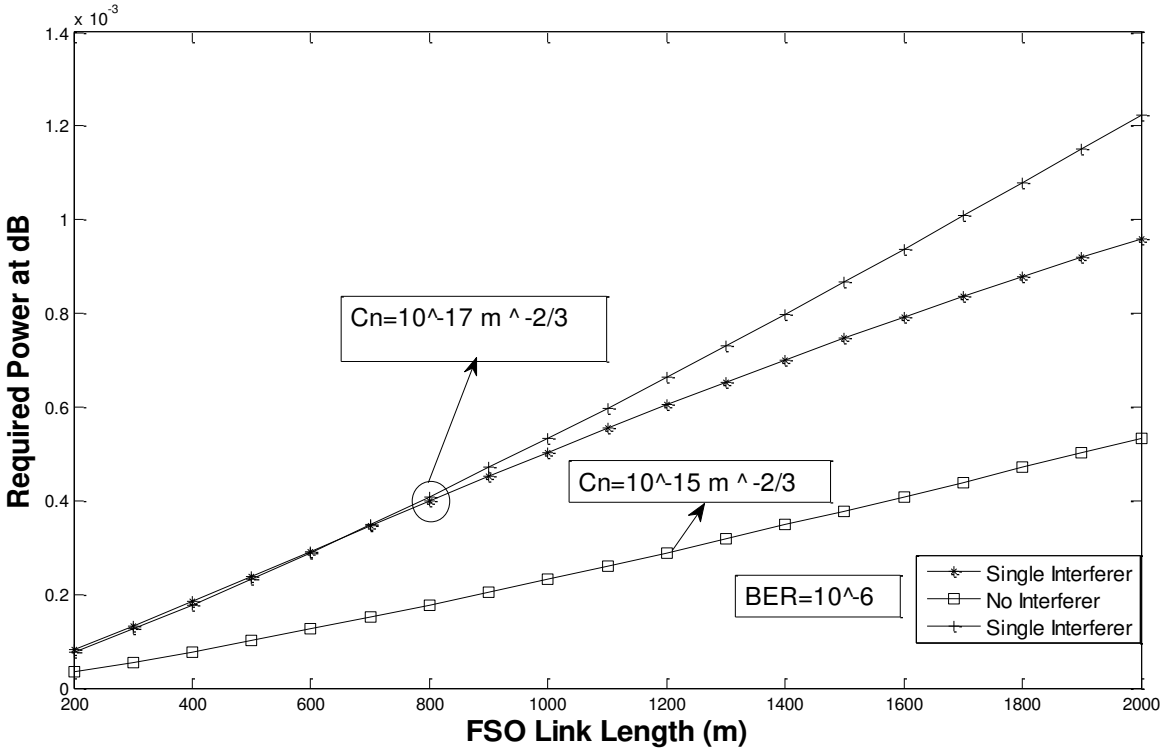

Fig. 5 Downstream required transmitted optical power (dBm) at target BERs of 10^{-6} as a function of the FSO link length (m) for no interferer and single interferer cases for l_{demux} = 15 dB.

Fig. 5 shows the downstream required transmitted optical power (dBm) at target BERs of 10^{-6} as a function of the transmitter divergence angle (rad) with $\mathrm{l_{fso}} = 1000$ m, for no interferer and single interferer cases with l_{demux} = 15 dB. It can be seen that the required to optical power increases with the OLT transmit divergence and turbulence strength [27]. The atmospheric channel becomes more turbulent, the required optical power increase, both the no interferer and single interferer cases have very similar required transmit power, due to the high signal to crosstalk ratio. If the transmitted power can be increase to a high 10 dBm, it can compensate for the turbulence effects for all Cn^2 values. If the OLT transmit power is fixed at 10 dBm, it can be deduced that the FSO link close to 2000 m can be used to achieve a BER of 10^{-12}.

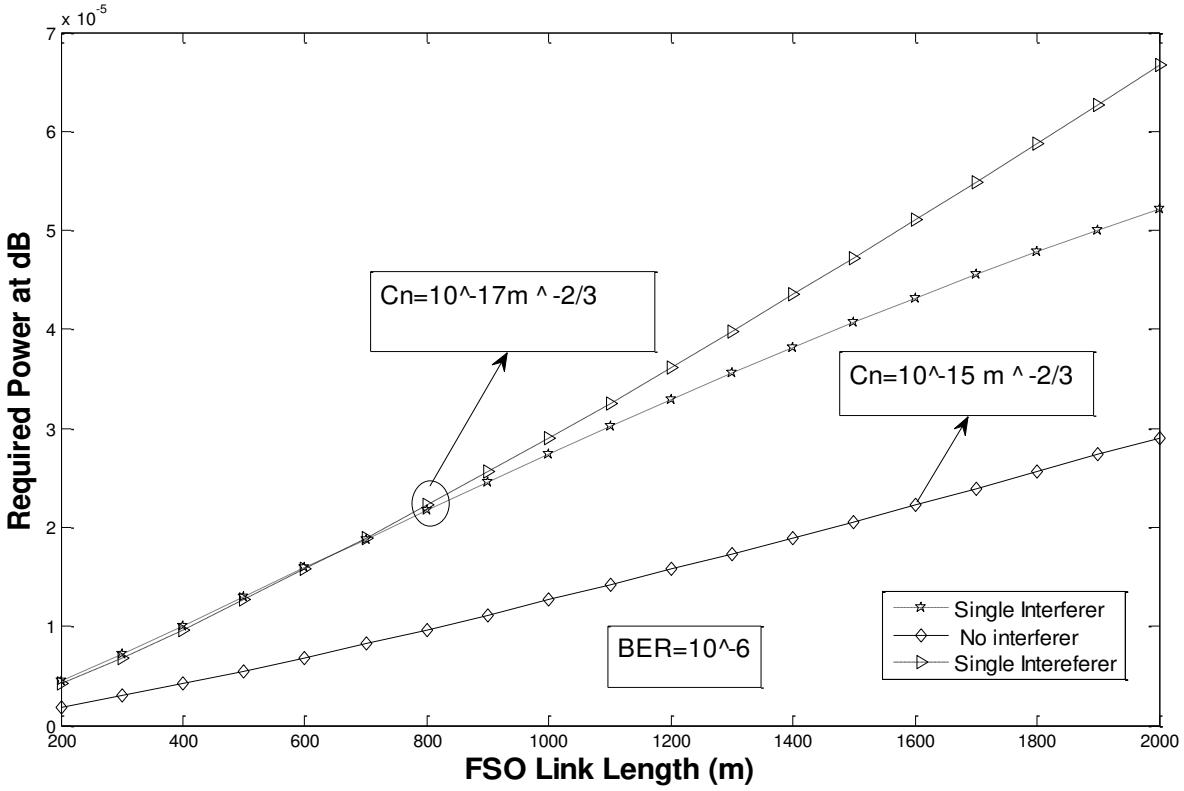

Fig. 6 Upstream required transmitted optical power (dBm) at target BERs of 10^{-6} as a function of the FSO link length (m) with equal signal and interferer FSO link lengths, l_{demux} = 15 dB.

Fig. 6 shows the upstream required transmitted optical power (dBm) at target BERs of 10^{-6} as a function of the FSO link length (m) with equal signal and interferer FSO link lengths, l_{demux} = 15 dB. It can be seen in both cases that, as the FSO link lengths and turbulence strength increase the ONU transmit power required to attain the target BER increase as well. Further, in the upstream the ONU transmit power can be up to 20 dB, which fulfills eye safety conditions for a C-band wavelength range [31], it can be seen that a FSO link length of about 2000 m can be used to achieve both target BER values for all atmospheric turbulence conditions with a single interferer.

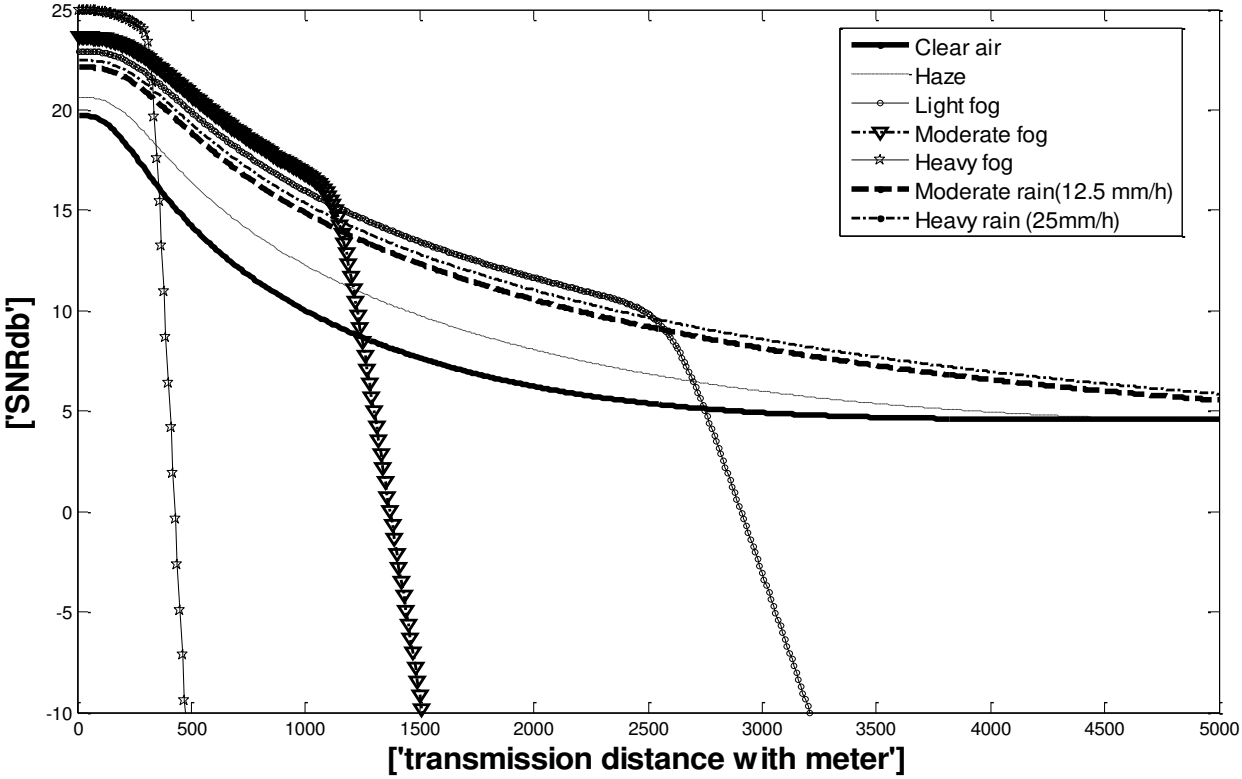

Fig. 7 The FSO link length Vs Signal-to-noise-ratio (SNR) at dB.

Table 2 The calculation results of Fig. 7 for the FSO link length and the signal-to-noise-ratio (SNR) at dB in the network structure.

C_n^2 (Refractive Index Structure)	Distance	SNR at dB	Atmosphere Turbulence
$5.0\ e^{-14}\ m^{-2/3}$	5 km	20 dB	Clear air
$1.7\ e^{-14}\ m^{-2/3}$	5 km	21 dB	Haze
$3.0\ e^{-15}\ m^{-2/3}$	3.3 km	23 dB	Light fog
$2.0\ e^{-15}\ m^{-2/3}$	1.5 km	24 dB	Moderate fog
$1.0\ e^{-15}\ m^{-2/3}$	0.5 km	25 dB	Heavy fog
$5.0\ e^{-15}\ m^{-2/3}$	5 km	22 dB	Moderate fog (12.5 mm/h)
$4.0\ e^{-15}\ m^{-2/3}$	5 km	23 dB	Heavy rain (2 mm/h)

8. FSO Link Performance under the Effect of Atmospheric Turbulence.

Atmospheric turbulence is known to cause signal fading in the channel. There are many different types of modulation schemes that are suitable for optical wireless communication systems. The effect of atmospheric turbulence-induced fading on the following techniques: On-Off Keying (OOK), Pulse Position Modulation (PPM), and phase-shift keying pre-modulated subcarrier intensity modulation. The classical modulation technique used for FSO is OOK [28]. This is primarily because of the simplicity of its design and implementation. The PPM requires no adaptive threshold and is predominantly used for deep space free-space optical communication links because of its enhanced power efficiency compared to the OOK signaling.

8.1. DPSK-Modulated Subcarrier

The DPSK pre-modulated SIM-FSO is demodulated by comparing the phase of the received signal in any signaling interval (with the phase of the signal received in the preceding signaling interval [28] as shown in Fig. 8. The demodulation of DPSK-based SIM-FSO is feasible during atmospheric turbulence because the turbulence coherence time, which is of the order of milliseconds, is far greater than the typical duration of two consecutive data symbols. This implies that the properties of the channels are fixed during a minimum of two symbol durations are prerequisites for non-coherent demodulation of the DPSK subcarrier signal.

The conditional BER of the DPSK pre-modulated subcarrier is given by [28].

$$P_{ec} = 0.5\exp((-0.5\gamma(I)) \quad 14$$

In the presence of scintillation, the following unconditional BER P_e is derived using the Gauss–Hermite quadrature integration approximation as written in [28].

$$\mathrm{P_{ec}} = \frac{1}{2\sqrt{\pi}}\sum_{\mathrm{i}=1}^{\mathrm{n}} \mathrm{w_i}\exp\big((-\mathrm{K\hat{}2}\exp\big[\mathrm{x_i}\,2\sqrt{2}\;\;\sigma_1 - \sigma_1^2\big]\,)\big)\,, \quad 15$$

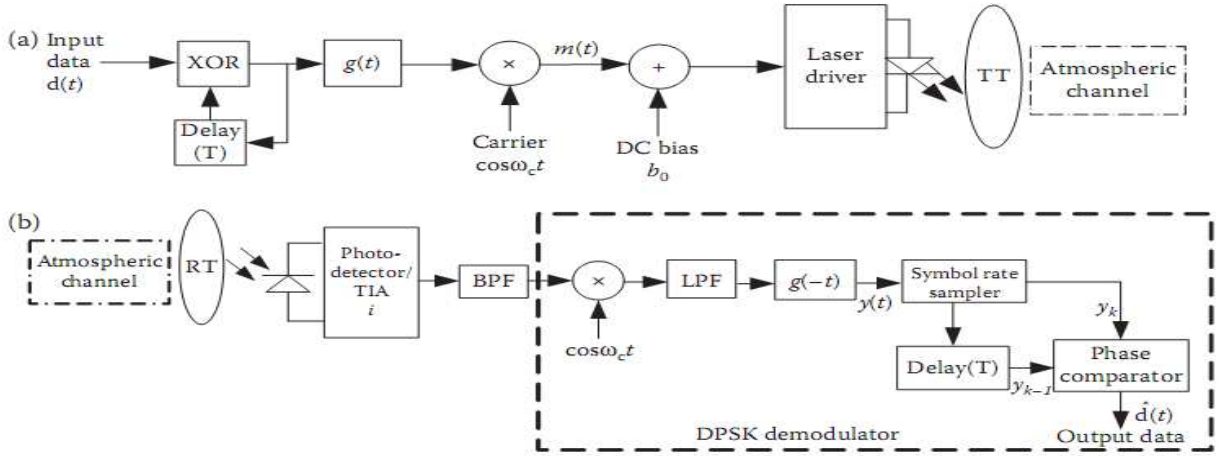

Fig. 8 Block diagram of an FSO link employing DPSK-modulated SIM for (a) Transmitter and (b) Receiver. TIP-trans-impedance amplifier; TT-transmitter.

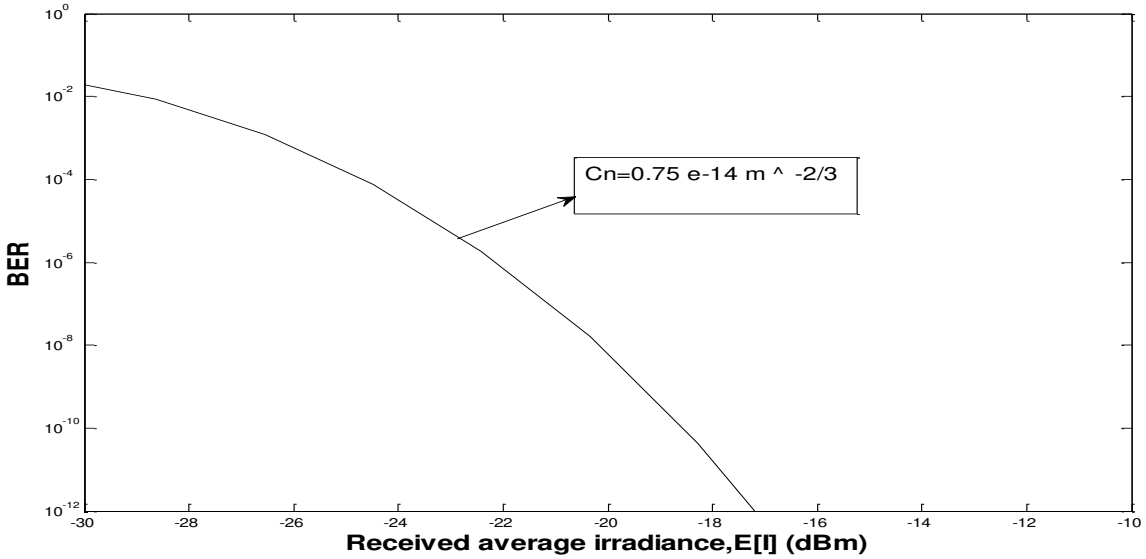

Fig. 9 BER against the received irradiance for SIM-FSO with different subcarrier modulation techniques in weak atmospheric turbulence for $\sigma_1^2 = 0.3$, $\lambda = 1550$ nm.

Here in Fig. 9, the BER of SIM-FSO based on different modulation techniques on the subcarrier is compared at a scintillation level of $\sigma_1^2 = 0.5^2$. The performance in a turbulence-free channel is included in the figure for the estimation of turbulence-induced fading penalty. The figure shows clearly the performance superiority of BPSK-modulated SIM in terms of the amount of SNR required to achieve a given BER Due to atmospheric turbulence-induced channel fading, a BPSK pre-modulated SIM-FSO system will incur a power penalty of ~ 5 dB at a BER of 10^{-6}; the penalty rises to ~ 10 dB when the error performance level is raised to a BER of 10^{-9}. This penalty is higher for other modulation techniques as shown in Fig. 9.

8.2. On-Off Keying

OOK is the dominant modulation scheme employed in commercial terrestrial wireless optical communication systems. This is primarily due to its simplicity and resilience to the innate nonlinearities of the laser and the external modulator. OOK can use either non-return-to-zero (NRZ) or return-to-zero (RZ) pulse formats. In NRZ-OOK, an optical pulse of peak power $\alpha_e P_T$ represents a digital symbol '0'while the transmission of an optical pulse of peak power P_T represents a digital symbol '1'. OOK is the most reported modulation technique for IM-DD in optical communication. A bit one is simply represented by an optical pulse that occupies the entire or part of the bit duration while a bit zero is represented by the absence of an optical pulse. In the NRZ scheme, a pulse with a duration equal to the bit duration is transmitted to represent while in the RZ scheme the pulse occupies only the partial duration of the bit. Fig. 10 shows the single mapping of OOK-NRZ and OOK-RZ with a duty cycle $\gamma = 0.5$ for average transmitted power of P_{avg} in [28] where the average energy per bit E_b is given by 17.

$$P_{e-bit-OOK} = Q\left[\sqrt{\frac{E_b}{N_0}}\right], \quad 16$$

$$E_b = \frac{E_P}{2} = 2\,(R_{PT})^2\,T_b \quad 17$$

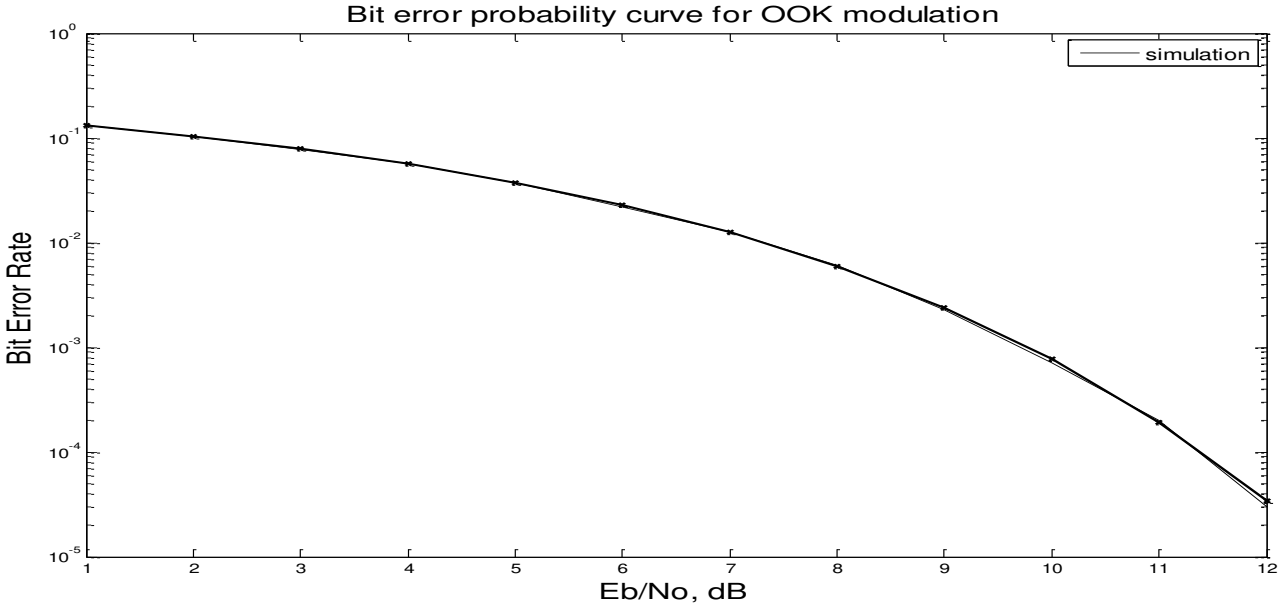

Fig. 10 Bit error rate probability curve for OOK Modulation.

This figure shows for a given value of P OOK-RZ $\gamma = 0.5$ has twice the ratio E_b/N_0 compared with OOK-NRZ, to achieve the same error performance, OOK-RZ, $\gamma = 0.5$ requires 3 dB less electrical power or 1.5 dB less average optical power compared with OOK-NRZ.

8.3. Pulse Position Modulation Scheme

In line-of-sight for the OWC links where the requirement for the bandwidth is not of major concern, PPM with its significantly better power efficiency seems to be the most attractive option for a range of applications PPM is an orthogonal modulation technique and a member of the pulse modulation family (see Fig. 11). The PPM modulation technique improves the power efficiency of OOK but at the expense of an increased bandwidth requirement and greater complexity. To achieve the same throughput as OOK, PPM slot duration $T_{s,PPM}$ is shorter than the OOK bit duration T_b by a factor L/M that is [28].

$$\mathbf{T_{s\_PPM}} = \frac{\mathbf{T_b M}}{\mathbf{L}} \qquad 18$$

The transmit pulse shape for L-PPM is given by [28].

$$x(t)_{PPM} = \left\{ \begin{array}{cc} 1 & \text{for } t \in \left[(m-1)T_{s_{PPM}}, mT_{s_{PPM}}\right] \\ 0 & \text{else where} \end{array} \right\}$$

Where $m \in \{1,2, \ldots . L\}$. 19

Hence, the PPM symbol sequence is given by [28].

$$\mathbf{x(t)_{PPM}} = \mathbf{LP_t} \sum_{\mathbf{k=0}}^{\mathbf{L-1}} \mathbf{C_k p}\left(\mathbf{t} - \frac{\mathbf{KT_{symb}}}{\mathbf{L}}\right) \qquad 20$$

Where $C_k \in \{c_0, c_1, c_2, \ldots . , c_L\}$ is the PPM symbol sequence, p (t) is the pulse shaping function of unity height and of duration T_{sysmb}/L, $T_{sysmb}(=T_bM)$ is the symbol interval and LP_{avg} is the peak optical power of PPM symbol.

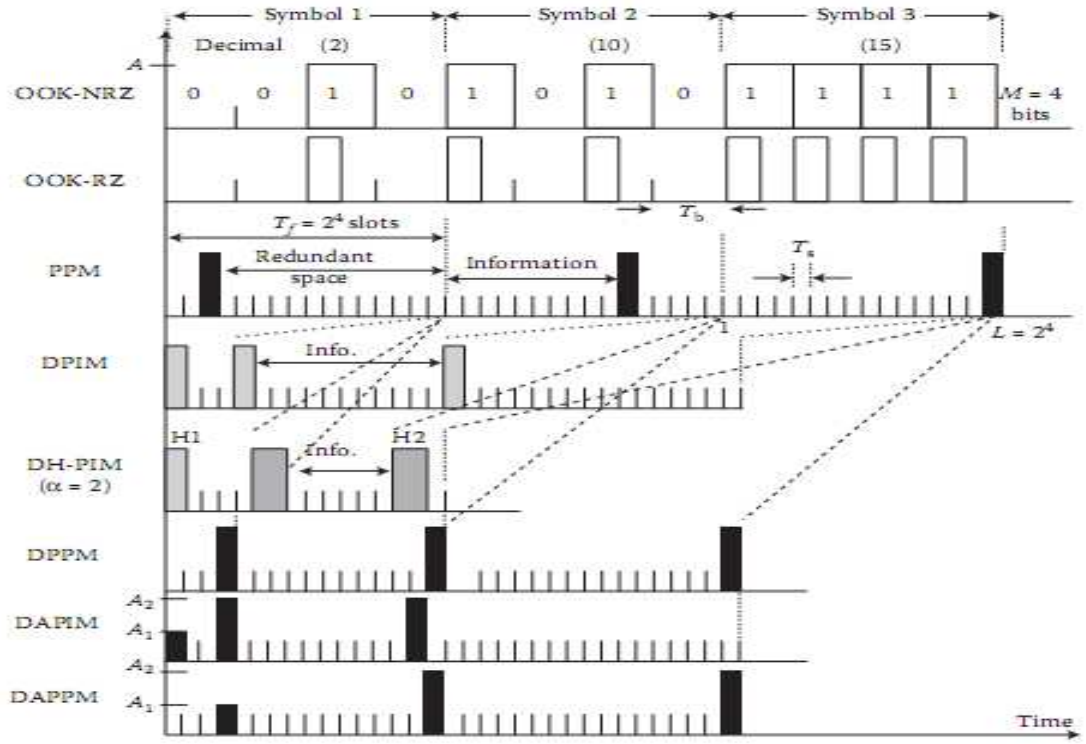

Fig. 11 Time waveforms for OOK, PPM, DPI, DH-PIM, DPPM, DAPIM and DAPPM signals.

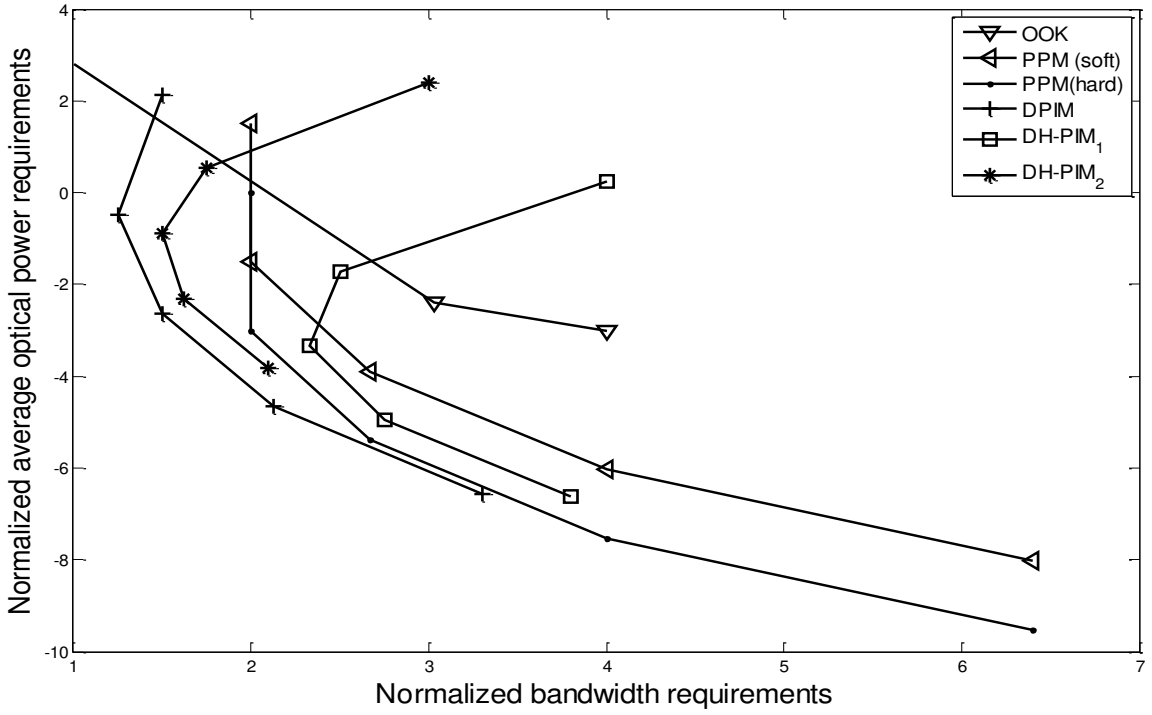

Fig. 12 Optical power requirement normalized to the OOK-NR versus bandwidth requirement normalized to the bit rate for OOK, PPM, PIM, DH-PIM$_1$ and DPIM$_2$, the numbers indicate the values of L.

Here in Fig. 12, the average optical power requirements and bandwidth requirements of OOK (NRZ and RZ), PPM, DPIM, and DH-PIM generated using Matlab. Figure 12 shows the trade-off between the bandwidth requirements and average power requirements. For OOK- RZ, the power requirements decrease with the duty cycle but the bandwidth increases. For PPM, DPIM, DH-PIM, average optical power requirements decrease as (average symbol length (L)) increase, however, the bandwidth requirements increase with L.

9. The Atmospheric Turbulence Models:

9.1. Log-Normal Turbulence Model

In describing the pdf of the irradiance fluctuation in a turbulence atmosphere, the beam is first represented by $\bar{E}$ Electric field as shown in Fig. 13

Figure 13 is shown log-normal pdf with E [I] =1 for a range of log irradiance variance σ_1^2.

$$E[I] = \frac{\sigma_1^2}{2} \qquad 21$$

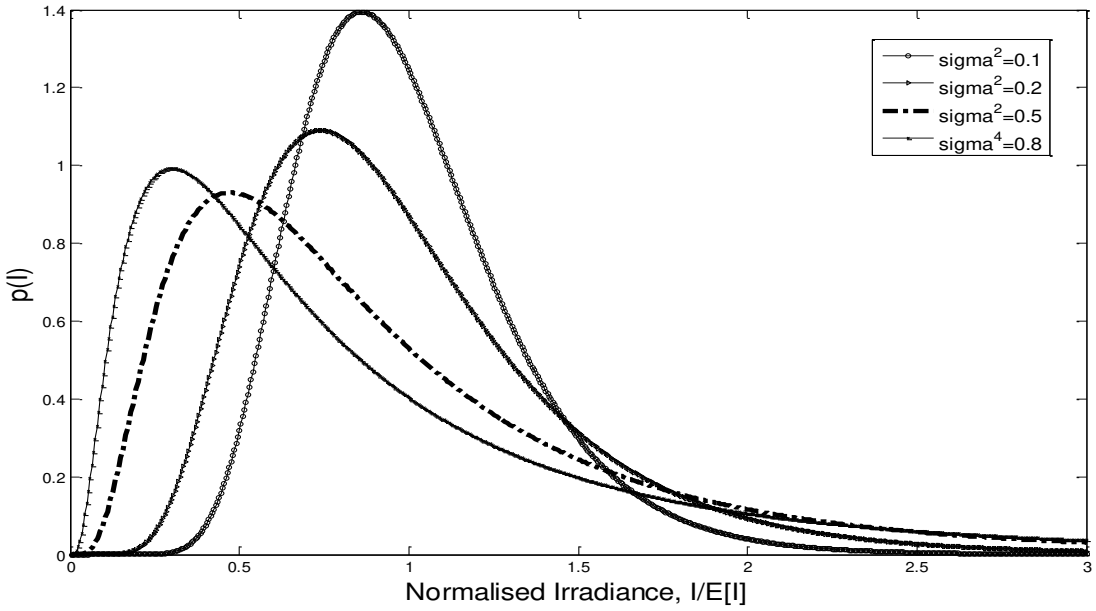

Fig. 13 Log-normal pdf with E [I] = 1 for a range of log irradiance variance σ_1^2.

The log-normal pdf is plotted in Fig. 13 for different values of log-irradiance variance of σ_1^2. As the value of σ_1^2 increases, the distribution becomes more skewed with tails in the infinity direction there is fluctuation of the irradiance.

9.2. Gamma-Gamma Turbulence Model

There is fluctuation of light radiation traversing a turbulent atmosphere is assumed to consist at small-scale (scattering) and large-scale (refraction) effects as shown in Fig. 14 as written in [27, 31]

$$\alpha = \left\{ \exp\left[\frac{0.49\sigma_{\mathrm{l}}^2}{(1+1.11\sigma_{\mathrm{l}}^{12/5})^{\frac{7}{6}}} \right] - 1 \right\}^{-1}, \quad 22$$

$$\beta = \left\{ \exp\left[\frac{0.51\sigma_{\mathrm{l}}^2}{1+0.69\sigma_{\mathrm{l}}^{12/5})^{5/6}} \right] - 1 \right\}^{-1}, \quad 23$$

$$\sigma_N^2 = \exp\left[\frac{0.49\sigma_{\mathrm{l}}^2}{(1+1.11\sigma_{\mathrm{l}}^{12/5})^{\frac{7}{6}}} + \frac{0.51\sigma_{\mathrm{l}}^2}{1+0.69\sigma_{\mathrm{l}}^{12/5})^{5/6}} \right] - 1 \quad 24$$

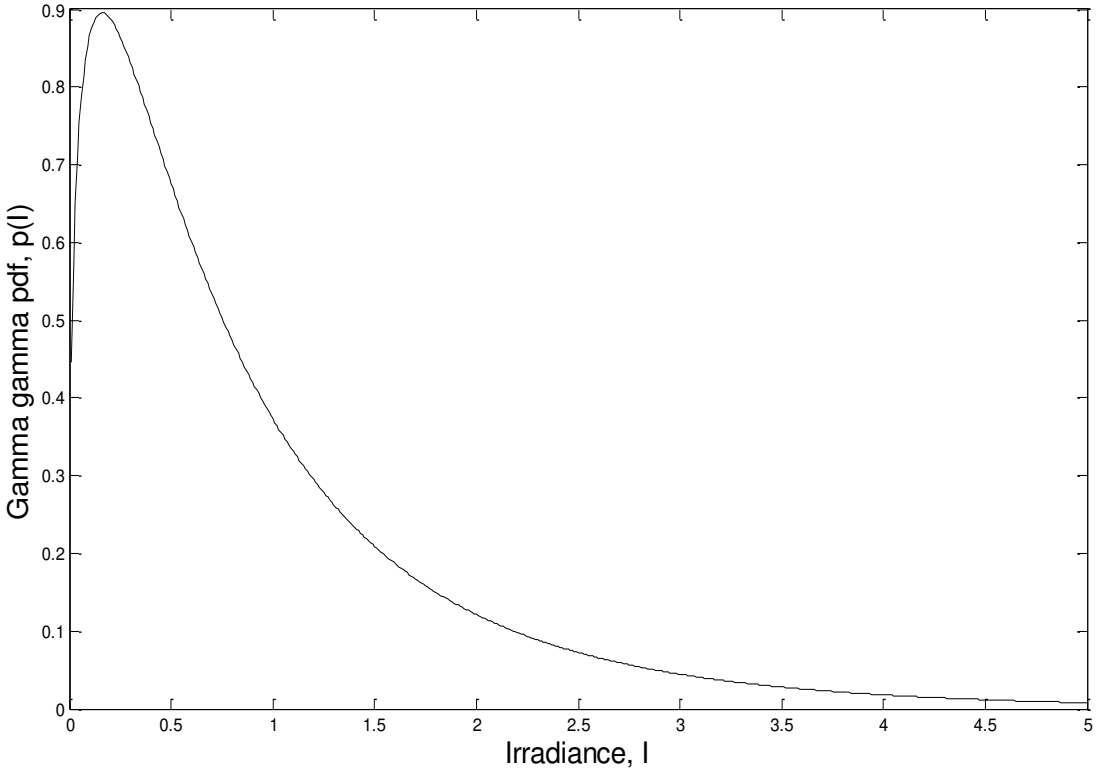

Fig. 14 Gamma–Gamma pdf for turbulence regime, strong $\alpha = 4.2, \beta = 1.4, \sigma_1^2 = 3.5$.

The plot shows that as the turbulence increases from the weak to the strong regime, the distribution spreads out more, with an increase in the range of possible values of the irradiance.

9.3. Analysis of the Atmospheric Turbulence

We analyze laser transfer turbulent atmosphere, spot scale, offset angle and light intensity fluctuation are related.

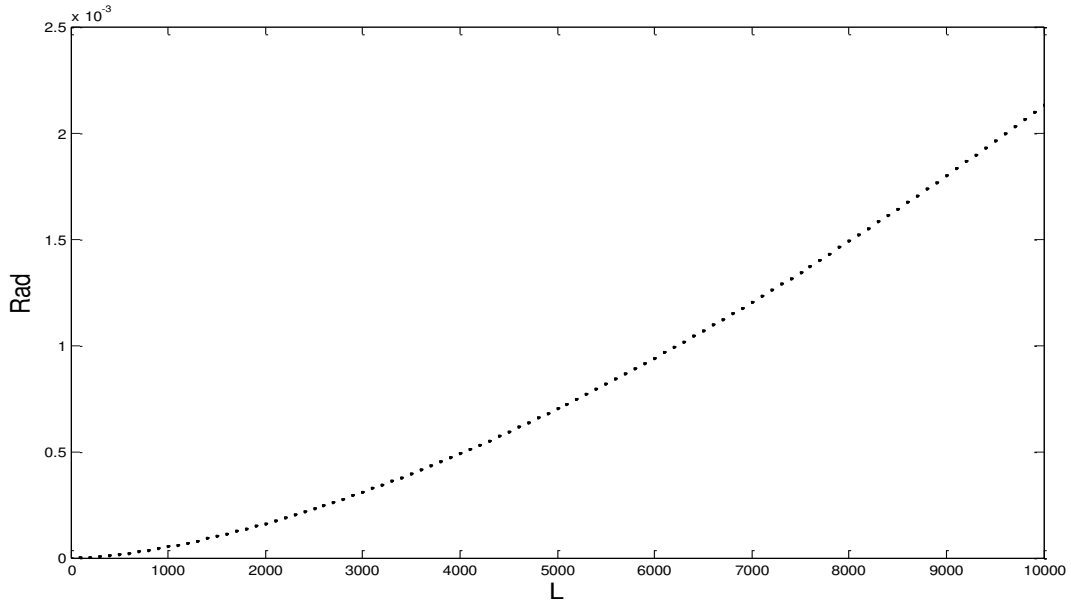

Fig. 15 FSO link length (L) vs Rad (beam divergence).

When the distance increases to 10 km, the beam divergence increase to (2×10^{-3}) rad. This system type would be required to have greater beam-widths to compensate for any motions due to buildings way. For systems with automatic pointing and tracking, the transmit divergence angle can be narrowed sufficiently with $<$ 1 mrad as shown in Fig. 15.

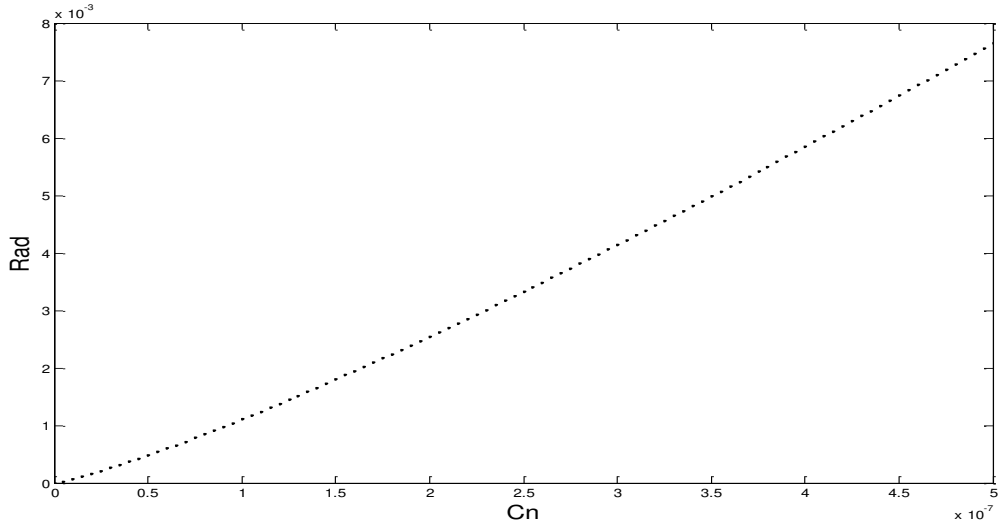

Fig. 16 Refraction Index Structure (Cn) vs beam divergence. When Cn is increasing, beam divergence is increasing.

Here in Fig. 16, the Cn = ($10^{-9}m^{-2/3}$), L =10 km.

$$\theta = 4.03 \times Cn^{5/6} \times 0.6328^{-1/5} \times l^{3/5} \quad (25)$$

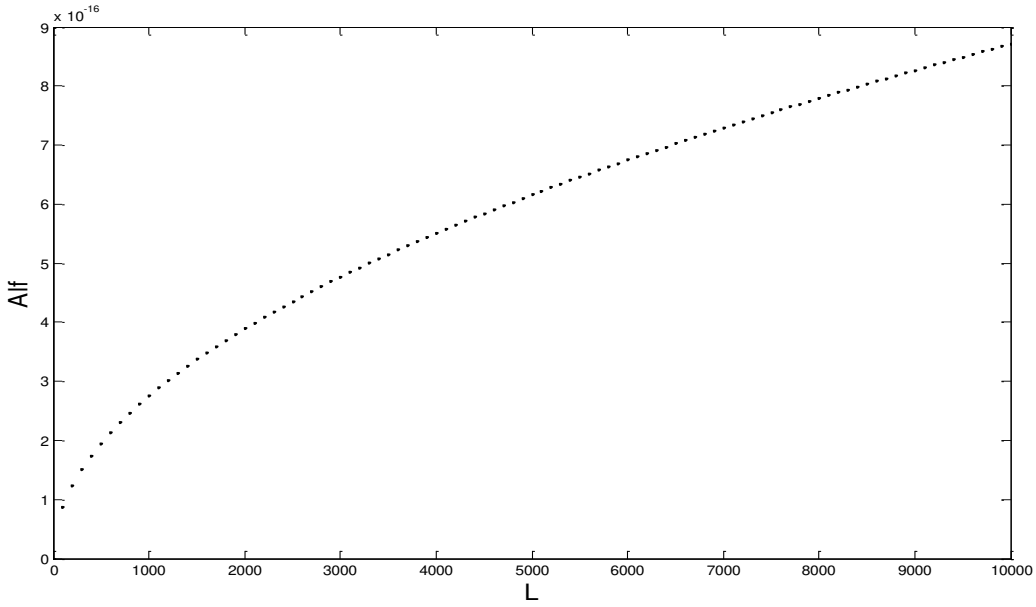

Fig. 17 FSO link length (L) vs Attenuation (α).

Attenuation is increased with longer distances. Here in Fig. 17, the Cn=$88 \times 10^{-9}m^{-2/3}$, L=10 km

$$\alpha = \sqrt{(1.75 \times Cn \times 1 \times 3.2^{-1/3}) \times 10^{-18}} \quad (26)$$

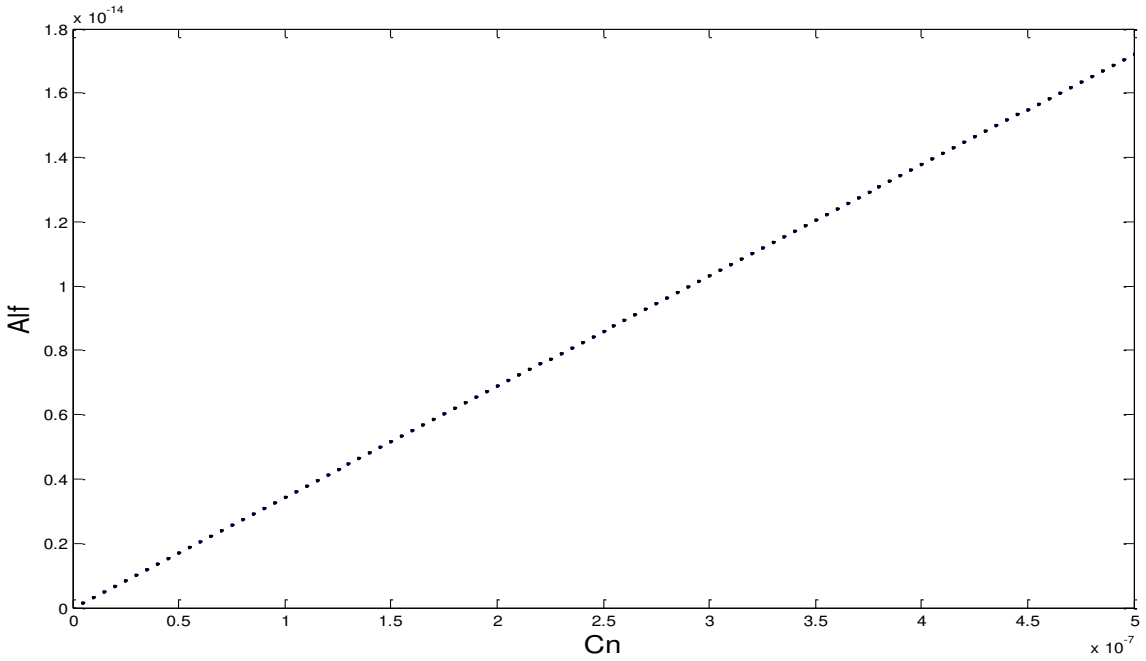

Fig. 18 Refractive Index Structure vs α (Attenuation).

Here in Fig. 18, the Cn is ($10^{-9}\ m^{-2/3}$), Attenuation is high when Cn is increase.

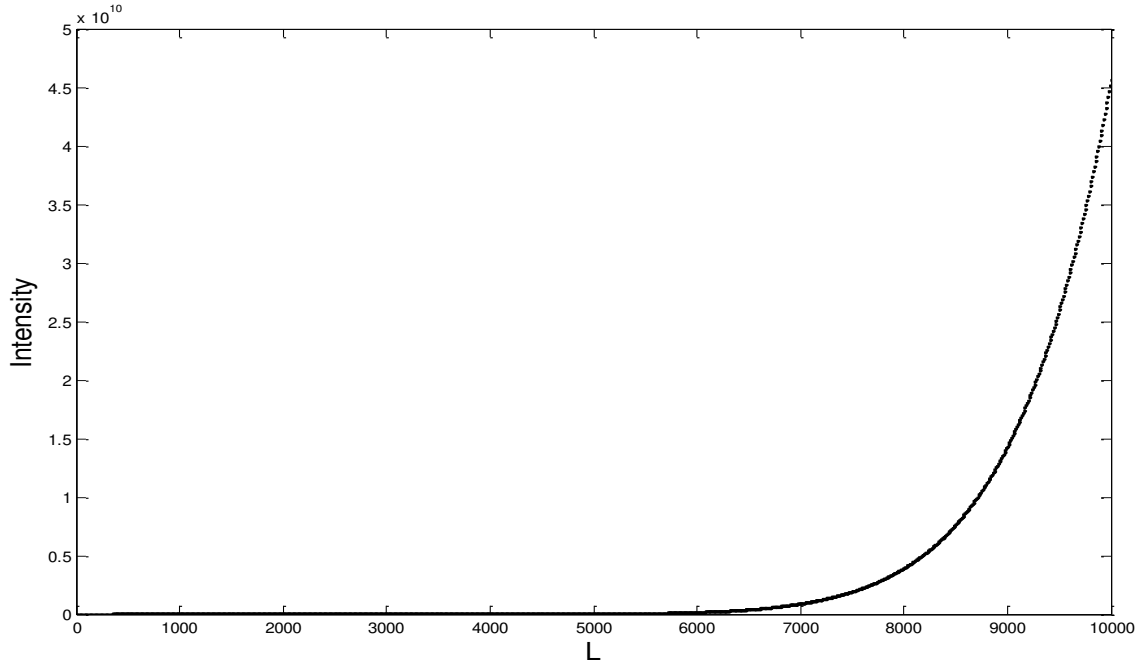

Fig. 19 FSO link length (L) vs Turbulence Intensity. Here in Fig. 19, the turbulence intensity is high when the L link is longer. B = 0.49, Cn = $10^{-9}\ m^{-2/3}$.

$$\text{I (Intensity)} = \text{B}\times \left(\frac{2\pi}{0.6328}\right)^{\frac{7}{6}} \times L^{11} \times Cn^2 \times 10^{-18} \qquad 27$$

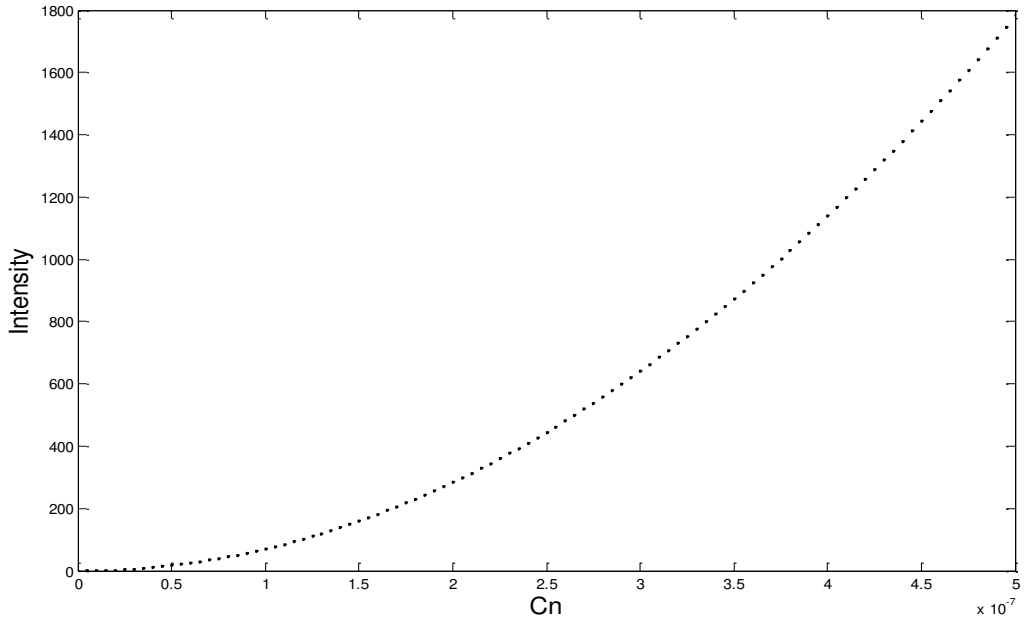

Fig. 20 Refractive Index Structure (Cn) vs Turbulence Intensity.

Refractive Index Structure (Cn) increase, Turbulence Intensity increase as shown in Fig. 20.

Cn ∝ I, Here Cn= $10^{-9}\ m^{-2/3}$

I (Intensity) = B× $(\frac{2\pi}{0.6328})^{7/6} \times L^{11} \times Cn^2 \times 10^{-18}$ 28

10. Wavelength-Division Multiplexing (WDM):

In fiber-optic communications, wavelength-division multiplexing (WDM) is a technology which multiplexes multiple optical carrier signals on a single optical fiber by using different wavelengths (colors) of laser light to carry different signals [32-42]. This allows for a multiplication in capacity, in addition to enabling bidirectional communications over one strand of fiber. This is a form of frequency division multiplexing (FDM) but is commonly called wavelength division multiplexing [32]. A WDM system uses a multiplexer at the transmitter to join the signals together, and a demultiplexer at the receiver to split them apart as shown in Fig. 21. With the right type of fiber, it is possible to have a device that does both simultaneously and can function as an optical add-drop multiplexer. The optical filtering devices used have traditionally been etalons, stable solid-state single-frequency Fabry-Perot interferometers in the form of thin-film-coated optical glass.

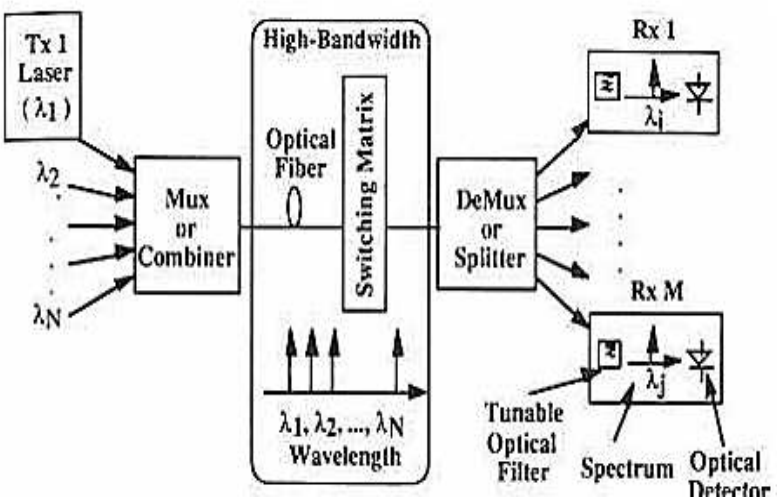

Fig. 21 Diagram of a Simple WDM System.

11. DWDM Systems:

Dense wavelength division multiplexing, or DWDM for short, refers originally to optical signals multiplexed within the 1550 nm band to leverage the capabilities (and cost) of erbium-doped fiber amplifiers (EDFAs) (see Fig. 22), which are effective for wavelengths between approximately 1525-1565 nm (C band), or 1570-1610 nm (L band) [33]. EDFAs were originally developed to replace SONET/SDH optical-electrical-optical (OEO) regenerators, which they have made practically obsolete. EDFAs can amplify any optical signal in their operating range, regardless of the modulated bit rate. In terms of multi-wavelength signals, so long as the EDFA has enough pump energy available to it, it can amplify as many optical signals as can be multiplexed into its amplification band (though signal densities are limited by choice of modulation format) [34-39]. EDFAs allow a single-channel optical link to be upgraded in bit rate by replacing only equipment at the ends of the link while retaining the existing EDFA or series of EDFAs through a long haul route. Furthermore, single-wavelength links using EDFAs can similarly be upgraded to WDM links at a reasonable cost. The EDFAs cost is thus leveraged across as many channels as can be multiplexed into the 1550 nm band [40-42].

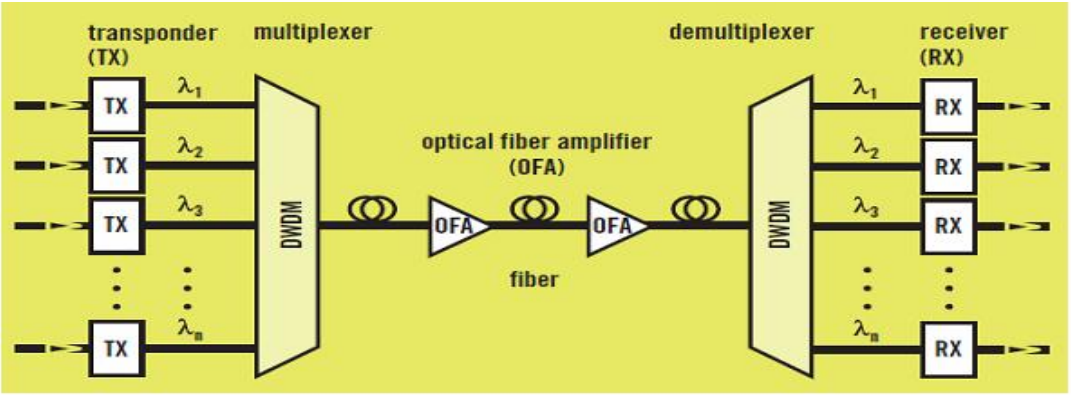

Fig. 22 Multichannel DWDM Transmission System.

12. Limitations of WDM:

Crosstalk will be one of the major limitations for the introduction of OXC in all-optical networks as shown in Fig. 23. Crosstalk occurs in devices that filter and separate wavelengths [35, 39-46].

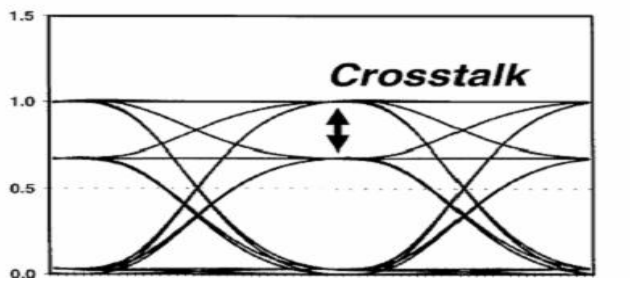

Fig. 23: Definition of Crosstalk.

The crosstalk within the same wavelength slot is called intra-band crosstalk. Moreover, In-band crosstalk can be divided into coherent crosstalk and incoherent crosstalk. Coherent crosstalk is that whose phase is correlated with the signal considered and incoherent crosstalk, whose phase is not correlated with the signal. On the other hand, Inter-band crosstalk is crosstalk situated in wavelengths outside the channel slot (wavelengths outside the optical bandwidth) and considered as a less severe phenomenon as shown in Fig. 24. However, in the DWDM technique this can be very predominant and degrades the network performance severely. The different classes of crosstalk are clarified in Fig. 25.

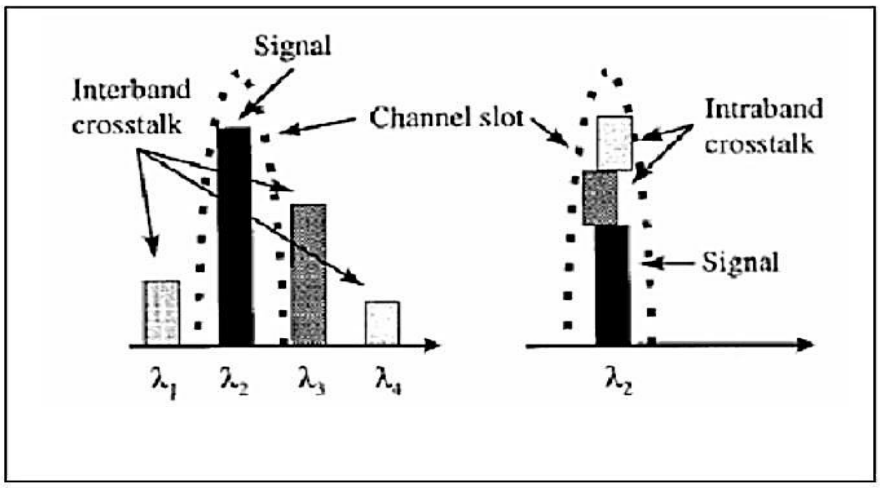

Fig. 24 Inter-band and intra-band crosstalk.

12.1 Types of Crosstalk :

a) Interband crosstalk: Interband crosstalk is the crosstalk situated in wavelengths outside the channel slot (wavelengths outside the optical bandwidth).

b) Intraband Crosstalk: The crosstalk within the same wavelength slot is called intraband crosstalk. It cannot be removed by an optical filter and therefore accumulates through the network.

13. Analysis of Crosstalk in WDM system:

a) WDM System Block Diagram

The OXC uses the N number of (M × 1) multiplexers and (1 × M) demultiplexers and the M number of (N × N) optical switches. The demultiplexer of OXC separates M wavelengths. The optical switch takes the N number of the same wavelength signals coming from all the N input fibers and routes each wavelength to any of the N output fibers according to the destination address. The multiplexer of OXC again combines M number of wavelengths and sends them to a single fiber. The output demultiplexer of Fig. 24 separates the M wavelengths and sends them to the individual user terminal.

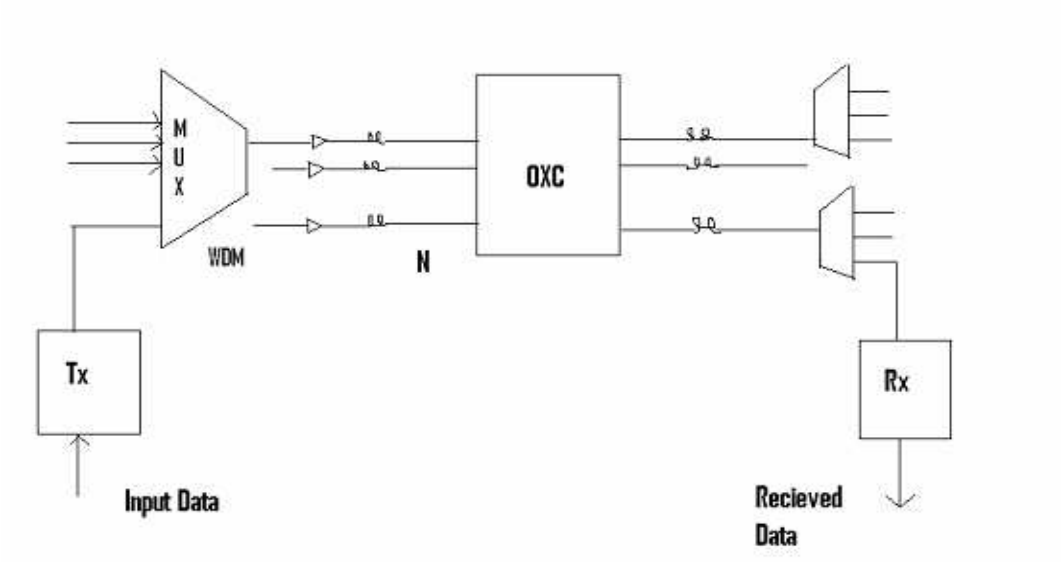

Fig. 25 Simple block design.

b) Analysis of Bit Error Rate without Crosstalk:

The BER can be calculated with and without Crosstalk using some equations. In this section, the ideal case is shown. So Crosstalk is taken to be zero. The equation for crosstalk is given in the next section. BER is the number of bit errors that occur within the space of one second. This measurement is one of the prime considerations in determining signal quality. The higher the data transmission rate the greater the standard.

BER can be calculated with and without Crosstalk using some equations.

$$BER = 0.5\ \mathrm{erfc}(Q/\sqrt{2}) \quad (29)$$

Here Q is a function proportional to the receiver signal-to-noise ratio (SNR).

It is expressed as [37].

$$Q=(R_b * P_s)\text{^}2/\sqrt{\sigma ase\text{^}2 + \sigma c\text{^}2)} \quad (30)$$

Rb = Bit Rate; in telecommunications and computing, bitrate (sometimes written bit rate, Ps = Signal power in dBm.

σc = Crosstalk.

σase = ASE (amplified spontaneous emission) noise-induced by parametric gain and spontaneous Raman scattering in optical fiber Ramen amplifier. βo = Band Width a measure of the width of a range of frequencies, measured in hertz. In the ideal case, σc = 0; which is with no cross talk, equation 30 becomes:

$$Q=(R_d \times P_s)\text{^}2/\sigma ase \qquad [\sigma c = 0 \text{ for ideal case}] \qquad 31$$

c) Analysis of Bit Error Rate with Crosstalk

In practical case zero crosstalk is not possible. So BER is calculated with equation 29 taking in the value of σc. Here Q is a function proportional to the receiver signal-to-noise ratio (SNR). It is expressed as equation 30.

14. Numerical Results and Discussions:

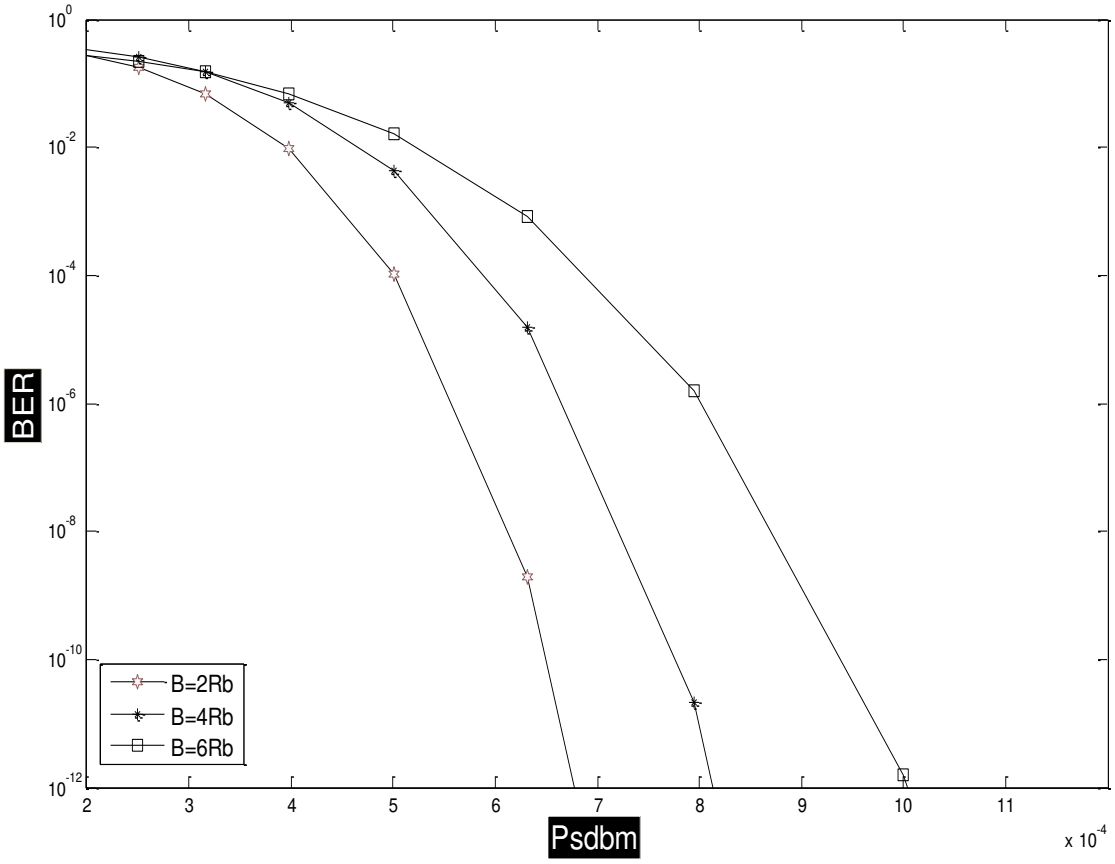

Fig. 26 BER vs input power for different Bandwidth.

The resulting graph Fig. 26 of the BER vs. the input power has plotted above. We have plotted this graph for three different bandwidths. It is seen that the BER increases with an increase in the input power. It is also shown that to use more

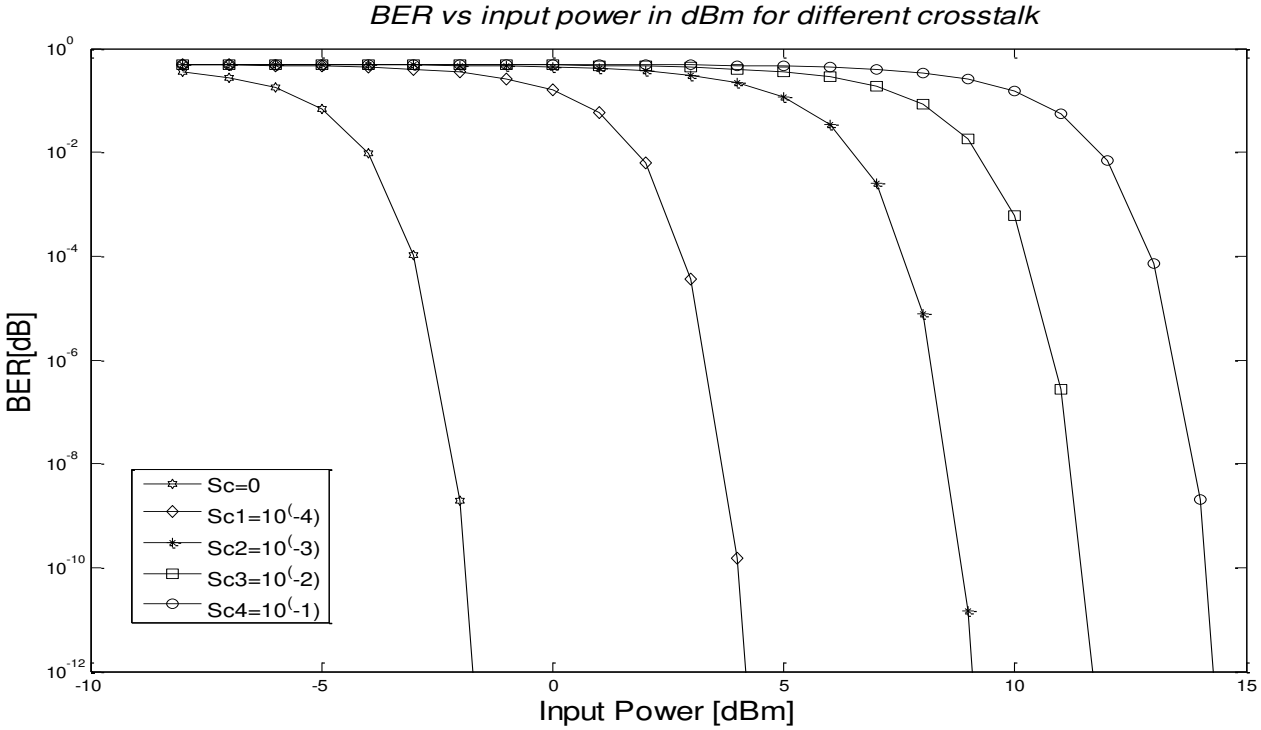

bandwidth we need more input power.

Fig. 27 BER vs input power in dBm for different crosstalk.

Here in Fig. 27, we show that BER increase for increasing crosstalk. For using more input power we get more crosstalk. For example, when 1.8 dBm is used as input power, the crosstalk is and for 9.1dBm input power, crosstalk is. At the same time, the BER is also increasing.

For using more input power we get more crosstalk. Fig. 28 shows the crosstalk plotted against the number of channel in a WDM system. Here we calculated crosstalk from the equation [29, 30] as written in [35-39].

$$\sigma^2 = \mathrm{M}.\mathrm{b}^2.{\mathrm{R}_\mathrm{d}}^2.{\mathrm{P}_\mathrm{S}}^2\left[2\acute{\varepsilon}_{adj} + (N-3)\acute{\varepsilon}_{nonadj} + X_{switch}\right] \quad 32$$

ɛ́ad = Effective adjacent channel crosstalk.

ɛ́nonad = Effective Non-adjacent channel crosstalk.

Xswitch = Crosstalk value (in linear units) of the optical switch fabric.

Where, M= number of hop.

b= bit ratio of signal peak power.

R= detector resistance.

Ps= input power.

ε = effective adjacent and effective non-adjacent.

N= number of channels.

X= switch.

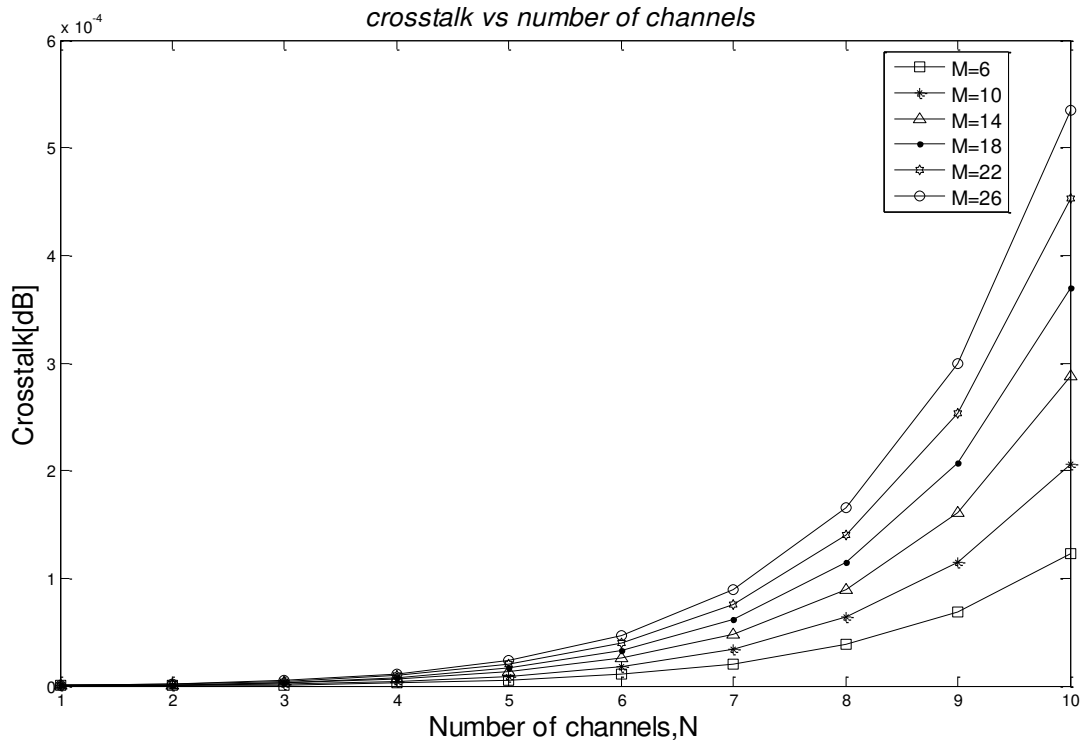

Fig. 28 Crosstalk vs the number of channels.

It can be said that if we increase the number of hop then crosstalk also increases.

Values taken for Fig. 28:

b = 1

R=0.85

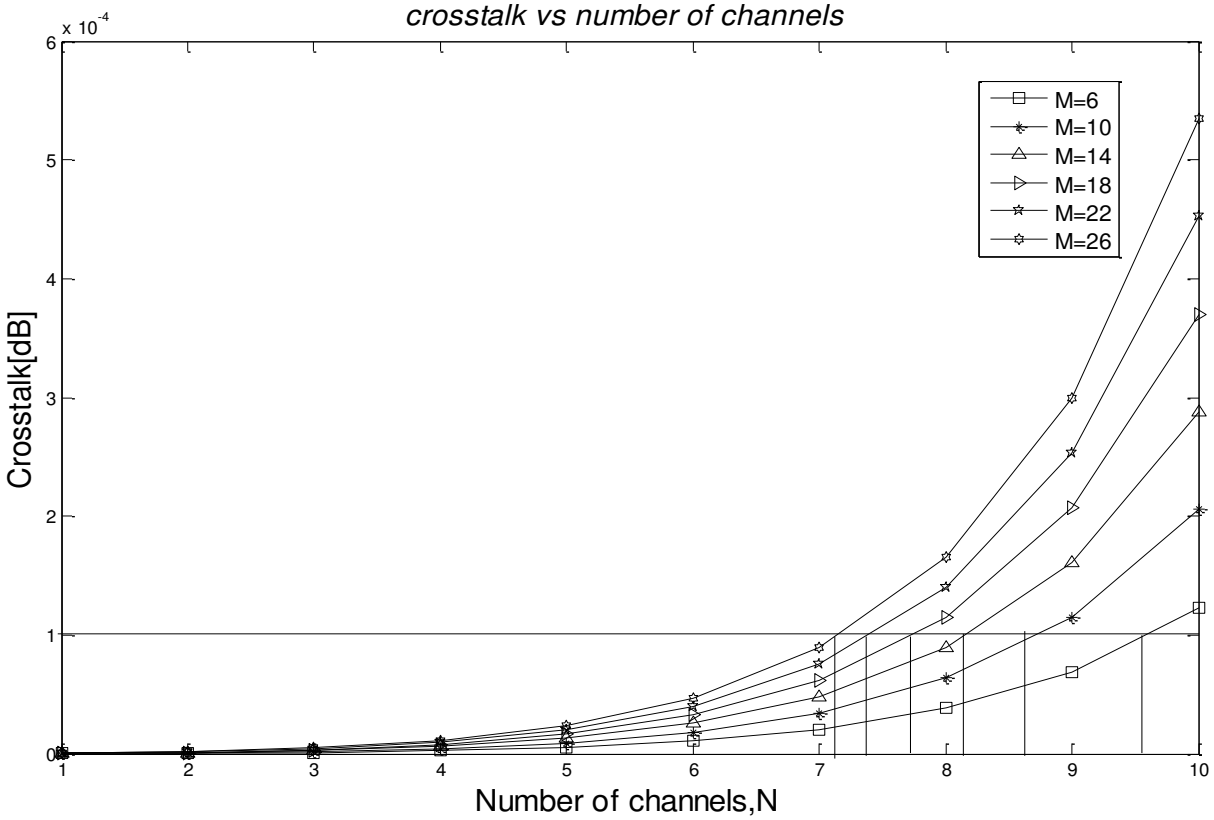

Fig. 29 The number of channels and hops for related crosstalk.

For this graph in Fig. 29, we can find out the number of channels and hops for related crosstalk. For example for power penalty 8.1dB we got the corresponding crosstalk to be -40dB which is 10^{-4}. From the above graph, we can find combinations of hops and channels. Here, the combinations are :

Hoops	Channels
6	9.7 = 10(approx.)
10	8.6 = 9 (approx.)
14	8.1 = 8 (approx.)
18	7.8 = 8 (approx.)
22	7.4 = 7 (approx.)
26	7.1 = 7 (approx.)

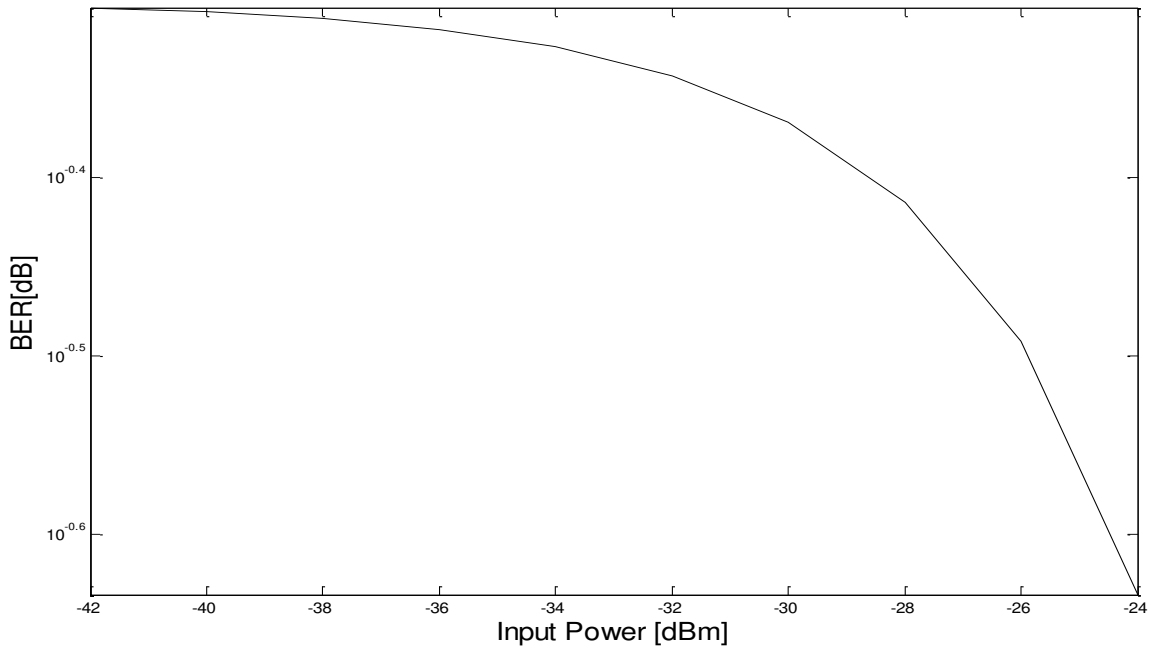

Fig. 30 BER for with crosstalk.

Fig. 30 shows the plotting of the BER corresponding to the BER with crosstalk The graph shows that BER is minimum when there is no crosstalk.

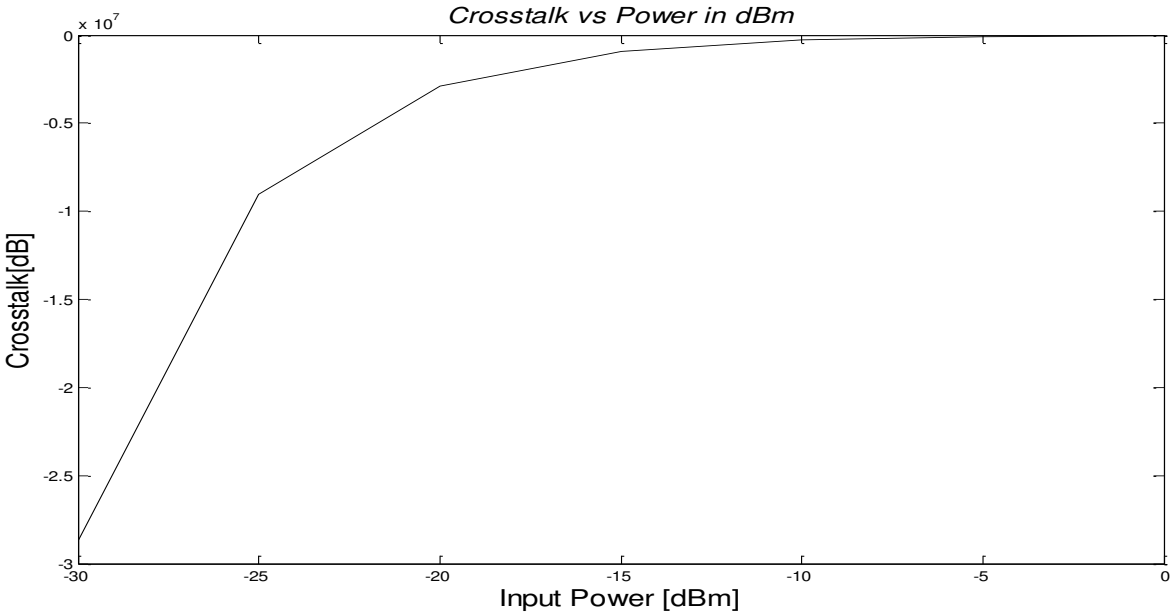

Fig. 31 Topology 1: Crosstalk for various input power.

For this topology in Fig. 31, we assumed -30 dB input power and increased it significantly. the graph shows us that when input power is getting greater, the crosstalk is increasing slightly.

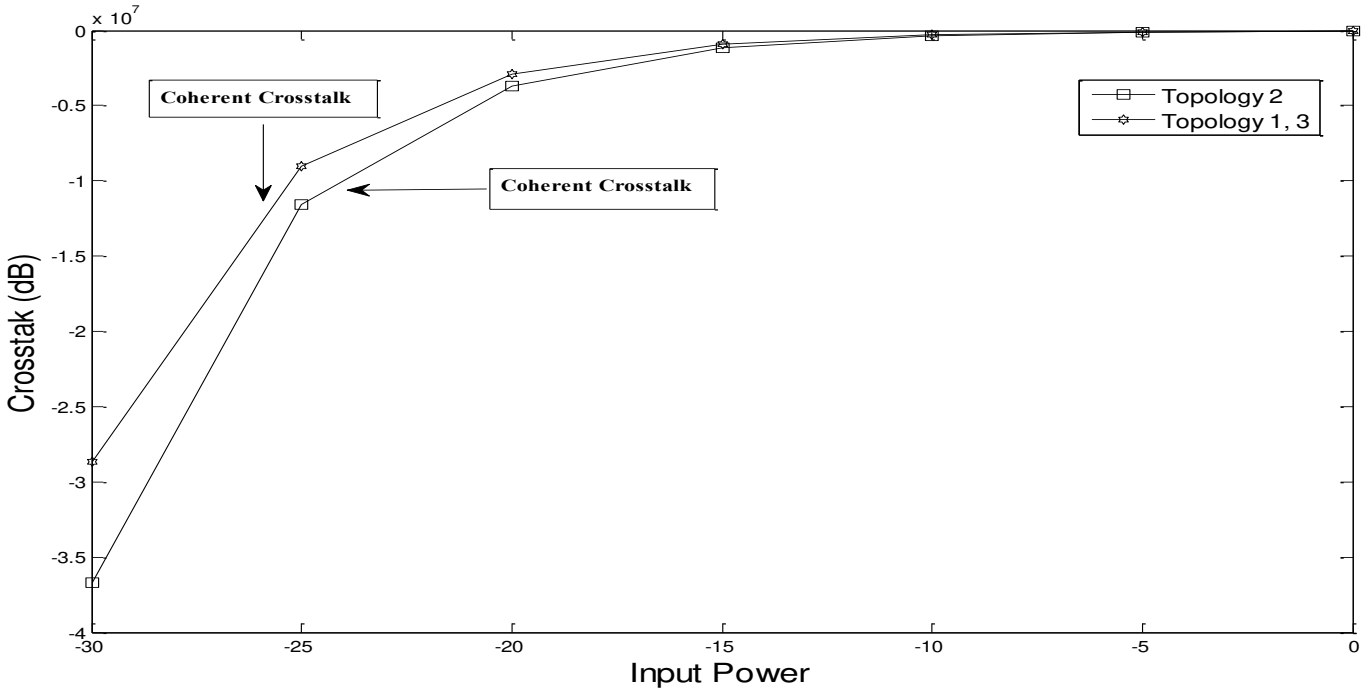

Fig. 32 Crosstalk (coherent) in the function of the number of OXC's cascaded for three topologies. The highest crosstalk is obtained for the first and second topologies. Both topologies perform equally. The better performance is shown by the second topology. Due to the low crosstalk values of the space switch as shown in Fig. 32.

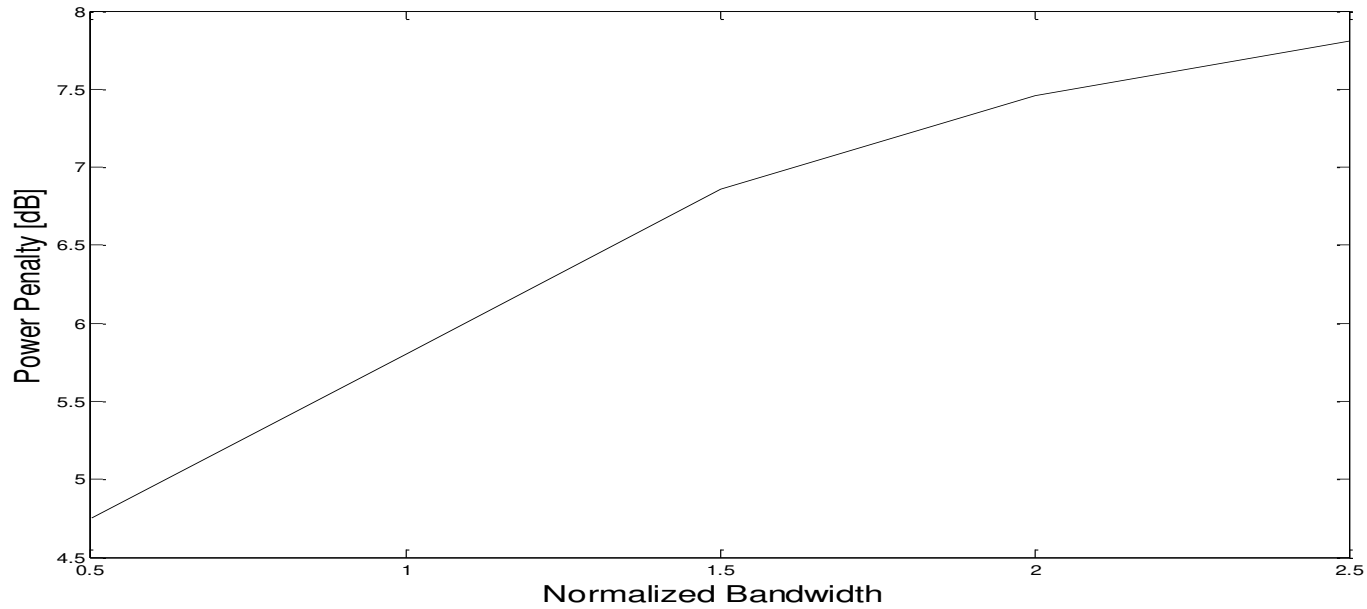

Fig. 33: Power penalty (at BER=10^{-12}) versus channel spacing with crosstalk for a bit rate of 4.5 Gb/ps.

- This curve from Fig. 33 is calculated from the BER curve with crosstalk. The difference between BER with crosstalk and BER without crosstalk at the BER of 10^{-12}. The result shows that the power penalty increases with decreasing channel spacing.
- The power penalty can be defined as the increase in signal power required (in dB) to maintain the same BER in the presence of impairments.

15. Conclusion and Future works:

We analyzed a hybrid fiber and DWDM-FSO/PON network and the effects of turbulence-accentuated interchannel crosstalk, it could be seen that DPPM systems required lower optical power compared to the OOK systems. It can be deduced from this analysis the interchannel crosstalk,turbulence-induced scintillation, and ASE noises are dominant causes of system degradation, especially in the upstream transmission, causing the BER to increase by several orders of magnitude and also we have used some basic equations to optimize the relation between hoops and channels. No new equation was derived or used to form this relationship. The figures were plotted manually using the graphs plotted with the basic equations of BER and Crosstalk in Matlab software. At the first, a graph for BER vs. the input power was plotted using the BER equation. Then a graph of crosstalk vs. number of channels was plotted for a different number of hops. From this graph, the power penalty was found out. This power penalty was used to plot a graph of the power penalty vs. the crosstalk. Work can be carried out to evaluate the performance of a WDM system with bi-directional OXC and find the limitations due to crosstalk and optimum system parameters.

References

[1] C. H. Lee, W. V. Sorin, and B. Y. Kim, "Fiber to the home using a PON infrastructure," Journal of Lightwave Technology, vol. 24, pp. 4568-4583, 2006.

[2] J. Prat, Next-generation FTTH passive optical networks: research towards unlimited bandwidth access, Springer Science, 2008.

[3] S. Bloom, E. Korevaar, J. Schuster, and H. A. Willebrand, "Understanding the performance of free-space optics," Journal of Optical Networking, vol. 2, pp. 178-200, June 2003.

[4] D. O. Caplan, "Laser communication transmitter and receiver design," Journal of Optical Fibre Communication Report, vol. 4, pp. 225-362, 2007.

[5] T. H. Carbonneau and D. R. Wisely, "Opportunities and challenges for optical wireless; the competitive advantage of free space telecommunications links in today's crowded marketplace," Proc. SPIE Wireless Technologies and Systems: Millimeter-Wave and Optical, vol. 3232, pp. 119-128, January 1998.

[6] D. Killinger, "Free space optics for laser communication through the air," Optics and Photonics News, vol. 13, pp. 36-42, October 2002.

[7] S. Karp, R. M. Gagliardi, S. E. Moran, and L. B. Stotts, Optical channels: fibers, clouds, water and the atmosphere, New York: Plenum Press, 1988.

[8] R. Ramaswami and K. N. Sivarajan, Optical networks-a pratical perspective, Second Edition, Academic Press, London, 2002.

[9] R. P. Davey, D. B. Grossman, M. Rasztovits-Wiech, D. B. Payne, D. Nesset, A. E. Kelly, A. Rafel, S. Appathurai, and S. Yang, "Long-reach passive optical networks," Journal of Lightwave Technology, vol. 27, pp. 273-291, Feb. 2009.

[10] E. Ciaramella, Y. Arimoto, G. Contestabile, M. Presi, A. D'Errico, V. Guarino, and M. Matsumoto, "1.28 terabit/s (32x40 Gbit/s) WDM transmission system for free space optical communications," IEEE Journal on Selected Areas in Communications, vol. 27, pp. 1639-1645, 2009.

[11] L. Kazovsky, W. Shing-Wa, T. Ayhan, K. M. Albeyoglu, M. R. N. Ribeiro, and A. Shastri, "Hybrid optical wireless access networks," Proceedings of the IEEE, vol. 100, pp. 1197-1225, 2012.

[12] E. S. Son, K. H. Han, J. H. Lee, and Y. C. Chung, "Survivable network architectures for WDM PON," Optical Fiber Communication Conference (OFC), Anaheim, California, Mar., 2005.

[13] E. Leitgeb, M. Gedhart, and U. Birnbacher, "Optical networks, last mile access and applications," J. Opt. Fiber Commun., pp. 56-85, 2005.

[14] A. K. Majumdar, "Free-space laser communication performance in the atmospheric channel," Journal of Optical and Fiber Communications Research, vol. 2, pp. 345-396, 2005.

[15] J. C. Ricklin, S. M. Hammel, F. D. Eaton, and S. L. Lachinova, "Atmospheric channel effects on free-space laser communication," J.Opt. Fiber Commun., vol. 3, pp. 111-158, 2006.

[16] H. A. Willebrand and B. S. Ghuman, Free-space optics: enabling optical connectivity in today's networks, Sams Publishing, Indianapolis, Indiana 46240 USA, 2002.

[17] L. C. Andrews and R. L. Phillips, Laser beam propagation through random media, Second Edition, SPIE Press, Bellingham, Washington, 2005.

[18] E. Korevaar, I. Kim, and B. McArthur, "Atmospheric propagation characteristics of highest importance to commercial free space optics," Proc. of SPIE, San Diego, CA, vol. 4976, pp. 1-12, 2003.

[19] T. Kamalakis, I. Neokosmidis, A. Tsipouras, S. Pantazis, and I. Andrikopoulos, "Hybrid free space optical / millimeter wave outdoor links for broadband wireless access networks," IEEE 18th International Symposium on Personal, Indoor and Mobile Radio Communications, 2007, pp. 1-5.

[20] M. Abtahi, P. Lemieux, W. Mathlouthi, and L. A. Rusch, "Suppression of turbulence-induced scintillation in free-space optical communication systems using saturated optical amplifiers," Journal of Lightwave Technology, vol. 24, pp. 4966-4973, 2006.

[21] A. O. Aladeloba, A. J. Phillips, and M. S. Woolfson, "Improved bit error rate evaluation for optically pre-amplified free-space optical communication systems in turbulent atmosphere," IET Optoelectronics, vol. 6, pp. 26-33, February 2012.

[22] M. Razavi and J. H. Shapiro, "Wireless optical communications via diversity reception and optical preamplification," IEEE Transactions on Wireless Communications, vol. 4, pp. 975-983, 2005.

[23] A. J. Phillips, J. M. Senior, R. Mercinelli, M. Valvo, P. J. Vetter, C. M. Martin, M. O. Van Deventer, P. Vaes, and X. Z. Qiu,"Redundancy strategies for a high splitting optically amplified passive optical network,"Journal of Lightwave Technology, vol. 19, pp. 137-149, 2001.

[24] I. T. Monroy and E. Tangdiongga, Crosstalk in WDM communication networks, Kluwer Academic Publishers, Norwell, Massachusetts, USA, 2002.

[25] D. M. Forin, S. Di Bartolo, G. M. Toshi Beleffi, F. Curti, G. Cincotti, A. Vecchi, S. Ragana, and A. L. J. Teixeira, "Giga ethernet free-space passive optical networks," Fibre and Integrated Optics, vol. 27, pp. 229-236, April 2008.

[26] K. Wang, A. Nirmalathas, C. Lim, and E. Skafidas, "4X12.5 Gb/s WDM Optical Wireless Communication System for Indoor Applications," Journal of Lightwave Technology, vol. 29, pp. 1988-1996, July 2011.

[27] Ebrahim E. Elsayed, Bedir B. Yousif, and Mahmoud M. Alzalabani, "Performance enhancement of the power penalty in DWDM FSO communication using DPPM and OOK modulation", Optical and Quantum Electronics, vol. 50 (7), pp. 282, (26 June 2018).

[28] Optical Wireless Communications System and Channel Modelling with MATLAB® Z. GhassemlooyW. PopoolaS. Rajbhandari 2008, CRC PressTaylor & Francis Group6000 Broken Sound Parkway NW, Suite 300

Boca Raton, FL 33487-2742© 2013 by Taylor & Francis Group, LLC CRC Press is an imprint of Taylor & Francis Group, an Informa business. International Standard Book Number-13: 978-1-4398-5235-4 (eBook - PDF).

[29] Y. Dikmelik and F. M. Davidson, "Fiber-coupling efficiency for free-space optical communication through atmospheric turbulence," Applied Optics, vol. 44, 10 August 2005.

[30] F. S. Vetelino, C. Young, L. Andrews, and J. Recolons, "Aperture averaging effects on the probability density of irradiance fluctuations in moderate-to-strong turbulence," Applied Optics, vol. 46, pp. 2099-2108, April 2007.

[31] A. O. Aladeloba, A. J. Phillips, and M. S. Woolfson, "DPPM FSO communication systems impaired by turbulence, pointing error and ASE noise," 14th International Conference on Transparent Optical Networks (ICTON), 2012, pp. 1-4.

[32] Bobby Barna, Monirnl Islam, “Evaluate the Effect of Stimulated Raman Scattering in DWDM Transmission System with Direct Detection Binary WSK Receiver” IEEE/OSA/IAPR International Conference on Infonnatics, Electronics & Vision ICIEV 2012.

[33] K, A Taher, "Minimization of the effect of Cross Phase Modulation in a WDM Optical Transmission System", M,Sc,Thesis, dept. of EEE, BUET, 2005.

[34] E. Iannone, and R. Sabella, “Optical path technologies: A comparison among different cross-connect architectures,” J. Lightwave Technol., vol. 14, no. 10, pp. 2184 - 2194, Oct. 1996.

[35] H. Takahashi, K. Oda, and H. Toba, “Impact of crosstalk in an arrayed waveguide multiplexer on N×N optical interconnection," J. Lightwave Technol., vol. 14, no. 6, pp. 1120 - 1126, June 1996.

[36] S. D. Dods, J. P. R. Lacey, and R. S.Tucker, “Homodyne crosstalk in WDM ring and bus networks,” IEEE Photon.Technol. Lett., vol. 10, no. 3, pp. 457 - 458, Mar. 1998.

[37] K. P. Ho, C. K. Chan, F. Tong, and L. K. Chen, “Exact analysis of homodyne crosstalk induced penalty in WDM networks,” IEEE photon. Technol. Lett., vol. 9, no. 3, pp. 1285 - 1287, Sept. 1997.

[38] S. D. Dods, J. P. R. Lacey, and R.S. Tucker, “Performance of WDM ring and bus network in the presence of homodyne crosstalk,” J. Lightwave Technol., vol. 17, no. 3, pp. 388 - 396, Mar. 1999.

[39] Y. Shen, K. Lu, and W. Gu, “Coherent and incoherent crosstalk in WDM optical networks," J. Lightwave Technol., vol. 17, no. 5, pp. 759 - 764, May 1999.

[40] C. Chen, H. Yang, H. Jiang, J. Fan, C. Han, and Y. Ding, "Mitigation of Turbulence-Induced Scintillation Noise in Free-Space Optical Communication Links Using Kalman Filter," IEEE Congress on Image and Signal Processing, Hainan, China, vol. 5, pp. 470-473, May 2008.

[41] Ebrahim E. Elsayed and Bedir B. Yousif, "Performance enhancement of M-ary pulse-position modulation for a wavelength division multiplexing free-space optical systems impaired by interchannel crosstalk, pointing error, and ASE noise", Optics Communications, vol. 475, pp. 126219, (15 November 2020).

[42] E. E. Elsayed and B. B. Yousif, “Performance evaluation and enhancement of the modified OOK based IM/DD techniques for hybrid fiber/FSO communication over WDM-PON systems,” *Opt. Quantum Electron.*, vol. 52, no. 9, 2020, doi: 10.1007/s11082-020-02497-0.

[43] B. B. Yousif, E. E. Elsayed, and M. M. Alzalabani, “Atmospheric turbulence mitigation using spatial mode multiplexing and modified pulse

position modulation in hybrid RF/FSO orbital-angular-momentum multiplexed based on MIMO wireless communications system," *Opt. Commun.*, vol. 436, pp. 197–208, 2019, doi: 10.1016/j.optcom.2018.12.034.

[44] Ebrahim E. Elsayed and Bedir B. Yousif, "Performance enhancement of the average spectral efficiency using an aperture averaging and spatial-coherence diversity based on the modified-PPM modulation for MISO FSO links", Optics Communications, vol. 463, pp. 125463, (15 May 2020).

[45] E. E. Elsayed and B. B. Yousif, "Performance enhancement of hybrid diversity for M-ary modified pulse-position modulation and spatial modulation of MIMO-FSO systems under the atmospheric turbulence effects with geometric spreading," *Opt. Quantum Electron.*, vol. 52, no. 12, 2020, doi: 10.1007/s11082-020-02612-1.

[46] B. B. Yousif and E. E. Elsayed, "Performance Enhancement of an Orbital-Angular-Momentum-Multiplexed Free-Space Optical Link under Atmospheric Turbulence Effects Using Spatial-Mode Multiplexing and Hybrid Diversity Based on Adaptive MIMO Equalization," *IEEE Access*, vol. 7, pp. 84401–84412, 2019, doi: 10.1109/ACCESS.2019.2924531.

Compliance with Ethical Standards

Conflict of interest: The author declares that there is no conflict of interest regarding the manuscript. The author is responsible for the content and writing of this article. The author declares that he has no known competing financial interests or personal relationships that could have appeared to influence the work reported in this paper.

Figures

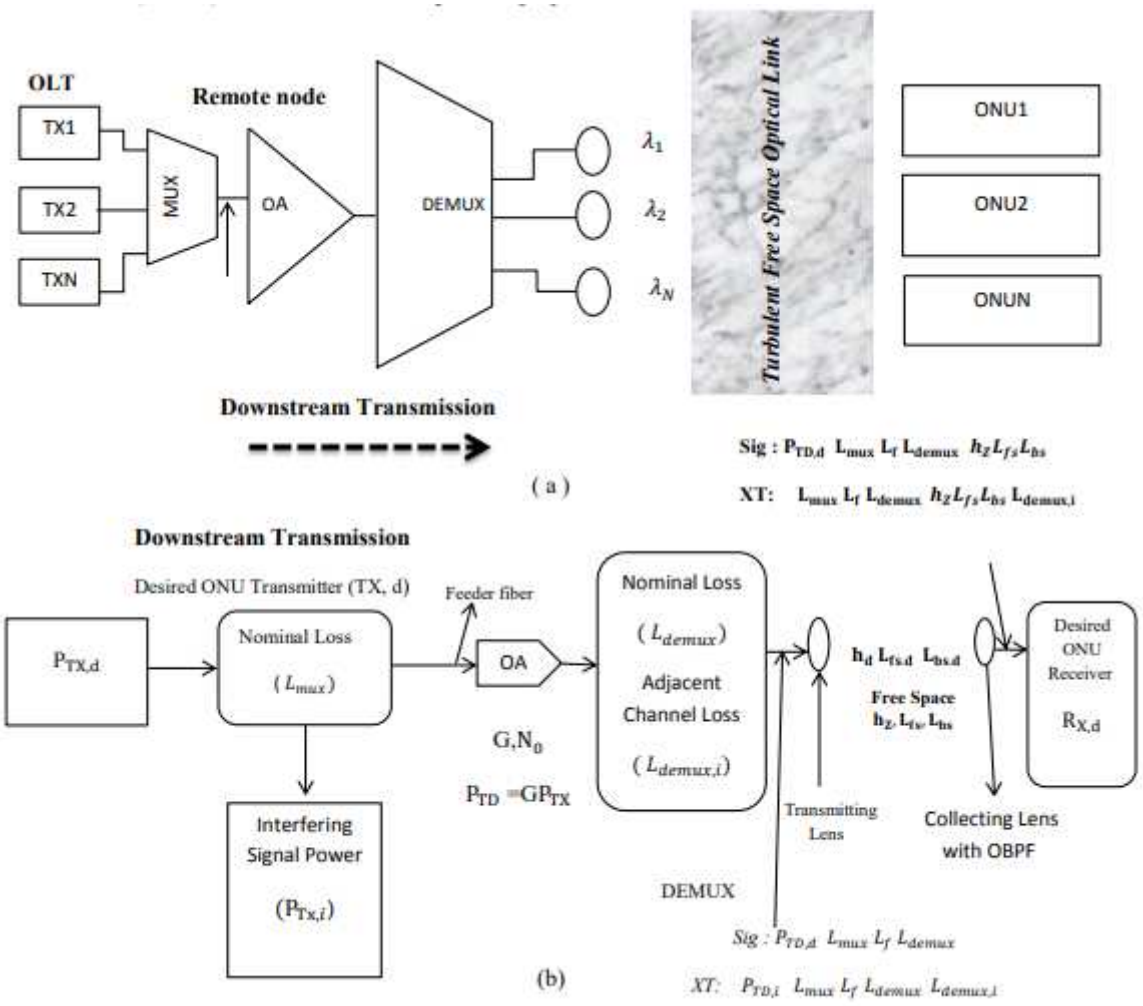

Figure 1

Optically Pre-amplified WDM DPPM Network: a) Downstream system diagram and b) (Downstream) functional diagram.

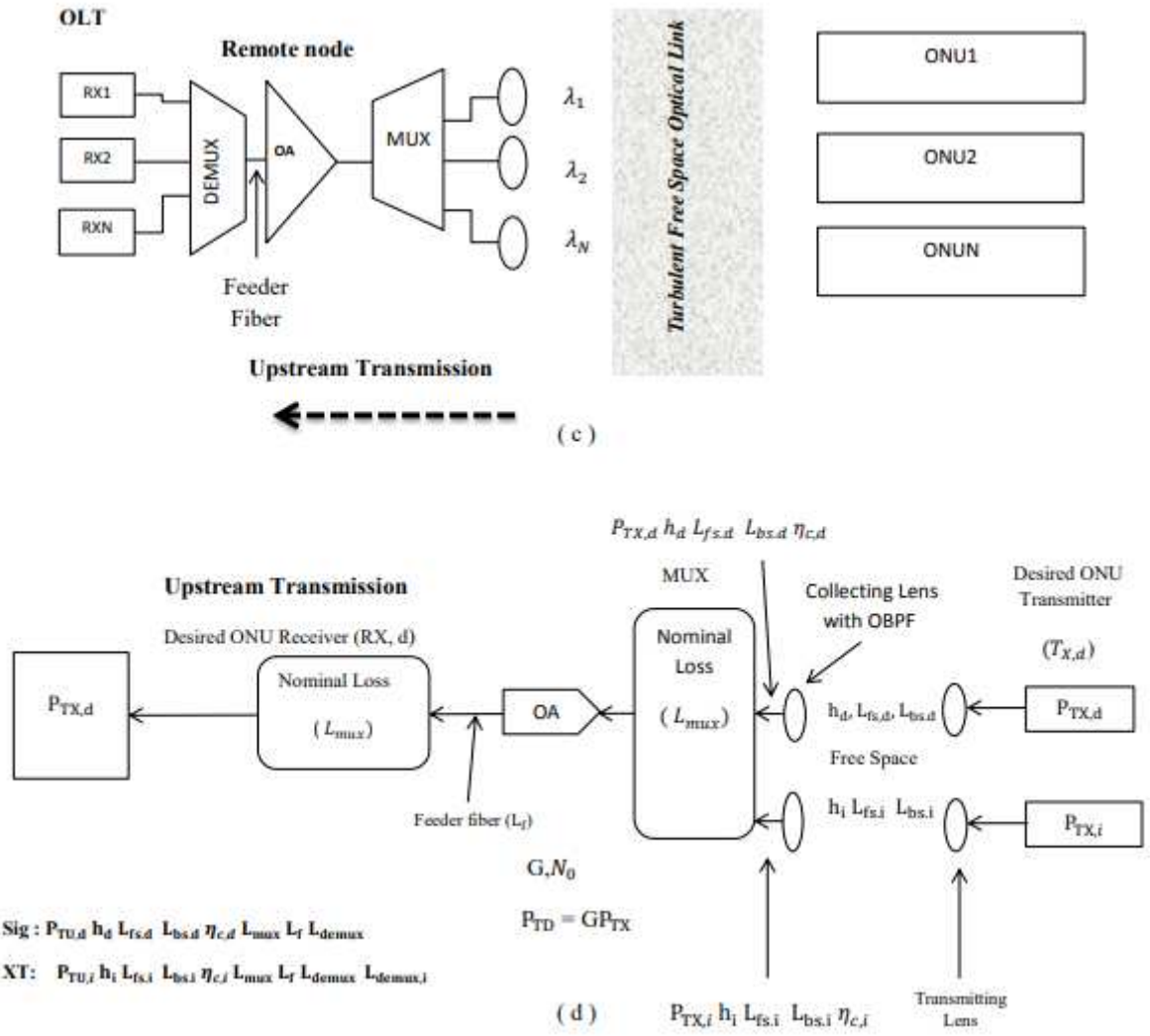

Figure 2

Optically Pre-amplified WDM DPPM Network: (c) Upstream system diagram (d) Upstream functional diagram.

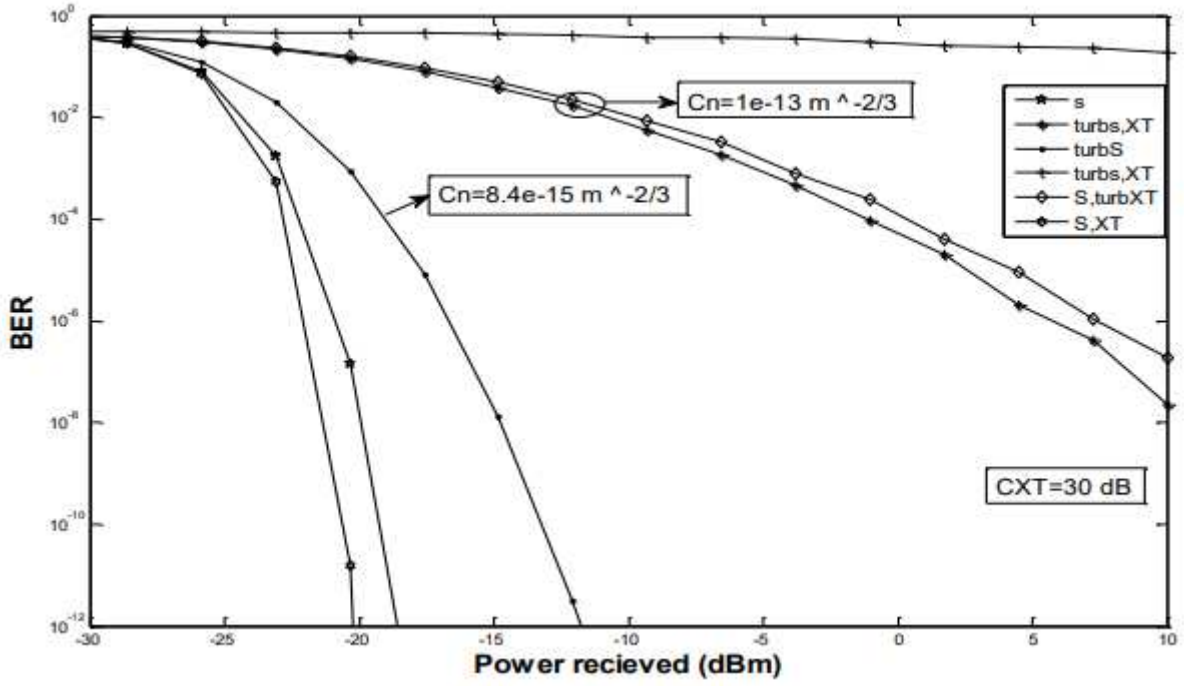

Figure 3

BER versus average received signal optical power (dBm) for WT and ST (no amplifier) with crosstalk CXT= 30 dB.

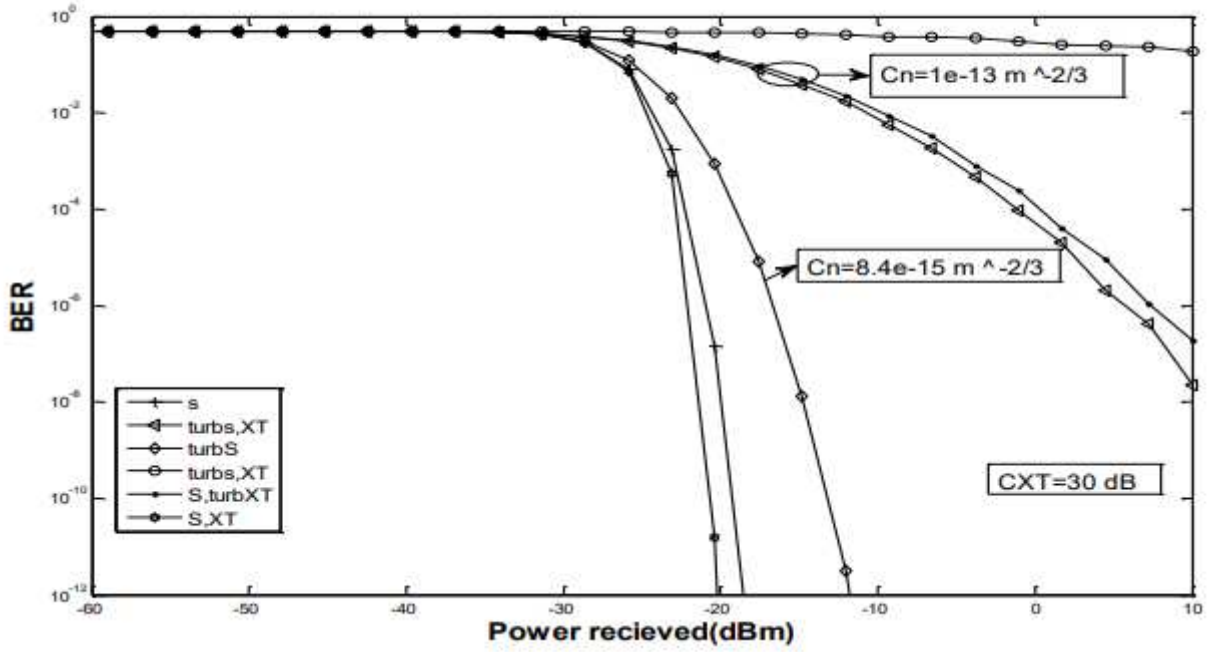

Figure 4

BER versus average received signal optical power (dBm) for WT and ST (with amplifier) with crosstalk CXT= 30 dB.

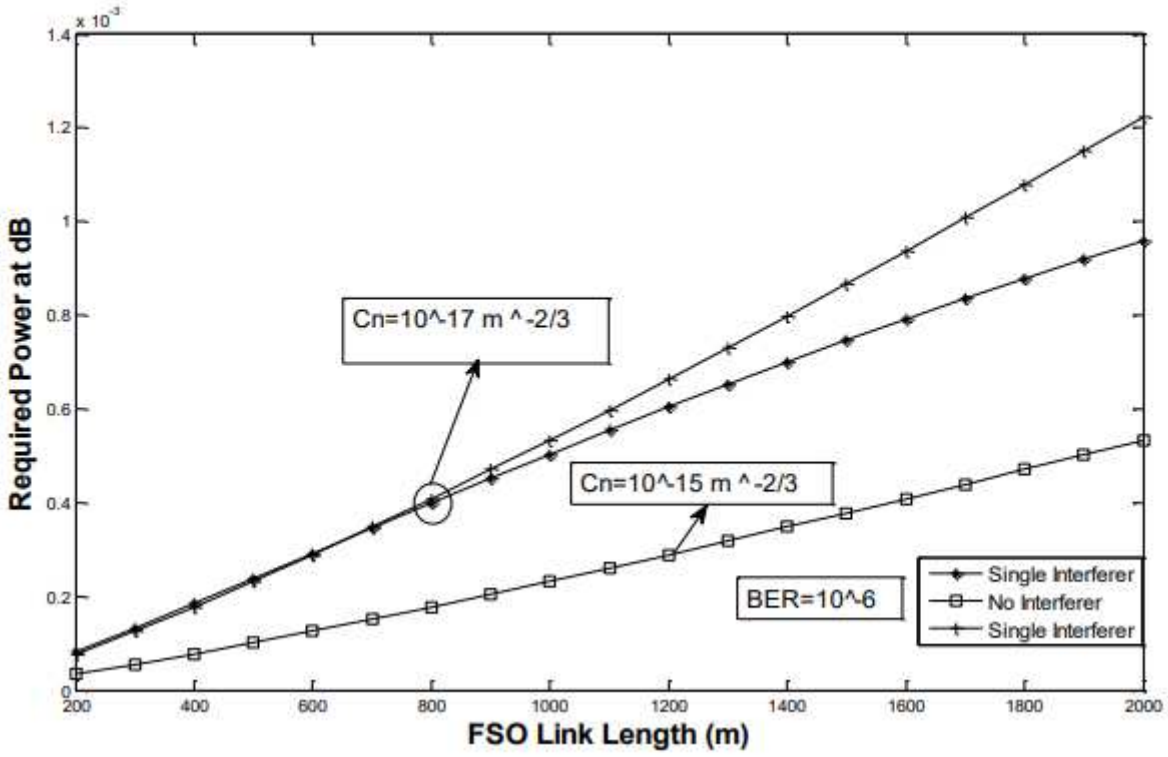

Figure 5

[Please see the manuscript file to view this figure caption.]

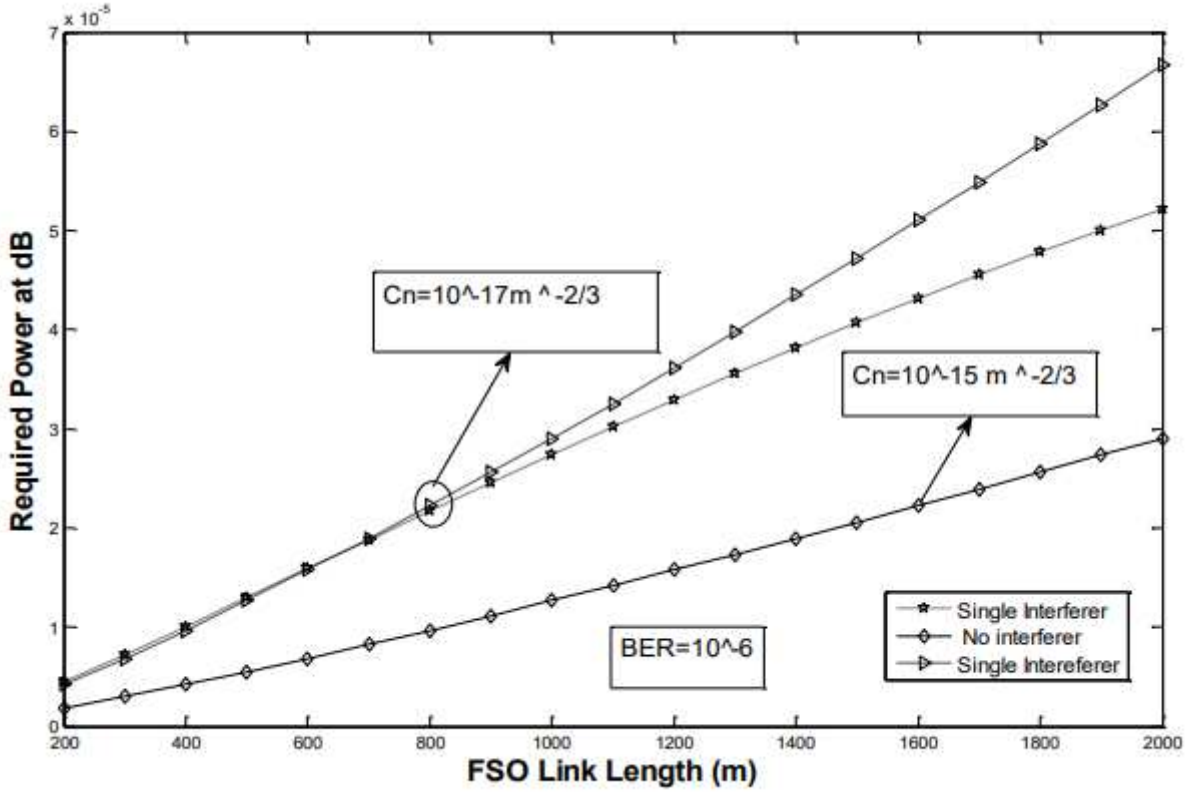

Figure 6

[Please see the manuscript file to view this figure caption.]

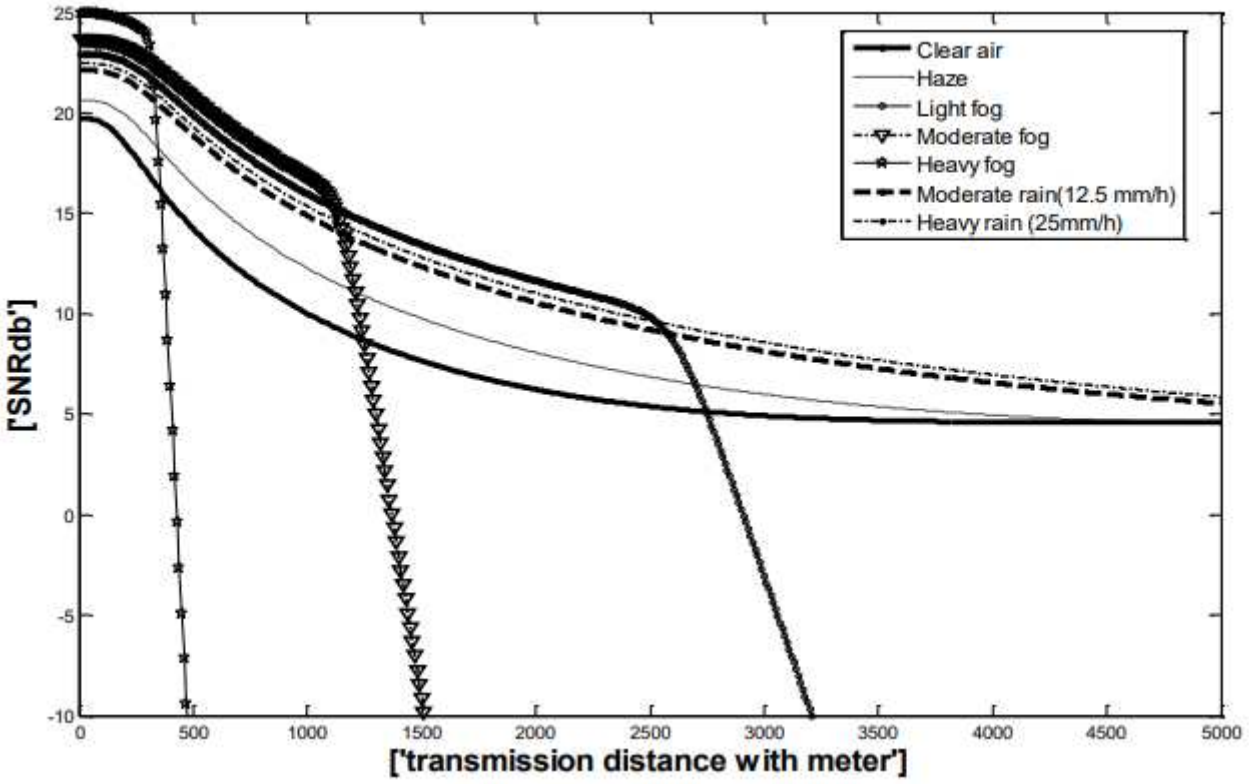

Figure 7

The FSO link length Vs Signal-to-noise-ratio (SNR) at dB.

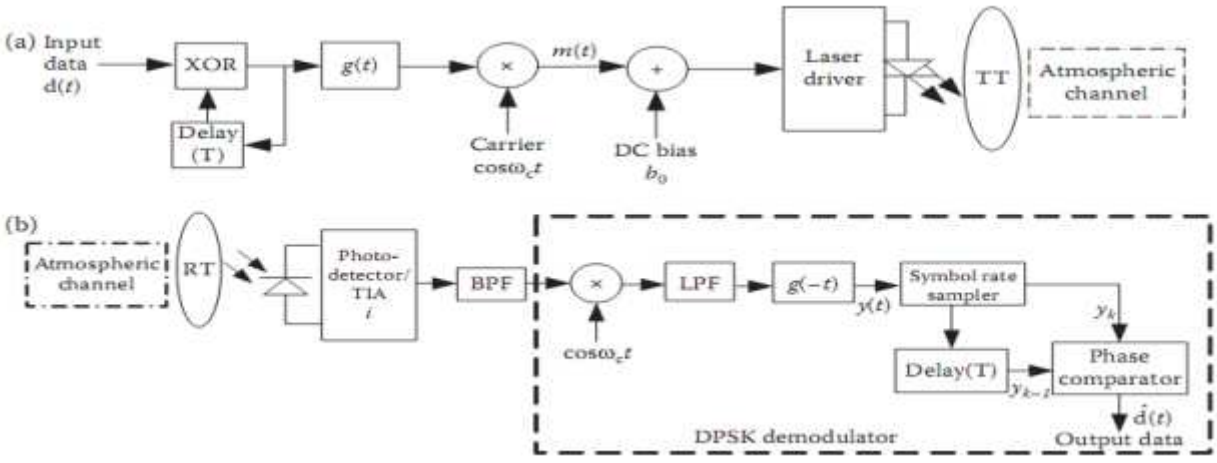

Figure 8

Block diagram of an FSO link employing DPSK-modulated SIM for (a) Transmitter and (b) Receiver. TIP-trans-impedance amplifier; TT-transmitter.

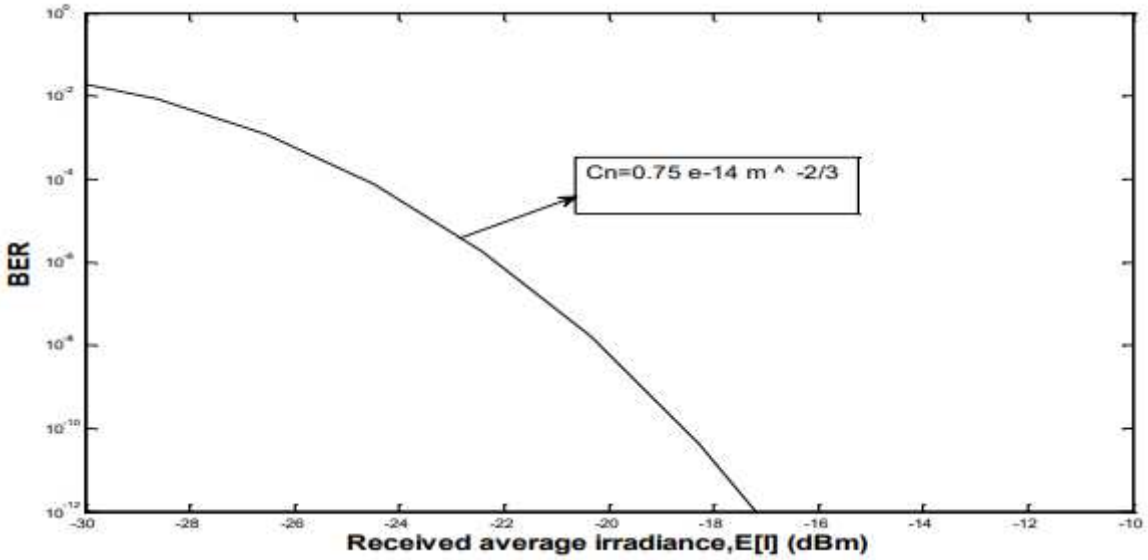

Figure 9

BER against the received irradiance for SIM-FSO with different subcarrier modulation techniques in weak atmospheric turbulence for λ = 1550 nm.

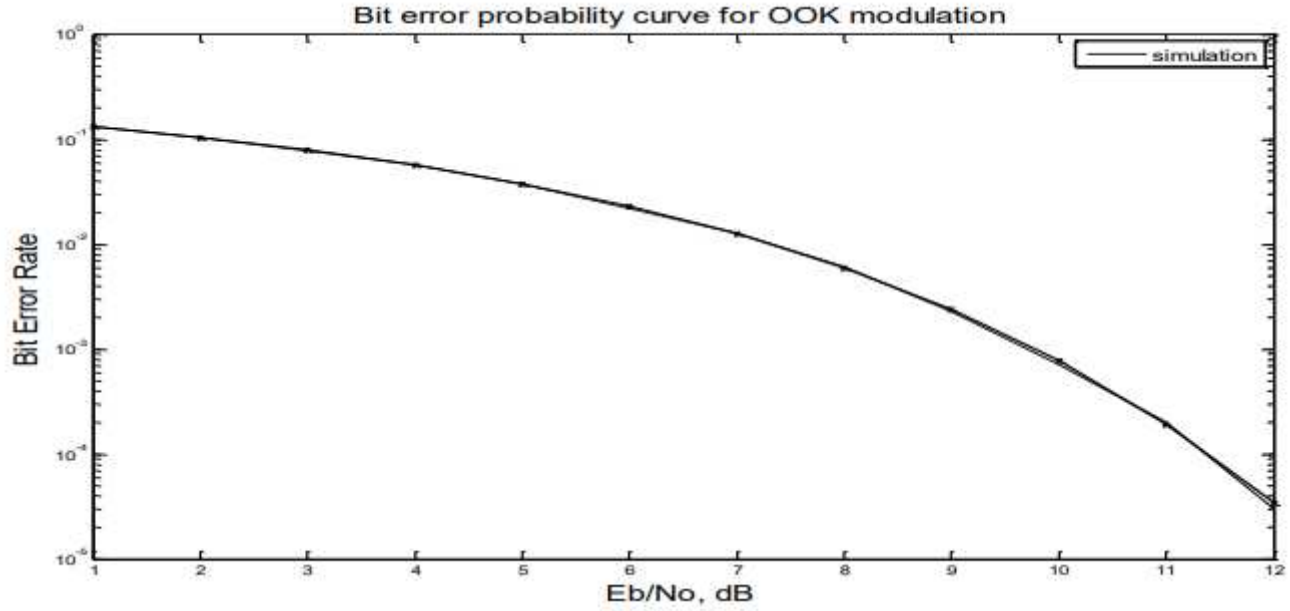

Figure 10

Bit error rate probability curve for OOK Modulation.

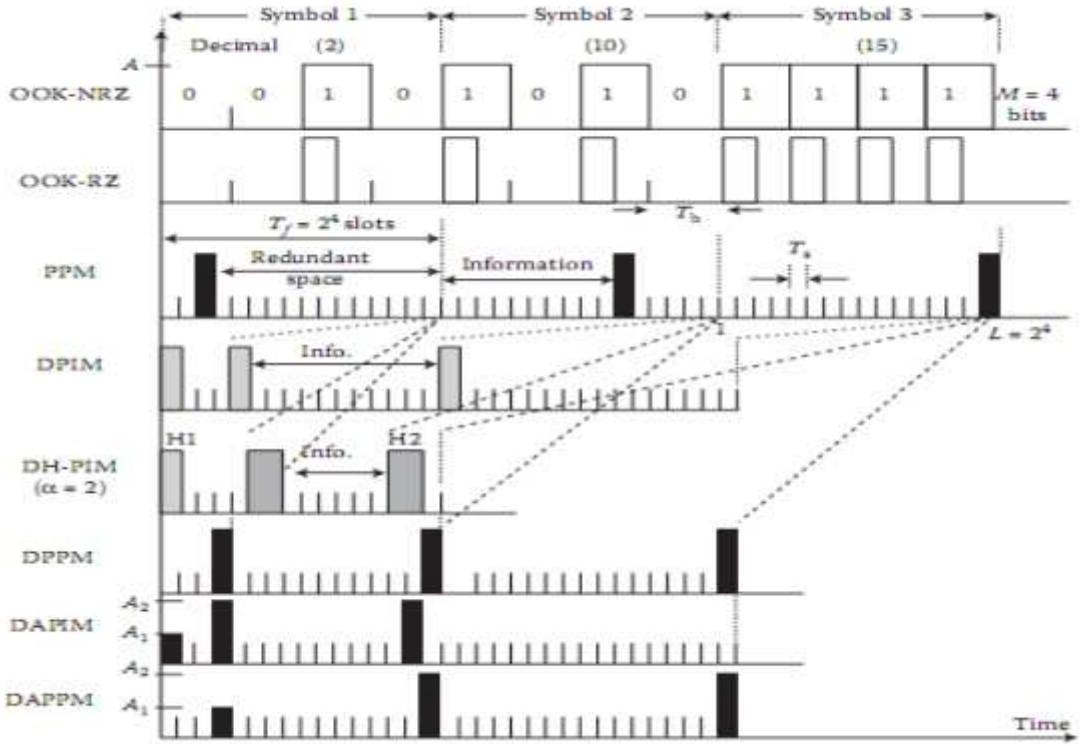

Figure 11

Time waveforms for OOK, PPM, DPI, DH-PIM, DPPM, DAPIM and DAPPM signals.

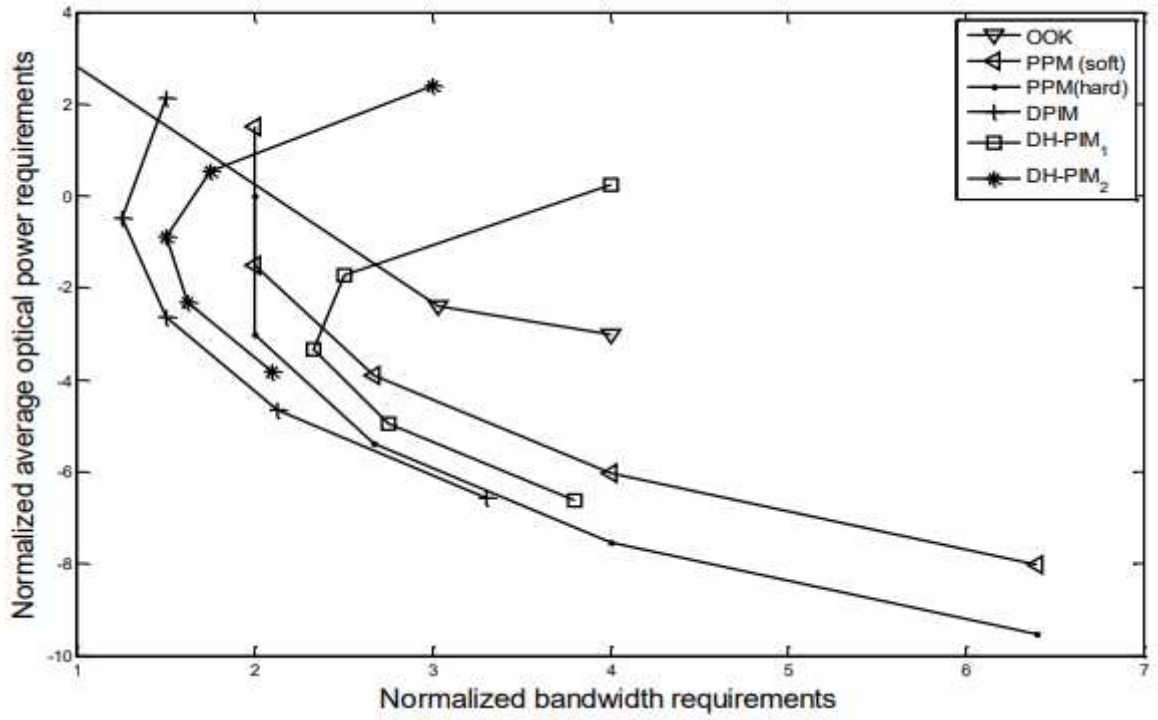

Figure 12

[Please see the manuscript file to view this figure caption.]

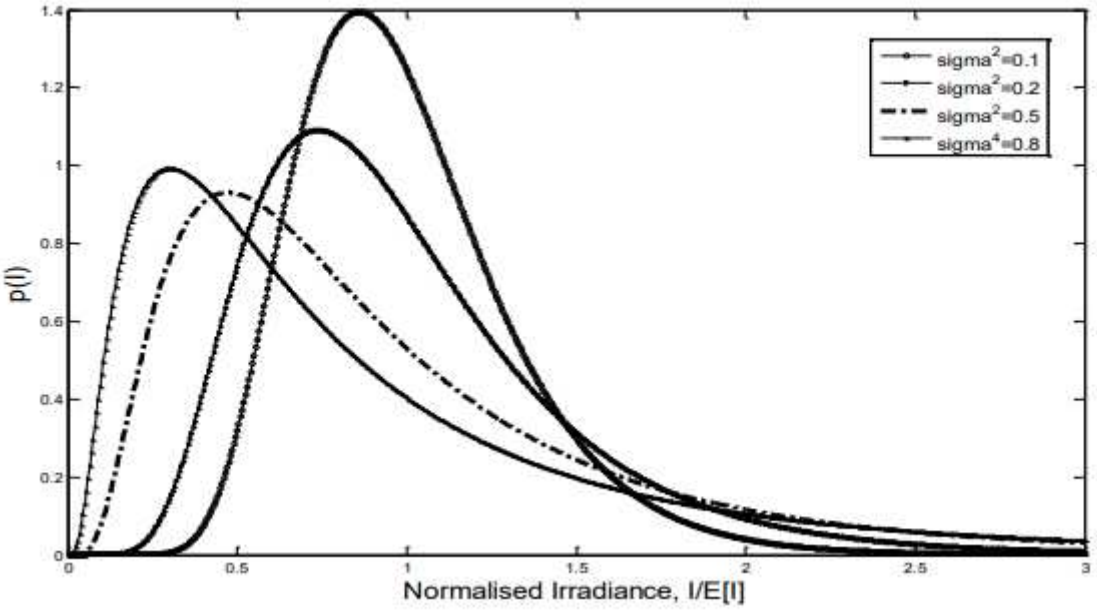

Figure 13

[Please see the manuscript file to view this figure caption.]

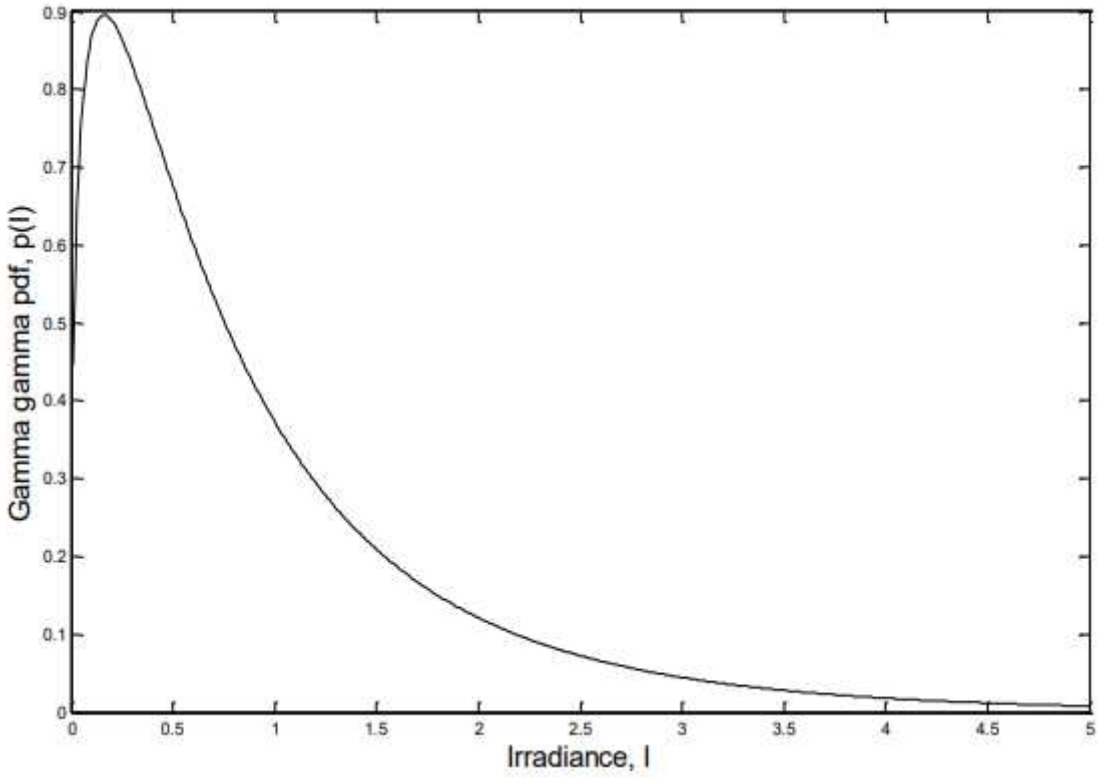

Figure 14

[Please see the manuscript file to view this figure caption.]

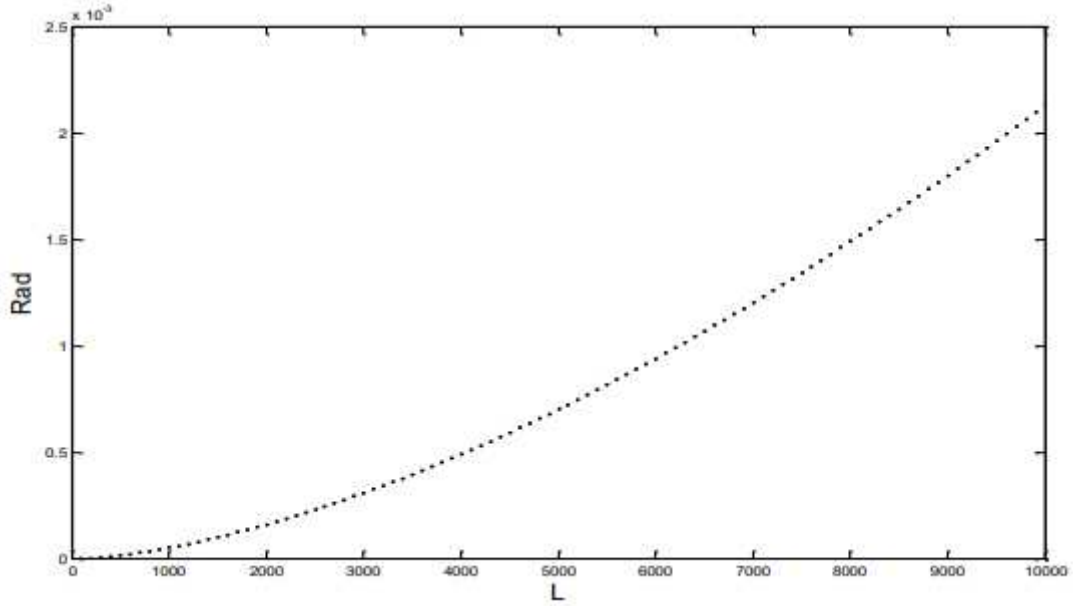

Figure 15

FSO link length (L) vs Rad (beam divergence).

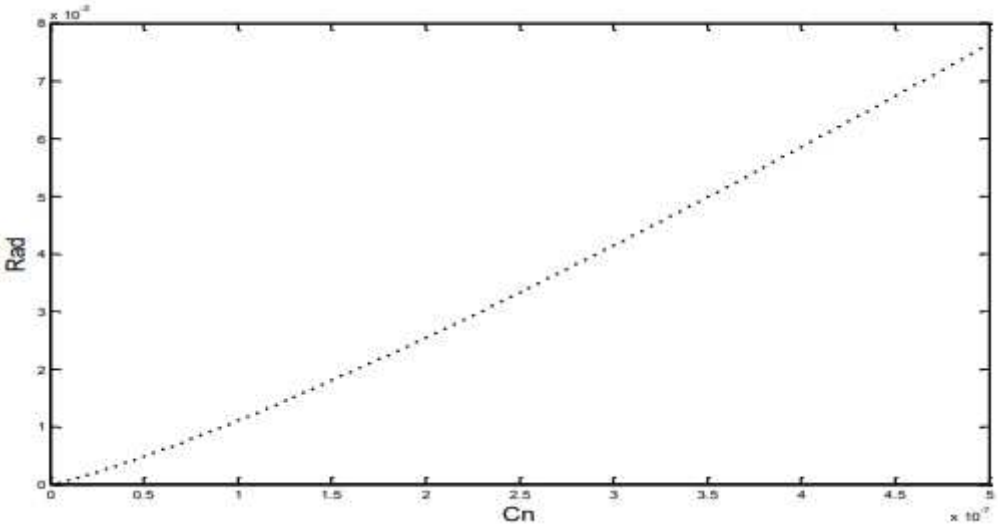

Figure 16

Refraction Index Structure (Cn) vs beam divergence. When Cn is increasing, beam divergence is increasing.

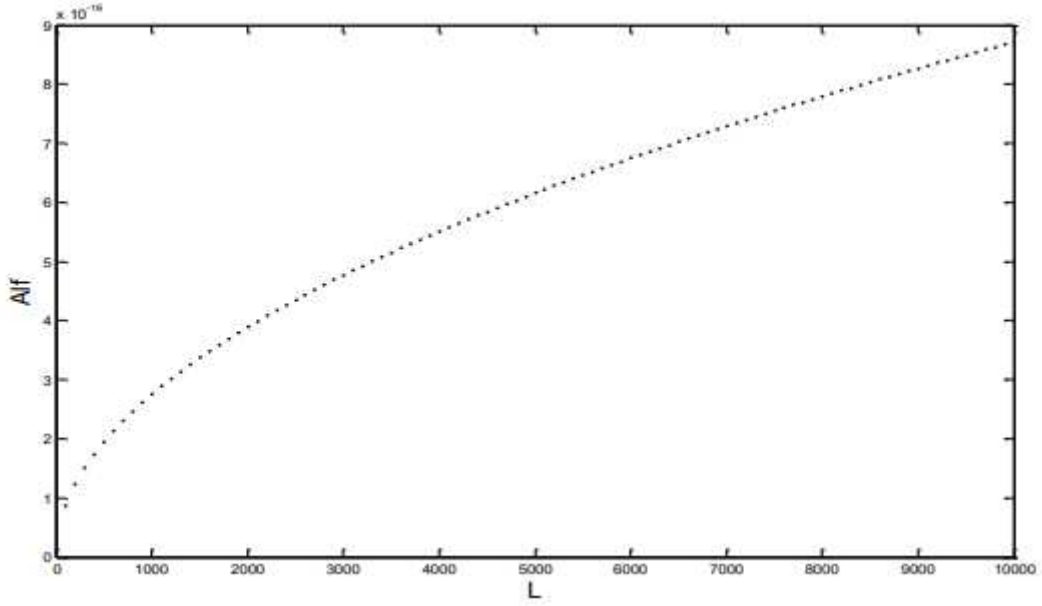

Figure 17

[Please see the manuscript file to view this figure caption.]

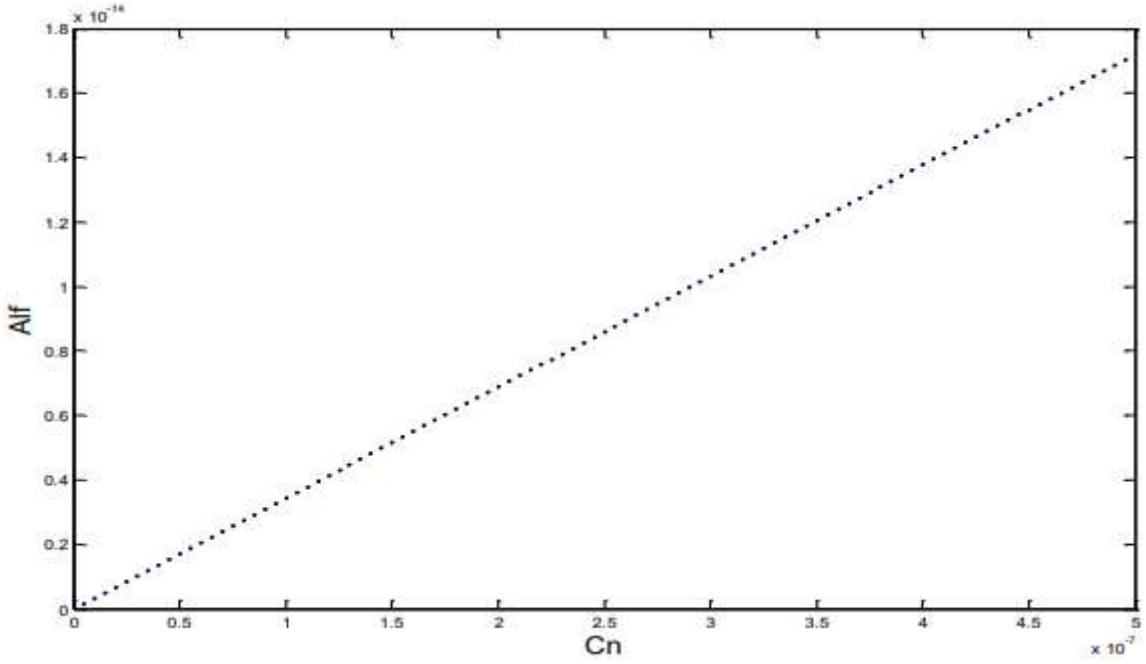

Figure 18

[Please see the manuscript file to view this figure caption.]

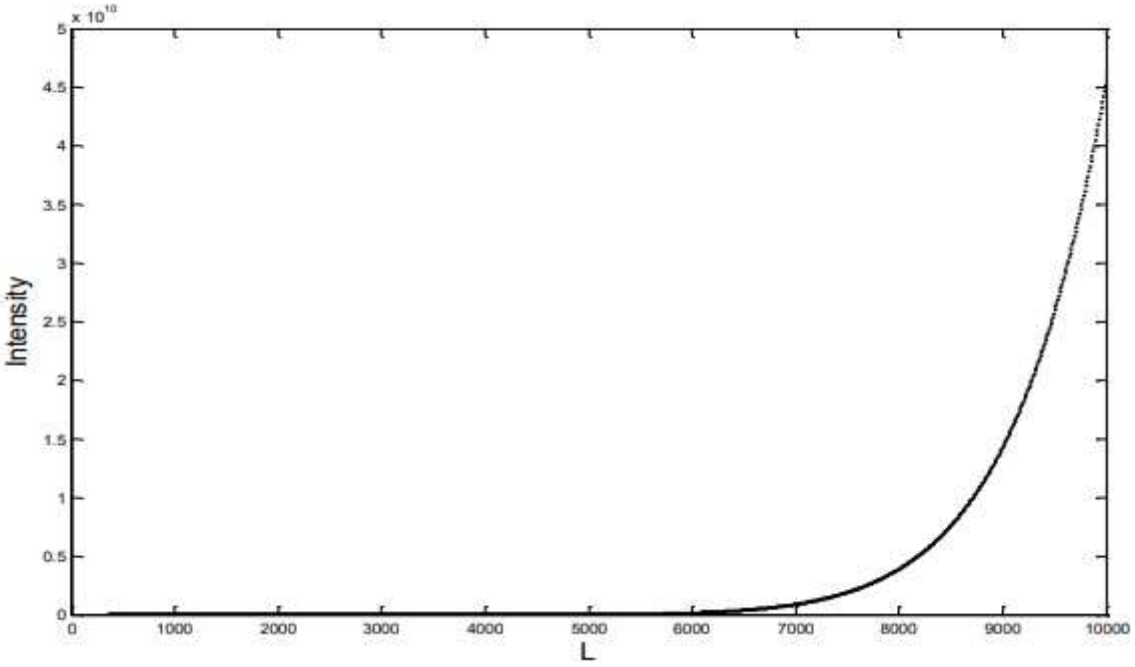

Figure 19

[Please see the manuscript file to view this figure caption.]

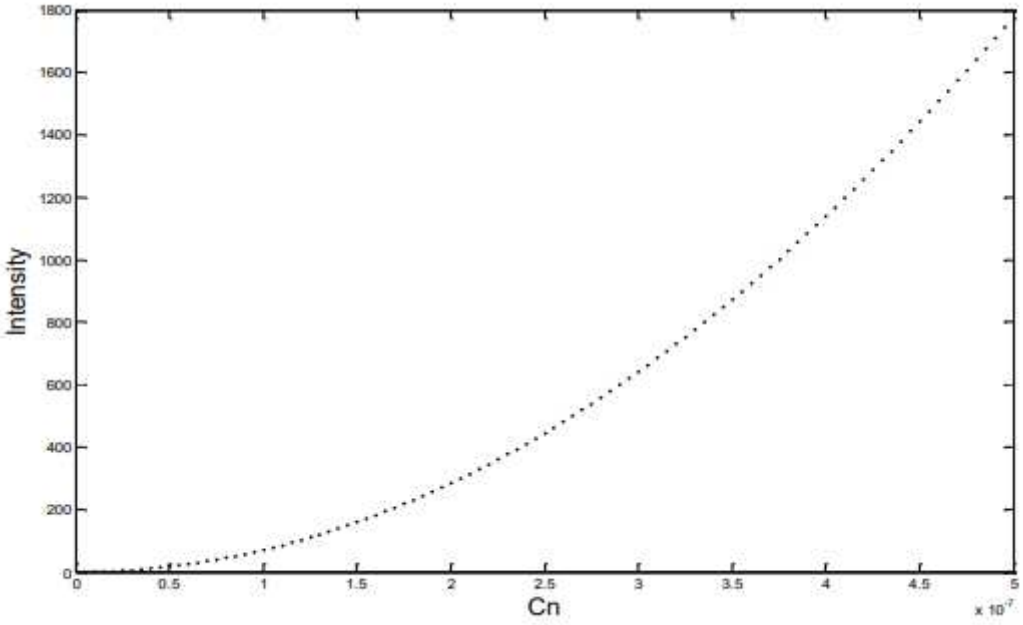

Figure 20

Refractive Index Structure (Cn) vs Turbulence Intensity.

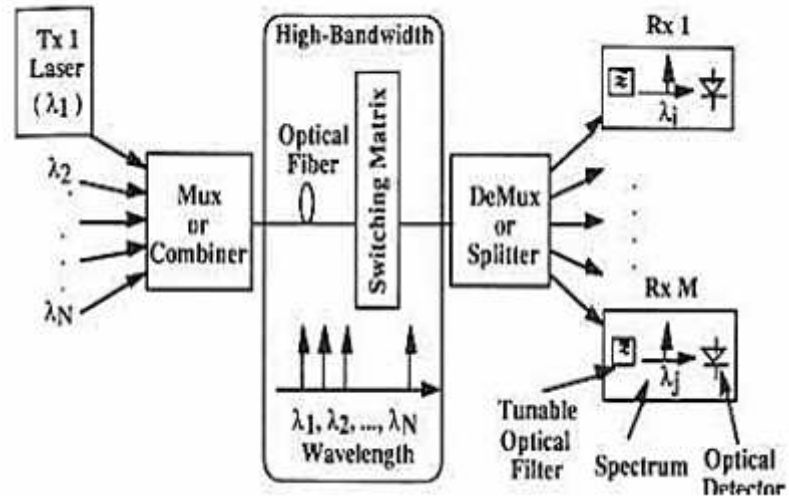

Figure 21

Diagram of a Simple WDM System.

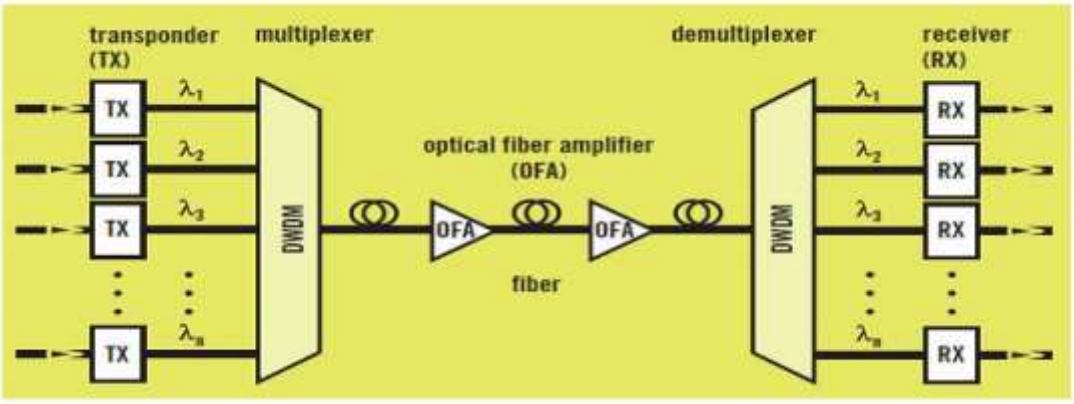

Figure 22

Multichannel DWDM Transmission System.

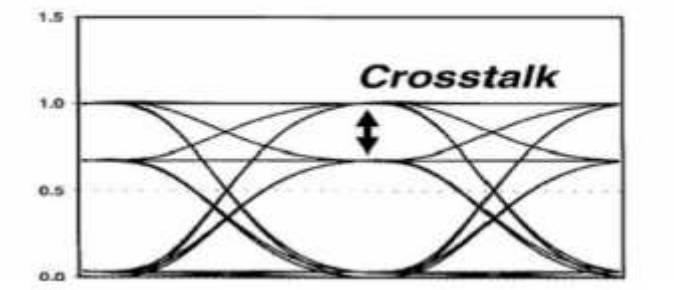

Figure 23

Definition of Crosstalk.

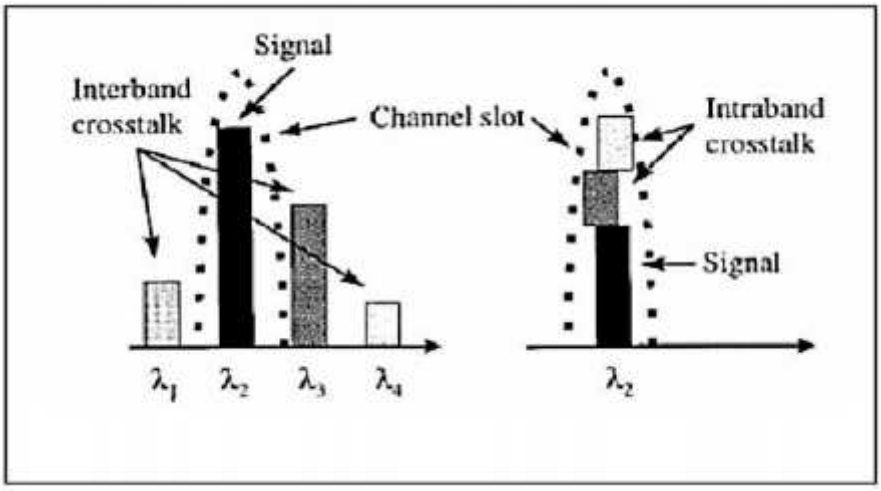

Figure 24

Inter-band and intra-band crosstalk.

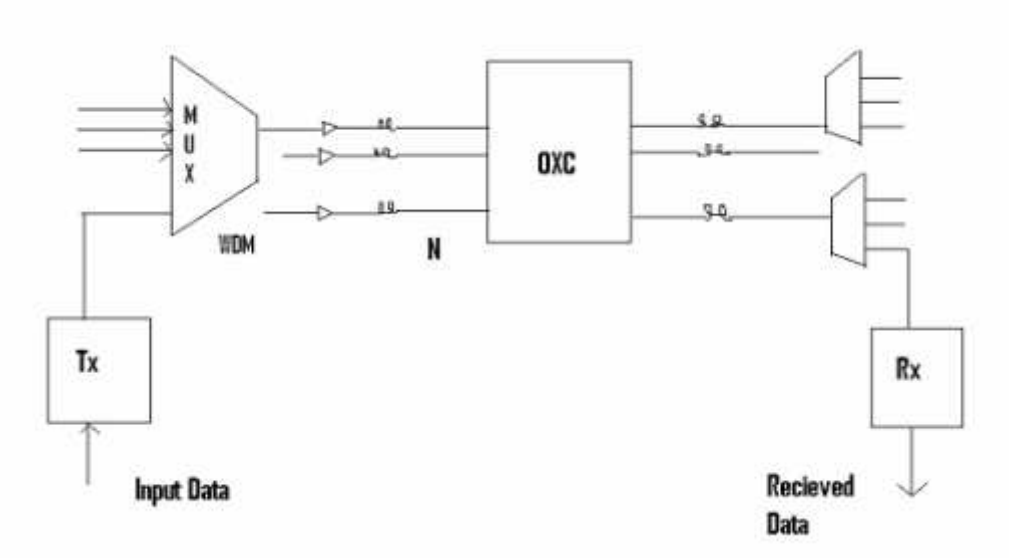

Figure 25

Simple block design.

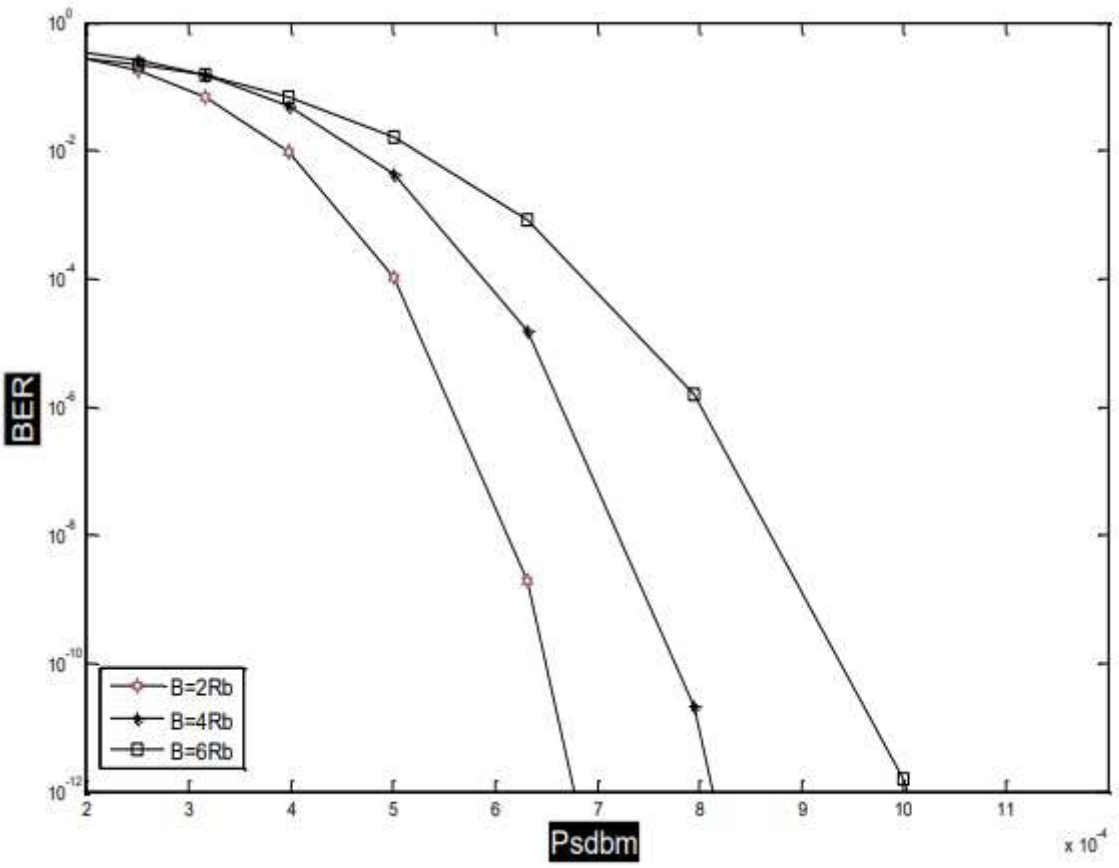

Figure 26

BER vs input power for different Bandwidth.

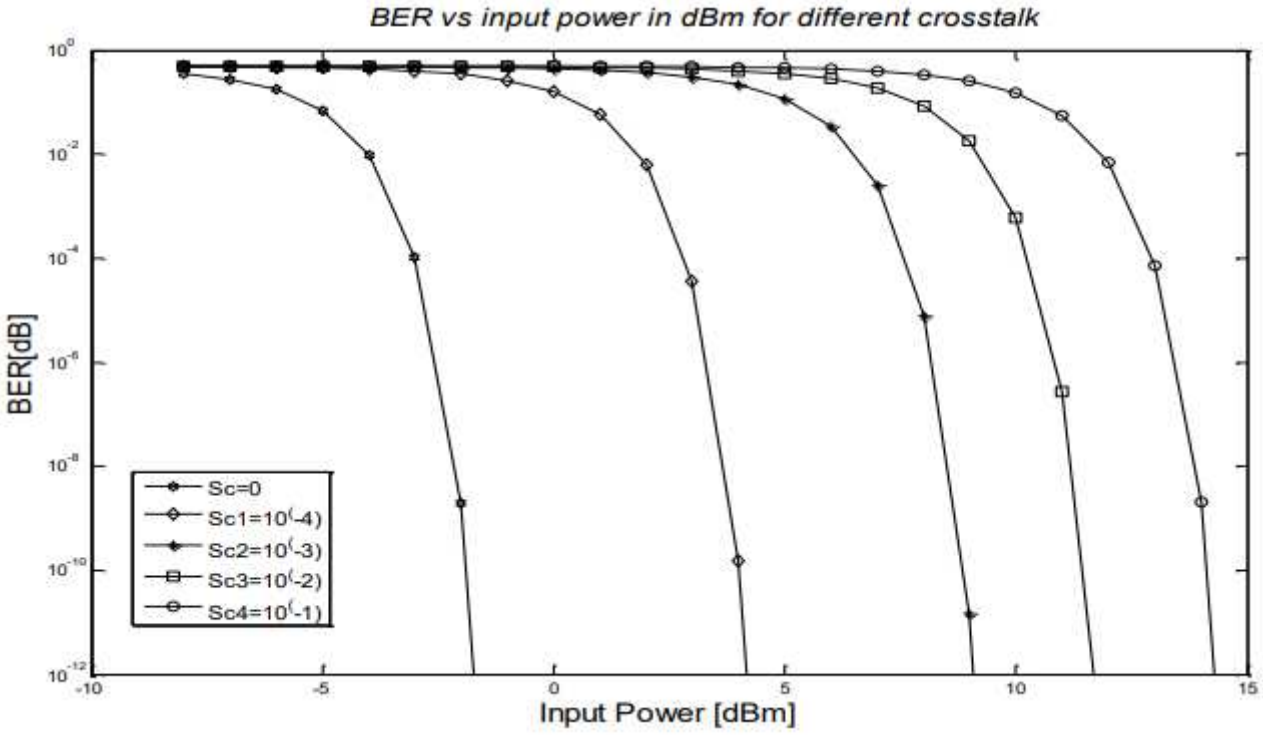

Figure 27

BER vs input power in dBm for different crosstalk.

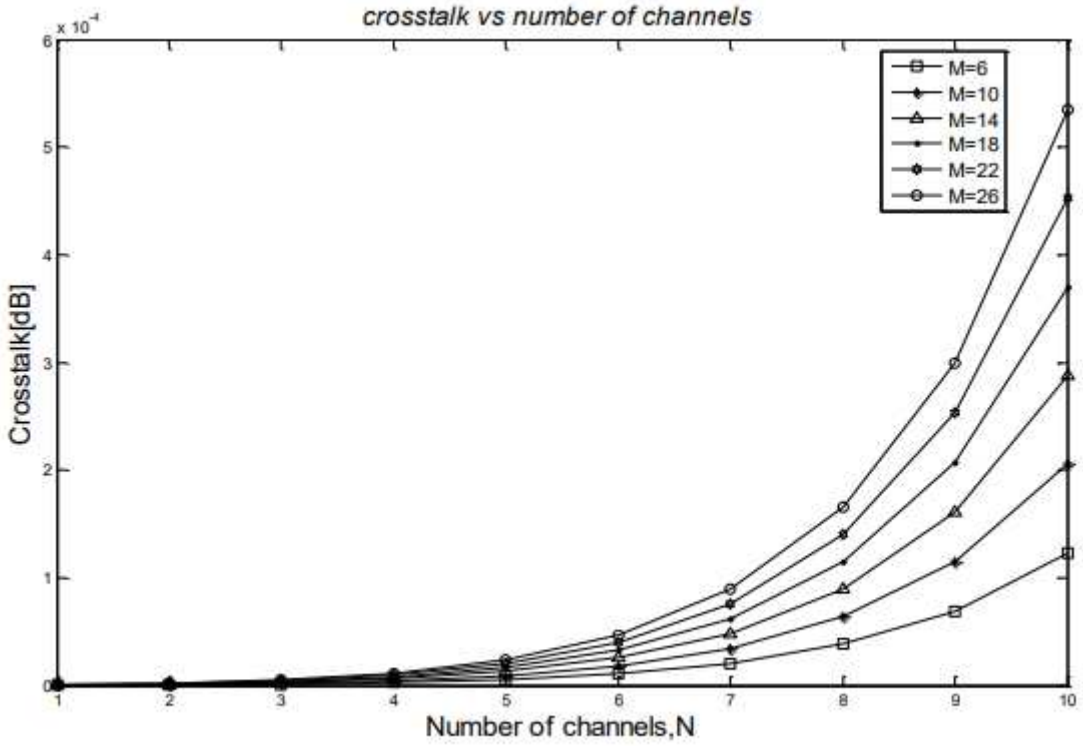

Figure 28

Crosstalk vs the number of channels.

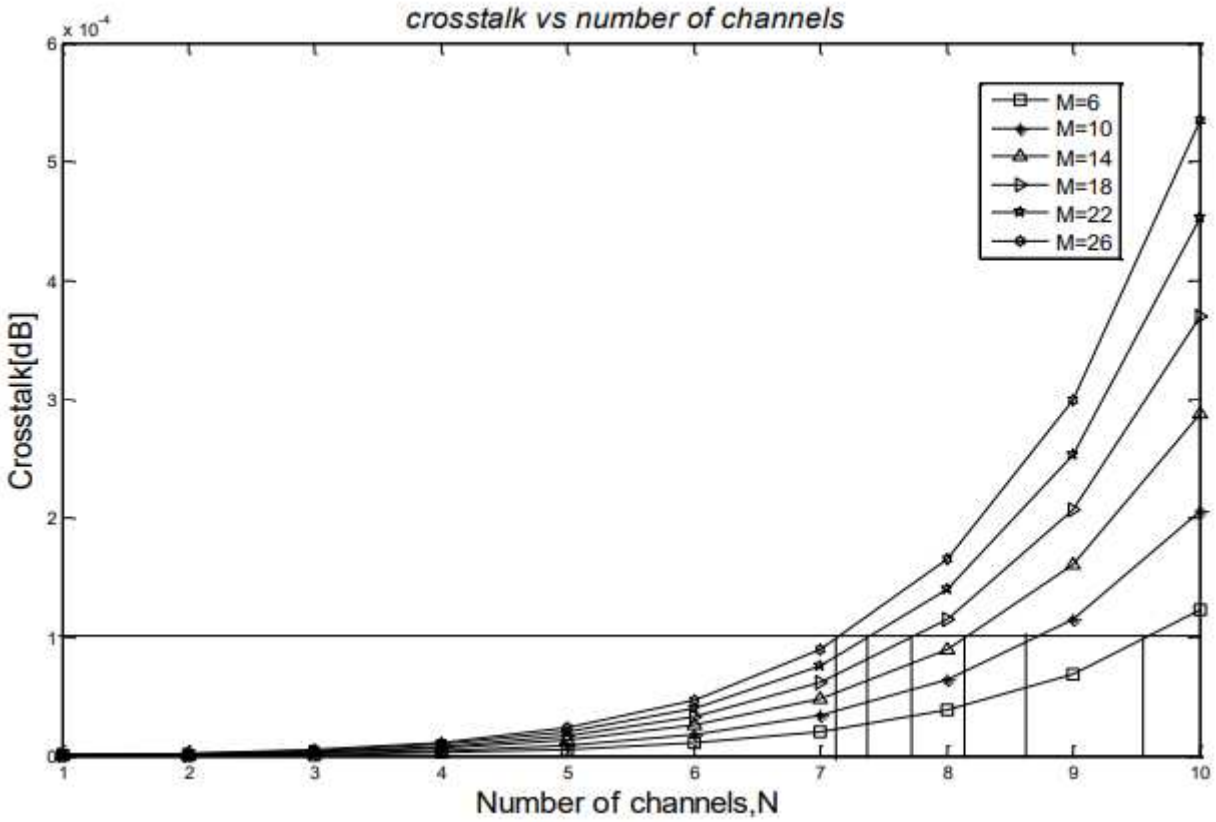

Figure 29

The number of channels and hops for related crosstalk.

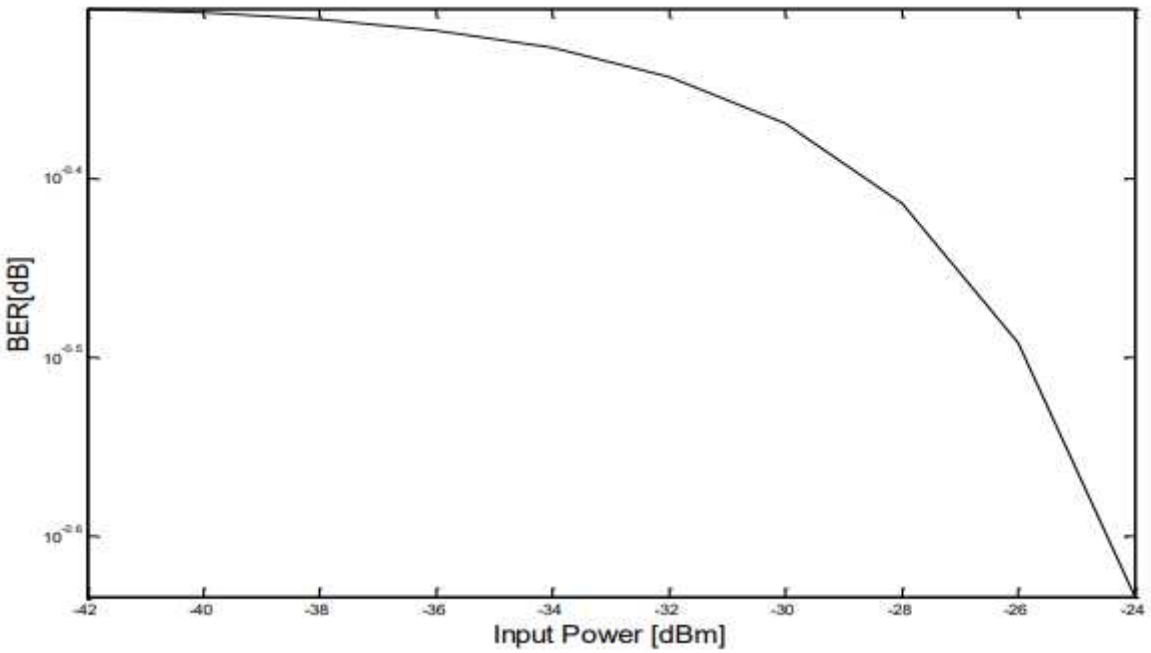

Figure 30

BER for with crosstalk.

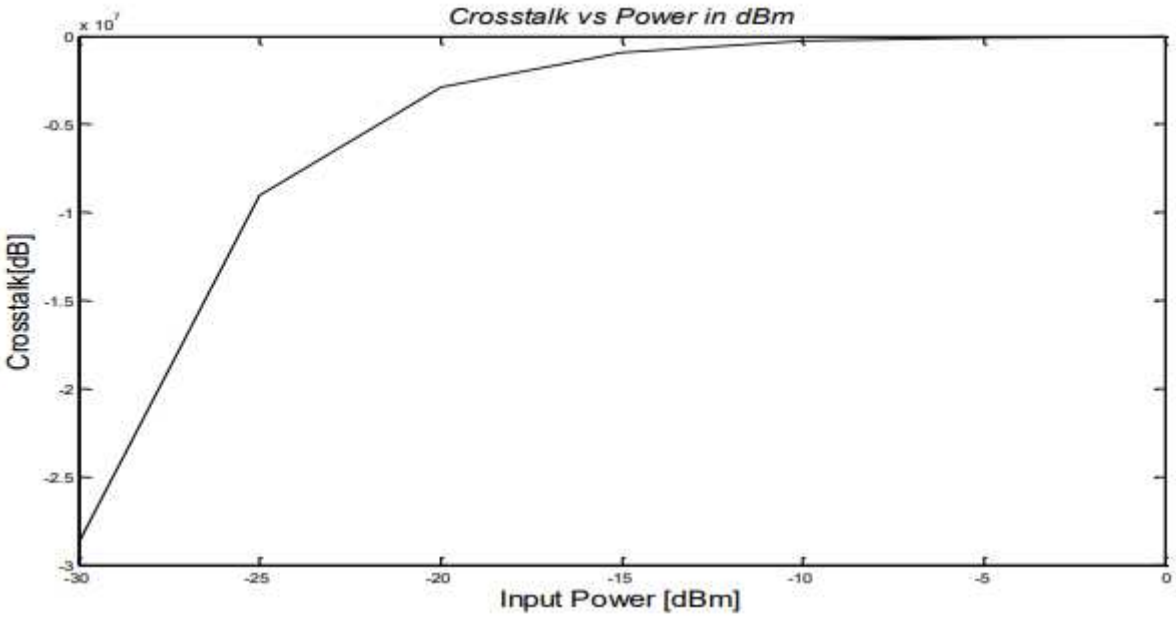

Figure 31

Topology 1: Crosstalk for various input power.

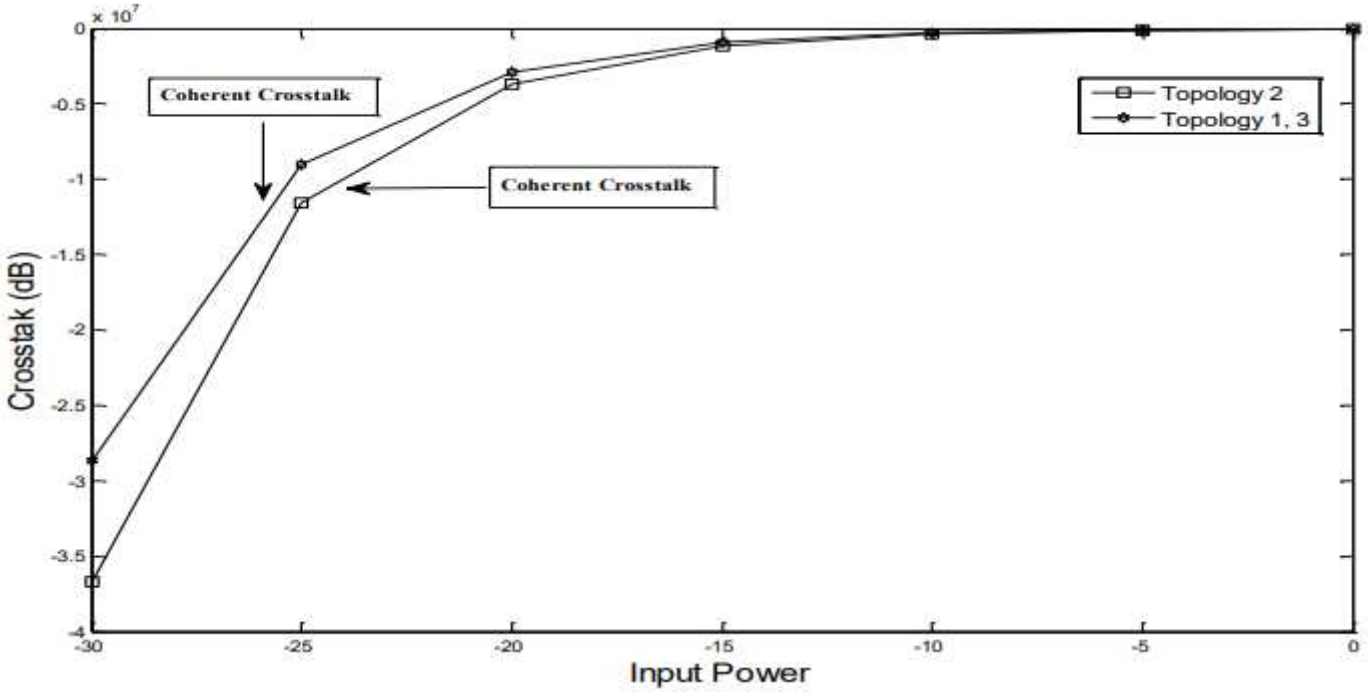

Figure 32

Crosstalk (coherent) in the function of the num er of OXC s c sc e for three topologies. The highest crosstalk is obtained for the first and second topologies. Both topologies perform equally. The better performance is shown by the second topology. Due to the low crosstalk values of the space switch as shown in Fig. 32.

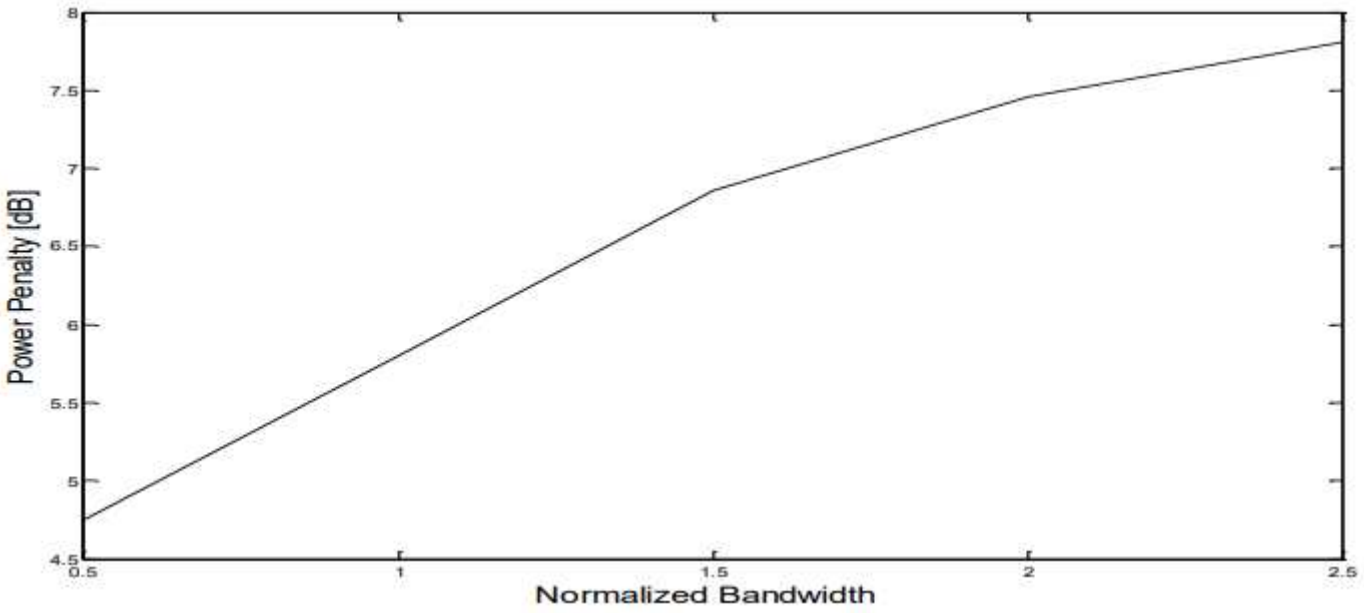

Figure 33

Power penalty (at BER= ;12) versus channel spacing with crosstalk for a bit rate of 4.5 Gb/ps.